



Hiroshima University

Graduate School of Advanced Science and Engineering

Electrical, Systems and Control Engineering Program

**Comprehensive Design for Enhancing
Resilience in Prosumer-Based
Microgrid Operations through
Modeling and Optimization**

PhD Dissertation

Mumbere Kihembo Samuel

March 2024

Comprehensive Design for Enhancing Resilience in Prosumer-Based Microgrid Operations through Modeling and Optimization

by

Mumbere Kihembo Samuel

D214393

A Thesis

Submitted to the Graduate School of Advanced Science and Engineering

Hiroshima University

in partial fulfillment of the requirements for the degree of

Doctor of Philosophy

(Electrical, Systems and Control Engineering)



Hiroshima University, Japan

March 2024



Hiroshima University
Graduate School of Advanced Science and Engineering

Kagamiyama, 1-4-1 Higashi-Hiroshima City
Hiroshima, Japan 739-8527
TEL: +81-82-424-7505
FAX: +81-82-422-7039

CERTIFICATE

To whom it may concern

We hereby certify that this is a copy of the original doctoral thesis by Mr. Mumbere Kihembo Samuel. This Ph.D. thesis was successfully defended and officially accepted in partial fulfillment of the requirements for the degree of Doctor of Philosophy in Electrical, Systems and Control Engineering.

Advisory and Examination committee:

Professor Yoshifumi ZOKA

Specially-appointed Professor. Naoto YORINO

Professor Katsuhiko TAKAHASHI

Professor Ichiro NISHIZAKI

Associate Professor Yutaka SASAKI

Abstract

As the integration of renewable energy sources into power systems continues to grow, the efficient operation of microgrids has become increasingly crucial. However, the inherently variable nature of solar energy introduces challenges for maintaining grid reliability and efficiency. This thesis tackles these challenges by developing and optimizing models for accurate photovoltaic (PV) power prediction within prosumer-based microgrids. Employing a comprehensive blend of machine learning algorithms and advanced optimization techniques, this research makes significant contributions to enhance microgrid operation and reliability. Specifically, this work utilizes the capabilities of MATLAB/Simulink for simulation and MATLAB's Optimization Toolbox for advanced computational analysis.

The research's novelty lies in its multi-faceted approach to flexible microgrid modelling that leverages fast and accurate solar power prediction and harmonizing predicted and real-time optimization. Firstly, the thesis introduces a resilient prosumer model for microgrids, which employs resilience hardening control schemes that include PV curtailment (PVC), non-critical load shedding (NCLS), and flexible load switching (FLS) to complement the inbuilt voltage and frequency control schemes in an energy management system (EMS), battery energy storage systems (BESS), PV systems, and. This model, validated through simulations and case studies executed via MATLAB/Simulink, marks a pioneering effort in existing literature.

Secondly, the research presents a novel solar power prediction model which employs an Iterative Network Pruning (IP) Technique in feedforward neural networks (FNNs), leading to significant gains in forecast accuracy and computational efficiency. The weather-based FNNs (WFNNs) employ weather clustering algorithms to further refine prediction accuracy under different weather conditions. The model considers the setting of confidence intervals, thereby providing a reliability measure for the forecasts.

Thirdly, this thesis utilizes predictive linear programming and model predictive optimization strategies for real-time energy management in microgrids. This novel approach incorporates adjustments for discrepancies between forecasted and actual energy production and consumption, offering a more dynamic and responsive EMS for mitigating uncertainties and prioritizing critical loads.

Considering the simulation results presented in this research, it is evident that the proposed models and methodologies significantly enhance the resilience and adaptability

of microgrid operations. The advanced prosumer model, with its integrated BESS and PV systems, demonstrates robust performance under varying weather conditions and in post-disaster scenarios, as validated by simulation. Furthermore, the solar power prediction model, utilizing the IP technique, effectively reduced computational load, maintaining high prediction accuracy, a crucial factor for real-time applications in microgrids. These results underscore the efficacy of the developed models and optimization strategies in managing the complexities and dynamic nature of microgrid operations, paving the way for more sustainable and reliable energy systems.

Acknowledgment

First and foremost, I extend my deepest gratitude to God for His endless grace, goodness, and blessings. His strength was pivotal in the successful completion of this study.

I am profoundly grateful to my colleagues at the Electric Power and Energy Systems Laboratory, Hiroshima University, for their assistance and the congenial environment they provided, which was crucial to my work. Special thanks to my advisor, Associate Professor Yutaka Sasaki, for his invaluable guidance, suggestions, and unwavering support throughout my research. His mentorship was a cornerstone in accomplishing my master's thesis.

I am equally thankful to my co-advisors, Specially-appointed Professor Naoto Yorino, Professor Yoshifumi Zoka, Professor Katsuhiko Takahashi, and Professor Ichiro Nishizaki, for their guidance and support. My colleagues, Yoshiki Tanioka and Sho Enomoto, deserve special mention for laying the groundwork for this thesis and for their assistance throughout my research journey. I am also grateful to Dr. Ahmed Bedawy for his invaluable guidance and Daigo Usami for his help, particularly in collecting weather data. I appreciate the support of Krifa Chiraz and Wang Weichao in discussions and travel preparations.

My sincere thanks to the staff of the Electric Power and Energy Systems Laboratory, especially Yukiko Yamauchi, for her invaluable assistance with logistics, organizing conference travels and financial reporting.

The Japanese Government MEXT deserves a special mention for providing the scholarship that supported my studies and stay in Japan.

Most importantly, my heartfelt thanks to my family: my wife for her unwavering patience, and my parents, siblings, and friends for their emotional and spiritual support. Their love and encouragement were the bedrock of my journey.

This thesis is dedicated to my beloved daughter, Colette, whose early years I missed while pursuing this degree. Her presence has been a constant inspiration.

Mumbere Kihembo Samuel

2024

| | |
|---|----|
| 2.1.3 Resilience in Microgrid Systems..... | 16 |
| 2.1.4 Microgrid Control Strategies..... | 19 |
| 2.1.5 The Robust Electricity Supply-Demand Manager (RESDM) | 21 |
| 2.2 Renewable Energy and Prosumer Models..... | 23 |
| 2.2.1 The Rise of Renewable Energy | 24 |
| 2.2.2 Concept of the Prosumer in Renewable Energy Systems..... | 24 |
| 2.2.3 Literature Review: Renewable Energy and Prosumer Models..... | 25 |
| 2.3 Solar Power Prediction Techniques..... | 26 |
| 2.3.1 Basics of Solar Power and Its Predictability | 27 |
| 2.3.2 Traditional Techniques and Their Limitations | 28 |
| 2.3.3 Neural Network-Based Forecasting..... | 29 |
| 2.3.4 Weather-Based Clustering Feedforward Neural Networks (WFNNs)..... | 29 |
| 2.3.5 Advantages Over Traditional Methods..... | 30 |
| 2.3.6 Advantages Over General Neural Network-Based Approaches:..... | 31 |
| 2.4 Optimization Techniques in Microgrids..... | 32 |
| 2.4.1 Traditional Optimization Techniques..... | 32 |
| 2.4.1.1 Linear Programming (LP) | 32 |
| 2.4.1.2 Mixed-Integer Linear Programming (MILP)..... | 33 |
| 2.4.1.3 Non-Linear Programming (NLP) | 33 |
| 2.4.2 Need for Advanced Techniques | 33 |
| 2.4.2.1 Model Predictive Control Coupled with LP | 33 |
| 2.4.2.2 Multi-objective Optimization..... | 35 |
| 2.4.2.3 Rolling Horizon Optimization..... | 36 |
| 2.4.3 Justification for Chosen Approaches | 39 |
| 2.5 Gaps in the Current Literature..... | 39 |
| 2.5.1 Modeling for Resilience | 40 |
| 2.5.2 PV Forecast Methodology..... | 41 |
| 2.5.3 Optimization Methodology | 41 |
| 2.6 Conclusion..... | 42 |

| | |
|---|-----------|
| Chapter 3: A Resilient Prosumer Model for Microgrids | 44 |
| 3.1 Introduction..... | 44 |
| 3.2 The Prosumer Model and Control Scheme | 44 |
| 3.2.1 Battery Energy Storage System (BESS) | 45 |
| 3.2.1.1 Battery Model Adopted by BESS | 45 |
| 3.2.1.2 DC Bus Control Scheme in BESS | 47 |
| 3.2.2 Photovoltaic System Architecture and Control Algorithms..... | 48 |
| 3.2.2.1 Modeling of the PV Array | 48 |
| 3.2.2.2 MPPT Controller and the Incremental Conductance Algorithm..... | 48 |
| 3.2.2.3 PV Output Limitations | 49 |
| 3.2.2.4 PV Curtailment Control (PVC) Method | 49 |
| 3.2.3 Electrical Load Modeling and Control Mechanisms | 50 |
| 3.2.3.1 Load Classification and Control | 50 |
| 3.2.3.2 Load Modeling and External Inputs | 51 |
| 3.2.3.3 Active and Reactive Power Components..... | 51 |
| 3.2.3.4 Current Reference Generation..... | 52 |
| 3.2.3.5 Limitations of the NCLS Mechanism | 53 |
| 3.2.4 The Single-Phase Synchronous Inverter (SSI): Principles and Operational Mechanics | 53 |
| 3.2.4.1 Basic Principle | 53 |
| 3.2.4.2 Input and Output Specifications..... | 53 |
| 3.2.4.3 Duty Ratio Calculation..... | 54 |
| 3.2.4.4 Adoption from Prior Research | 54 |
| 3.2.5 The proposed Energy Management System (EMS) Simulator | 54 |
| 3.2.5.1 Operating Principles of the EMS Simulator..... | 55 |
| 3.2.5.2 Algorithmic Control and Operational Modes | 56 |
| 3.3 Case Studies | 58 |
| 3.3.1 Simulation Set-up and Conditions | 58 |
| 3.3.2 Simulation Scenarios..... | 61 |
| 3.3.3 Results of the Simulated Test Scenarios | 62 |

| | |
|--|-----------|
| 3.3.4 Discussion of Findings | 67 |
| 3.3.5 Limitations..... | 68 |
| 3.4 Conclusion..... | 69 |
| Chapter 4: An Enhanced Solar Power Prediction Model..... | 70 |
| 4.1 Introduction | 70 |
| 4.2 Solar Power Prediction Using Iterative Network Pruning Technique for Microgrid Operation | 70 |
| 4.2.1 Overview | 70 |
| 4.2.2 Pre-processing of Weather Data and Feature Extraction..... | 70 |
| 4.2.3 Weather Clustering and Construction of WFNNs..... | 71 |
| 4.2.4 Confidence Intervals and Local Energy Management..... | 72 |
| 4.2.5 Feedforward Calculations and Activation Functions in Neural Networks..... | 72 |
| 4.2.6 Evaluation and Regularization techniques | 73 |
| 4.2.6.1 Evaluation methods | 73 |
| 4.2.6.2 Regularization Techniques | 74 |
| 4.2.7 Implementation of the Iterative Pruning (IP) Algorithm..... | 75 |
| 4.3 Case study..... | 77 |
| 4.3.1 overview | 77 |
| 4.3.2 Simulation and Results and Discussion..... | 77 |
| 4.3.2.1 Iterative Pruning Implementation..... | 77 |
| 4.3.2.2 Sunny Weather Prediction..... | 78 |
| 4.3.2.3 Cloudy Weather Prediction | 80 |
| 4.3.2.4 Rainy Weather Prediction..... | 82 |
| 4.4 Conclusion: Implications and Future Prospects | 83 |
| 4.4.1 Conclusion..... | 83 |
| 4.4.2 Practical Implications | 84 |
| 4.4.3 Future Works..... | 84 |
| Chapter 5: Forecast-Driven Optimization Strategy for Efficient Microgrid Management .. | 85 |
| 5.1 Introduction | 85 |

| | |
|---|------------|
| 5.2 SOC Estimation with Optimal Operation of Grid-Connected Microgrid Prosumers | 86 |
| 5.2.1 Introduction..... | 86 |
| 5.2.2 Proposed Optimization Approach..... | 87 |
| 5.2.2.1 Estimate the Optimal Operation for the Next Day..... | 87 |
| 5.2.2.2 Derive the Estimated Initial BESS SOC for the Next Day | 89 |
| 5.2.2.3 Manage Power Flow and Non-Critical Load for the Current Day | 90 |
| 5.2.3 Optimization Methodology | 92 |
| 5.2.3.1 Methodologies for Efficient Prosumer-Based Microgrid Management..... | 92 |
| 5.2.3.2 Solver: MATLAB's linprog Function | 92 |
| 5.2.4 Algorithm for Implementing Proposed Steps | 92 |
| 5.3 A Two-Stage Optimal Control Strategy for Mitigating Uncertainty in Microgrids | 93 |
| 5.3.1 Introduction..... | 93 |
| 5.3.2 Proposed Optimization Strategy | 94 |
| 5.3.2.1 Predictive Optimization (Stage 1)..... | 94 |
| 5.3.2.2 Re-Optimization (Stage 2) | 95 |
| 5.3.2.3 Objective Function and Constraints | 95 |
| 5.4 Case Studies..... | 96 |
| 5.4.1 SOC Estimation with Optimal Operation of a Grid-Connected Microgrid Prosumer .. | 96 |
| 5.4.1.1 Simulation Setup..... | 96 |
| 5.4.1.2 Simulation Results and Discussion..... | 96 |
| 5.4.2 The Two-Stage Optimal Control Strategy for a Grid-Connected Microgrid Prosumer | 98 |
| 5.4.2.1 Simulation Setup..... | 98 |
| 5.4.2.2 Simulation Result and Discussion..... | 100 |
| 5.5 Conclusion | 103 |
| Chapter 6: Conclusion and Future Work..... | 104 |
| 6.1 Summary of Findings..... | 104 |
| 6.2 Contributions..... | 104 |
| 6.3 Practical Implications..... | 105 |
| 6.4 Limitations and Future Work..... | 105 |

| | |
|--|------------|
| References | 107 |
| Appendix A: Detailed Description of Iterative Pruning | 115 |
| List of Publications by the Author | 116 |
| RESEARCH AWARDS | 118 |
| 1. IEEE PES Japan Joint Chapter Student Best Paper Award..... | 118 |
| 2. IEEE ISCIT 2021 Best Student Paper Award | 119 |
| 3. IEEE PES ISGT Europe 2021 Best Paper Award | 120 |
| 4. IEEJ Academic Encouragement Award | 121 |

List of Figures

| | |
|--|----|
| Figure 2.1. Historical Growth of Renewable Energies (World Bank Data) | 10 |
| Figure 2.2. Classification of grids by capacity..... | 12 |
| Figure 3.1. The Prosumer Model Configuration..... | 44 |
| Figure 3.2. Algorithm for MPPT and PV Curtailment..... | 49 |
| Figure 3.3. Electrical Load Model | 50 |
| Figure 3.4. Single-phase Synchronous Power Inverter..... | 54 |
| Figure 3.5. BESS SOC Operation Area Definition..... | 56 |
| Figure 3.6. EMS simulator Control Algorithm. | 57 |
| Figure 3.7. Interconnected Case Simulation setup..... | 59 |
| Figure 3.8. Prosumer Load Profiles. | 60 |
| Figure 3.9. Three-day weather data. | 60 |
| Figure 3.10. Three-day weather pattern possibilities. | 61 |
| Figure 3.11. Test Scenario 1 (Disconnected): Performance of prosumer X. | 62 |
| Figure 3.12. Test Scenario 1 (Disconnected): Performance of prosumer Y. | 62 |
| Figure 3.13. Test Scenario 2 (Disconnected): Performance of prosumer X. | 63 |
| Figure 3.14. Test Scenario 2 (Disconnected): Performance of prosumer Y. | 63 |
| Figure 3.15. Test Scenario 3 (Connected): Performance of prosumer X..... | 64 |
| Figure 3.16. Test Scenario 3 (Connected): Performance of prosumer Y..... | 64 |
| Figure 3.17. Test Scenario 4 (Connected): Performance of prosumer X..... | 65 |
| Figure 3.18. Test Scenario 4 (Connected): Performance of prosumer Y..... | 65 |
| Figure 3.19. Test Scenario 5 (Connected): Performance of prosumer X..... | 66 |
| Figure 3.20. Test Scenario 5 (Connected): Performance of prosumer Y..... | 66 |
| Figure 4.1. Basic structure of a WFNN | 71 |
| Figure 4.2. Confidence Interval Setting | 72 |
| Figure 4.3. Iterative Pruning Illustration..... | 75 |
| Figure 4.4. Iterative Pruning Strategy | 78 |
| Figure 4.5. Sunny Weather Prediction Result..... | 79 |
| Figure 4.6. Cloudy Weather Prediction Result | 81 |
| Figure 4.7. Rainy Weather Prediction Result | 82 |
| Figure 5.1. The Proposed Optimizer’s Role | 86 |
| Figure 5.2. The 2-Stage Optimization Algorithm. | 94 |
| Figure 5.3. Two-day Energy Trading Prices..... | 96 |
| Figure 5.4. 2-day Power Flow Curve..... | 97 |
| Figure 5.5. BESS SOC Over Time. | 97 |
| Figure 5.6. One Day Trading Prices. | 98 |

Figure 5.7. (a) Selling Weight vs Optimal Cost, (b) Selling Weight vs 24-hour Net Power Management Strategies 99

Figure 5.8. (a) The Stage 1 Optimal Result, (b) The Stage 2 Optimal Result 101

Figure 5.9. (a) λ vs Optimal Cost, (b) λ vs 24-hour Net Power Management Strategies 102

List of Tables

| | |
|---|-----|
| Table 2.1 Summary of Closely Related Works: Objectives and model..... | 14 |
| Table 2.2 Summary of Closely Related Works: Control parameters and features | 15 |
| Table 2.3 Recent Disaster Related Outages Worldwide | 17 |
| Table 3.1 SOC Settings for Each Prosumer | 59 |
| Table 3.2 Summary of test cases..... | 61 |
| Table 3.3 Summary of results. | 67 |
| Table 4.1 Summary of Results for Sunny Weather Prediction | 79 |
| Table 4.2 Summary of Results for Cloudy Weather Prediction..... | 80 |
| Table 4.3 Summary of Results for Rainy Weather Prediction..... | 82 |
| Table 5.1 Optimal Costs | 98 |
| Table 0.1 MAE for the Iterative Pruning Techniques for a Sunny Day..... | 115 |

Abbreviations

| | |
|-------|--|
| | |
| A | Ampere |
| AC | Alternating Current |
| ARIMA | Autoregressive Integrated Moving Average |
| BCP | Business Continuity Plan |
| BEMS | Building Energy Management System |
| BESS | Battery Energy Management Systems |
| CEMS | Community Energy Management Systems |
| CI | Confidence Interval |
| CNN | Convolutional Neural Network |
| CSC | Current Source Converter |
| DC | Direct Current |
| DER | Distributed Energy Resources |
| DNN | Deep Neural Networks |
| ECP | Electricity Continuity Plan |
| EMS | Energy Management System |
| FLS | Flexible Load Switching |
| FNN | Feedforward Neural Network |
| FVA | Fixed Value Addition |
| FVM | Fixed Value Multiplication |
| IP | Iterative Pruning |
| JEPX | Japan Electricity Market Exchange |
| JMA | Japan Meteorological Agency |
| LSTM | Long-Short Term Memory |
| HEMS | Home Energy Management System |
| MAE | Mean Absolute Error |
| MGO | Microgrid Operator |
| MILP | Mixed Integer Linear Programming |
| MOO | Multi-Objective Optimization |
| MPC | Model Predictive Control |
| MPP | Maximum Power Point |
| MPPT | Maximum Power Point Tracking |
| NCLS | Non-Critical Load Shedding |
| NLP | Non-Linear Programming |
| PCC | Point of Common Coupling |
| PCS | Power Conditioning System |
| PI | Proportional Integrator |
| PLL | Phase-locked Loop |
| PQ | Active and Reactive Power |
| PV | Photovoltaic Power |

| | |
|-------|--|
| P-V | Power -Voltage |
| PWM | Pulse Width Modulator |
| QSG | Quadrature Signal Generator |
| RDED | Robust Dynamic Economic Load Dispatch |
| RES | Renewable Energy Sources |
| RESDM | Robust Electricity Supply-Demand Manager |
| RHO | Rolling Horizon Optimization |
| RMSE | Root Mean Square Error |
| SDG | Sustainable Development Goals |
| SDG | Sustainable Development Goal |
| SOC | State of Charge |
| SOGI | Second-order Generalized Integrator |
| SSI | Single-phase Synchronous Inverter |
| TDF | Time-sequence Dynamic Feasible |
| V | Voltage |
| V-I | Voltage - Current |
| VRE | Variable Renewable Energy |
| VSC | Voltage Source Converter |
| WFNN | Weather-based Feedforward Neural Network |

Chapter 1: Introduction

1.1 Background

As the integration of renewable energy sources like solar power into modern electrical grids advances, the microgrid—a localized, decentralized energy system—has become a critical component for achieving greater energy sustainability and resilience. Despite the clear advantages of using microgrids and renewable energy, several challenges remain. Solar energy, in particular, is inherently variable due to weather conditions and the diurnal cycle, which can introduce complications in maintaining the grid's reliability and efficiency.

This variability calls for innovative solutions in energy prediction and system optimization. Solar power prediction is essential for ensuring that the energy produced by photovoltaic (PV) systems can be optimally integrated into the grid, allowing for better planning and operation. There is a significant need for accurate and reliable predictive models that can adapt to the fluctuating nature of solar energy, thereby making microgrid systems more reliable and efficient. Machine learning algorithms, especially feedforward neural networks (FNNs), have shown promise in predicting energy outputs based on historical data and real-time inputs, but there are still opportunities to improve their accuracy and computational efficiency.

The concept of a "prosumer"—an entity that not only consumes but also produces energy—has further complicated the landscape. The ability of prosumers to feed energy back into the grid demands sophisticated energy management systems (EMS) and control mechanisms, often incorporating battery energy storage systems (BESS) for better energy balancing. Control schemes for these prosumer models need to be robust, adaptive, and capable of dealing with both supply and demand-side dynamics.

Further complexities arise when considering real-time energy management in microgrids. Traditional static optimization models are insufficient as they, in some cases do not leverage recently popular prediction methods, and those that do fail to adjust dynamically to discrepancies between forecasted and actual energy production and consumption. Innovative strategies like Rolling Horizon Optimization (RHO) offer dynamic and responsive solutions for real-time energy management but are still under-explored.

It is against this backdrop of increasing renewable integration, technological innovation, and changing consumer behavior that this thesis is positioned. Utilizing advanced machine learning algorithms, optimization techniques, and simulation tools like MATLAB Simulink, this research aims to tackle these challenges comprehensively. Its primary contributions include the development of a resilient prosumer model incorporating BESS, PV systems, and EMS; a complementing iterative network pruning technique for speed, and to enhance solar power prediction accuracy; and a novel predictive optimization strategy for real-time energy management in microgrids.

The research is motivated by the increasing urgency to combat climate change and the international focus on reducing carbon emissions, as exemplified by recent pledges under the Paris Climate Agreement. Achieving greater reliability and efficiency in microgrid operations is not just an academic pursuit but a societal necessity. Hence, the research presented in this thesis has immediate and significant relevance, promising to contribute substantially to the evolution of sustainable energy systems. This research is based on our submitted peer-reviewed research journals [1], [2], and domestic and international conference articles [3]–[18].

1.2 Scope of Research

The scope of this research summarized in Fig. 1.1 is multi-faceted, encompassing three key areas essential for advancing the state of microgrid systems powered by renewable energy sources, particularly solar power. The following points outline the scope in detail:

Prosumer Models in Microgrids: This research introduces and validates a resilient prosumer model. The model proposes resilience hardening control schemes and is tailored to integrate seamlessly with existing EMS, BESS, and PV systems and modern control methods. The model's effectiveness is evaluated through simulations and case studies.

Solar Power Prediction: One of the primary focuses is on developing and optimizing predictive models for solar energy generation within microgrids. Employing machine learning algorithms and specialized techniques like Iterative Network Pruning, this research aims to improve both the accuracy and computational efficiency of solar power

forecasts. It also explores the incorporation of weather clustering algorithms to enhance prediction capabilities under varying weather conditions.

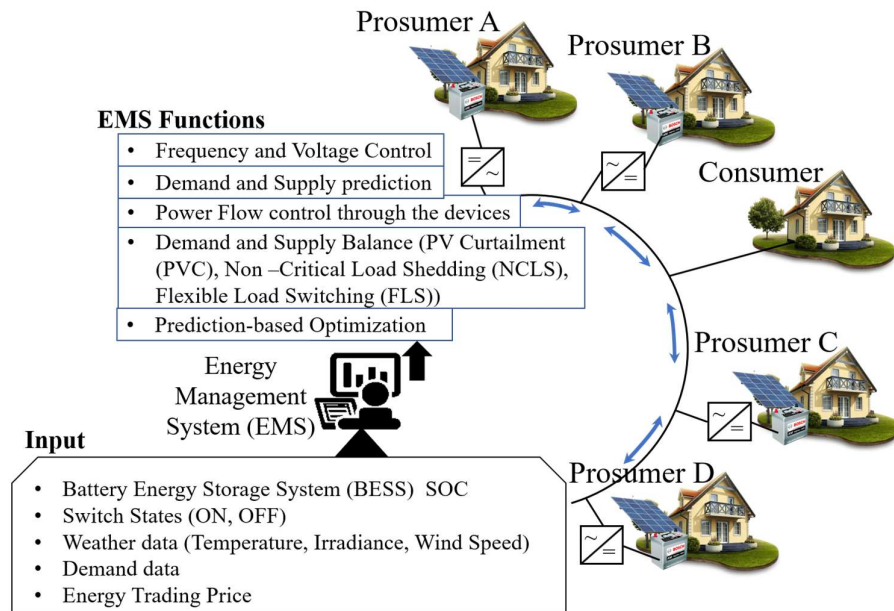


Figure 1.1 Overview of Research

Real-Time Energy Management: The scope extends to real-time energy management in microgrids, utilizing predictive RHO and two-stage optimization strategies. These strategies dynamically adjust to discrepancies between forecasted and actual energy outputs and consumptions. It offers a more robust, reliable, and flexible approach to energy management, critical for the efficient functioning of modern microgrids.

Optimization Strategies: In addition to prediction and real-time management, the research delves into advanced optimization techniques using MATLAB’s Optimization Toolbox. It includes strategies for optimal coordination and power balancing among prosumers, prioritizing critical loads and mitigating uncertainties.

Comparative Analysis: The research contrasts newly developed models and techniques with existing approaches in the field. It assesses the practical implications of the findings, identifying both strengths and limitations.

Toolset: The research extensively utilizes MATLAB Simulink for simulation and MATLAB’s Machine Learning and Optimization Toolboxes for computational analysis.

The aim is to provide a thorough, tool-supported validation of the proposed models and strategies.

Global and Environmental Context: While the technical aspects form the core of this research, it also considers the larger global context of renewable energy adoption and carbon emission reductions, tying in with international commitments like the Paris Climate Agreement.

Practical Implications: The research has been designed to be highly applicable to real-world scenarios. It aims to provide actionable insights and strategies that can be implemented in existing microgrids, thereby contributing to more reliable and efficient energy systems.

Future Work: Lastly, the research identifies potential areas for future exploration, offering a roadmap for subsequent scholarly endeavors.

This research aims to make significant contributions to the fields of renewable energy, machine learning, and optimization. In doing so, it advances the reliability and efficiency of microgrid systems, strives to contribute to the advancement of microgrid technologies, fosters the integration of renewable energy resources, and supports the development of resilient and reliable energy systems. Ultimately, this research aims to effectively meet the energy needs of communities and contribute to a sustainable future.

1.3 Research Objectives

The overarching aim of this research was to advance the reliability of prosumer-based microgrids by advancing the state-of-the-art of prosumer modeling, incorporating solar power prediction and microgrid optimization. This was achieved through the following specific objectives:

1.3.1 Develop a Resilient Prosumer Model for Enhanced Microgrid and Disaster Resilience

The objective was to create a resilient prosumer model tailored for microgrids, integrating BESS, PV systems, and an EMS to optimize energy usage and storage while facilitating the increased integration of renewable energy resources. This model was further applied to a simple radially distributed topology to enhance robustness, particularly in disaster scenarios. The aim was to enable the EMS to maintain uptime during critical post-disaster recovery periods, thereby contributing significantly to the

sustainability, resilience, and efficiency of global energy systems. Empirical validation of this integrated approach was conducted through simulations and case studies using MATLAB Simulink, demonstrating the effectiveness of the model in both standard operations and emergency situations.

1.3.2 Develop a Fast Accurate Photovoltaic Power Prediction Model

This objective aimed to create a highly accurate model for predicting the power output of PV systems under various weather conditions as part of the comprehensive resilient prosumer model. Utilizing machine learning algorithms and data-driven approaches, the research focused on optimizing prediction performance. This objective also included contrasting the developed model with existing approaches through comparative analysis and validation, thereby contributing to more efficient and reliable microgrid operation.

1.3.3 Optimize Day-Ahead and Real-time Energy Management in Microgrids

The objective was to develop and implement an optimal, resilient EMS that integrates both day-ahead and real-time strategies for microgrids. This involved employing a predictive optimization strategy to adjust for variances between forecasted and actual energy production and consumption, enhancing the dynamism and responsiveness of the EMS. Simultaneously, the focus was on optimizing day-ahead operations for grid-connected prosumer microgrids, where transactions between the grid, BESS, and non-critical load shedding were optimized based on predicted PV output power. This comprehensive approach leveraged MATLAB's Optimization Toolbox and Simulink for implementation and validation through case studies, aiming to enhance both day-ahead power security and overall microgrid reliability.

The system developed from achieving the three objectives presents a robust solution enhancing the resilience of prosumer-based microgrids. This research has made a substantial contribution to renewable energy, machine learning, and optimization disciplines. In doing so, it has facilitated the creation of microgrid systems that are not only resilient and reliable but also efficient, particularly in low and medium-voltage networks. The comprehensive Energy Management System (EMS) devised can be employed by operators to manage prosumer-based microgrid networks with greater efficiency.

1.4 Methodology

The methodology employed for this research was multi-faceted and designed to achieve the outlined research objectives. The following steps outline the methodological approach that was undertaken:

1.4.1 Data Collection

Load data was collected from different floors of the electric power and energy systems laboratory building at Hiroshima University, which followed a typical research facility profile. Weather data was also collected from the building's rooftop over various seasons, mainly focusing on summer conditions.

1.4.2 Pre-processing of Input Data

Public weather data was obtained from the Japan Meteorological Agency (JMA) website, which provided information at 1-hour intervals. Further, we selected various parameters like temperature, wind velocity, and precipitation based on their correlation with insolation, as investigated in our previous works.

1.4.3 Data Clustering

The collected past weather data was categorized into three clusters: sunny, cloudy, and rainy. This clustering facilitated the construction of weather-dedicated Feedforward Neural Networks (FNNs).

1.4.4 Prosumer Optimization Formulation

Temperature and irradiance data were used to generate a PV curve using MATLAB Simulink. Optimization decisions included the shedding of non-critical parts of the load to ensure power balance. Trading prices were sourced from the Japan Electricity Market Exchange (JEPX), which provided day-ahead pricing.

1.4.5 Mathematical Modeling and Optimization

Optimization problems were solved using MATLAB's optimization toolbox, utilizing linear programming techniques. We also tested our Rolling Horizon Optimization (RHO) against the Static Optimization Model (SOM) to adapt to real-time changes in energy demand and supply.

Through following this methodology, the research successfully contributed to the development of an effective control system for microgrid operation, enabled efficient

integration of distributed energy resources, and enhanced the resilience and reliability of microgrids in power networks.

1.5 Contributions

This research serves as a comprehensive extension of the authors' preceding master's degree research, substantially enriching the existing body of work in the field of prosumer models and microgrid systems. Below are the notable contributions of this research:

1.5.1 A Resilient Prosumer Model with Embedded EMS

The study develops an exhaustive MATLAB-based prosumer model that includes PV generation, BESS, and an electricity load system connected to the grid equipped with a real-time EMS simulator capable of adapting to local generation or external supply, with a monitoring system for operational efficiency. The model incorporates:

- Flexible Load Switching (FLS), adapting to local generation or external supply as needed.
- Integration of specialized functions like PV curtailment (PVC) to prevent over-generation and DC bus voltage control through a Proportional Integrator (PI) controller.
- A non-critical load shedding (NCLS) function that adds a layer of power security to the system.
- Real-time monitoring and alert systems that employ a color-coding scheme for each operating mode.

1.5.2 Computational Efficiency, Robustness and Accuracy

The methodology used for this research stands out for its computational efficiency, achieved using Linear Programming (LP) and iterative pruning-based PV forecasting. This allows for robust and flexible operations and is well-suited for sensitivity analysis and adaptability. The use of WFNNs for the prediction methodology as well as leveraging the prediction output through the proposed optimization method, harmonized with real-time data significantly improves the computation accuracy.

The research not only theorizes but also empirically validates the model through extensive practical implementation and experimentation, proving its advantages in energy cost reduction, PV power prediction accuracy, and system adaptability.

Through leveraging innovative optimization techniques and real-time data handling, this research lays the foundation for more efficient, flexible, and cost-effective energy systems, aligning with the global shift toward sustainability.

1.5.3 Novelty

The unique aspect of this study is its capacity to integrate real-time and day-ahead uncertainties using limited publicly available data for optimal microgrid operational control. Unlike traditional methods, the approach here successfully blends energy predictions, market dynamics, and user preferences into a unified framework. This is enabled by the proposed flexible prosumer model that enables the integration of these advanced control methods.

This research has significantly advanced the field, particularly in the development of robust and adaptive systems capable of mitigating the challenges faced by contemporary energy models by encompassing these contributions.

1.6 Organization of the Thesis

The thesis's research methods, findings, and comparative analyses are meticulously detailed below across seven chapters that include,

Chapter 1: This chapter lays the groundwork for the research by introducing the significance of microgrids and renewable energy, particularly solar power. It outlines the challenges tied to the unpredictability of solar power and presents the research objectives, methodologies, and contributions of this thesis.

Chapter 2: This chapter elucidates key concepts and definitions, such as what constitutes a microgrid, photovoltaic power, neural networks, and other terms pertinent to the research. This chapter then delves into existing literature concerning microgrids, photovoltaic systems, solar power prediction techniques, and optimization strategies in microgrids. The aim is to identify gaps in current research that this thesis aims to fill.

Chapter 3: This chapter focuses on the resilience of prosumer models within microgrids. It discusses various control schemes, including battery energy storage systems, photovoltaic systems, and energy management systems. The chapter also includes case studies and simulations to demonstrate the effectiveness of resilient prosumer models.

Chapter 4: An approach to solar power prediction is proposed based on Weather-based feedforward neural networks (WFNNs) followed by an iterative pruning (IP) technique to reduce the computational burden. The chapter also explores how to provide confidence intervals to increase the reliability of predictions.

Chapter 5: This chapter presents advanced optimization techniques to improve microgrid operation. It includes predictive optimization for energy management systems and discusses optimal coordination and power balancing among prosumers. Case studies focusing on a grid-connected prosumer along with simulations and results, demonstrate the efficacy of the proposed optimization techniques.

Chapter 6: This final chapter synthesizes the contributions of the thesis, summarizing key findings and making recommendations for future research endeavors.

Integrating advanced machine learning algorithms, MATLAB-driven simulation, and optimization techniques within a multi-disciplinary framework, this research serves as a crucial advancement in the fields of solar power prediction and microgrid optimization. It plays a key role in fostering more reliable and efficient microgrid operation, which is vital for the global shift toward sustainable energy systems.

Chapter 2: Literature Review and Basic Concepts

2.1 Microgrid and Photovoltaic Systems

The global energy landscape is undergoing a rapid transformation as indicated by statistics [19]–[22]. This accelerated transformation is driven by multiple factors, including massive population growth that is rapidly accelerating the depletion of traditional fossil-fuel energy resources and industrial expansion. Faced with these rising demands for energy, countries worldwide are setting ambitious goals for sustainable energy production, in alignment with the Sustainable Development Goals (SDGs) [23]. A noteworthy example is the Indian government, which has set a robust target to achieve 175 GW of renewable energy capacity. This ambitious goal is backed by initiatives from the Ministry of New and Renewable Energy and the National Institution for Transforming India [19]. These developments underscore the urgency and commitment to transition from fossil fuels to renewable energy sources [19]. Various countries, including Japan which has set its net-zero emission target for 2030 [24] are undertaking similar strides in line with the SDGs.

In recent years, there has been a marked increase in research and implementation of microgrid systems and PV technology. These technologies serve as pivotal elements in the global push towards sustainable energy solutions, contributing not only to energy

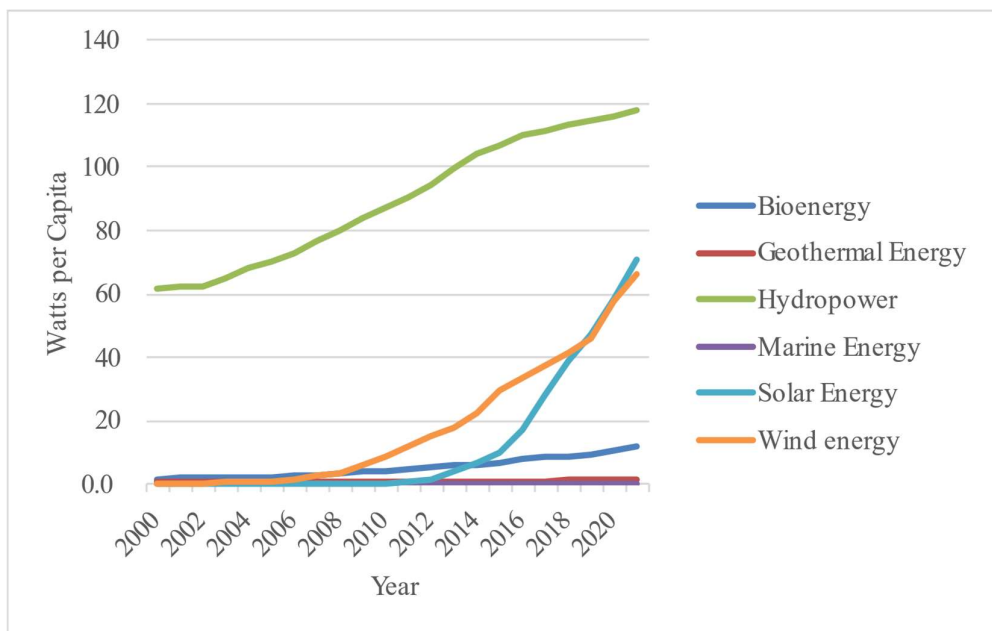


Figure 2.1. Historical Growth of Renewable Energies (World Bank Data)

security but also to improved living standards. Microgrids and PV systems are particularly relevant for remote and underserved regions, offering a decentralized approach to energy provision that aligns well with sustainable development objectives.

The data in World Bank statistics (Fig. 2.1) from [25] adds empirical weight to this focus on renewables, showcasing a 21-year growth trend in Watts per Capita from 2000 to 2021. While various renewable energy technologies like Bioenergy, Geothermal Energy, and Hydropower have shown some growth, solar energy (PV) emerges as a standout. Starting from a zero baseline in 2000, it has reached an extraordinary 71 Watts per Capita by 2021. This rate of growth is unparalleled when compared to other forms of renewable energy, even including the mature and established hydropower sector, which has shown only modest, linear growth over the same period.

This exponential growth in solar energy not only testifies to its established viability but also implies enormous untapped potential. Solar energy's ability to scale so impressively within just two decades points to its transformative capacity accelerated by advances in research that have focused on increasing its PV output efficiency as well as reducing its cost. This remarkable trajectory of PV systems serves as a compelling signal for its future potential, especially in a world that is urgently seeking ways to mitigate the impact of climate change through rapid decarbonization. Therefore, prioritizing solar energy in research agendas, as in this thesis, promises to deliver sustainable, high-impact solutions in the renewable energy sector.

2.1.1 Definition and Scope of Microgrids

The term "microgrid" refers to an integrated system that includes distributed energy resources (DERs), such as renewable energy sources, loads, and battery energy storage systems (BESSs), functioning cohesively as controllable units [26], [27]. A microgrid is a localized energy system that can operate independently or in conjunction with the main power grid. The scope of a microgrid can vary, ranging from simple, small-scale systems to more complex, large-scale setups. Some literature [28], [29] has used the terms 'microgrid' and 'minigrid' interchangeably. However, various authors agree that the distinction often lies in the size and capability of the DERs involved. Since a standardized classification for microgrids based on capacity or capability is currently lacking, this study attempts in [2], to categorize microgrids in terms of capacity, size, and capability in relation to a power system in, as illustrated in Figure 2.2.

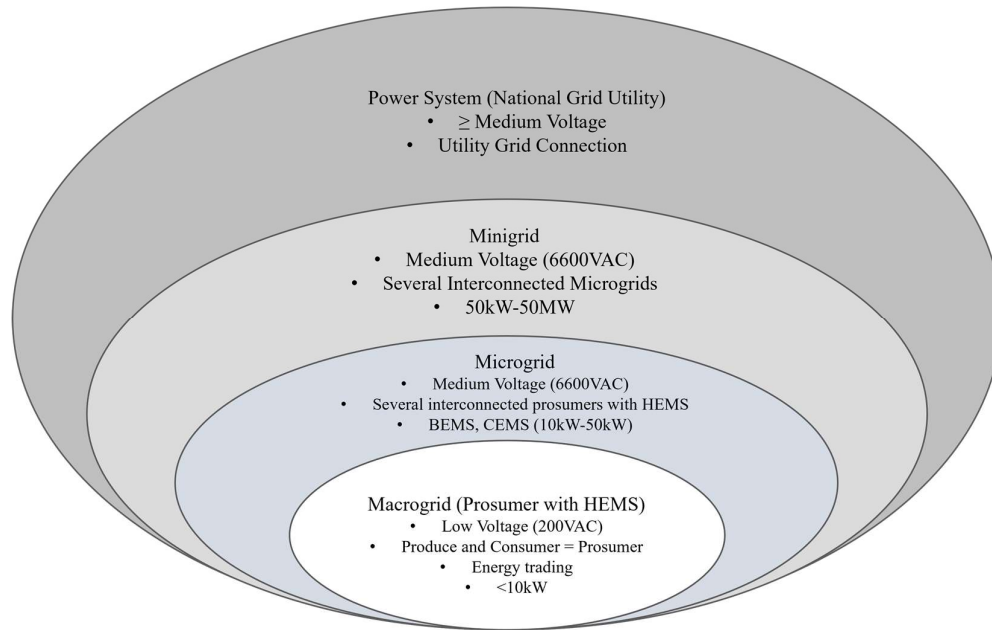


Figure 2.2. Classification of grids by capacity

The classification of grids based on capacity has been refined to incorporate various types, ranging from nanogrids to microgrids and minigrids, each serving different capacities and functionalities. This section further classifies these grids based on their voltage levels, specifically as per the Japan power system.

Nanogrid: Situated at the foundational tier of distributed energy systems, nanogrids predominantly comprise Home Energy Management Systems (HEMS). These are specialized, low-capacity installations, typically with a capacity of less than 10kW, designed for residential energy management. Nanogrids can function autonomously or be connected to a localized private grid. Significantly, for the framework of this study, a HEMS that possesses the capability for bi-directional power flow with its associated private grid earns the designation of a 'prosumer.' Operating at Low Voltage tiers, specifically 200VAC, prosumers in a nanogrid don't just consume electrical energy; they are also capable of generating it. The source of this generation is often renewable, typically hailing from solar panels or wind turbines. Furthermore, such prosumers can partake in energy trading activities, thereby transforming the nanogrid into an interactive, dynamic energy ecosystem.

Microgrid: Functioning at Medium Voltage levels, denoted as 6600VAC, microgrids are networks that consist of multiple interconnected prosumers, each equipped with their individual HEMS. With a typical capacity range of 10kW to 50kW,

microgrids offer an array of advanced features beyond the scope of nanogrids. These encompass energy trading, demand response mechanisms, and the seamless integration of renewable energy sources. Terms like Building Energy Management Systems (BEMS) and Community Energy Management Systems (CEMS) are frequently used as synonyms or specific instances of microgrids.

Minigrid: Also functioning within the Medium Voltage range of 6600VAC, minigrids serve as an aggregation of multiple microgrids, effectively forming a more complex network. With capacities generally ranging from 50kW to 5MW, minigrids provide an enhanced level of energy management, resilience, and operational efficiency. What distinguishes them further is their capability to connect to national utility grids, thereby augmenting their resilience and efficiency.

Power System (National Grid Utility): These are expansive, large-scale grid infrastructures that function at Medium Voltage levels or even higher. These complex systems serve as the backbone for the broad-scale distribution of electrical energy. Typically managed by national or regional utility corporations, these grids are pivotal in maintaining a stable and reliable electricity supply for large geographic areas.

This classification is essential for understanding the varying capacities and functionalities of these different grid types, especially in the context of renewable energy integration and the emerging prosumer models.

2.1.2 Challenges in Microgrid Deployment

As the integration of DERs into microgrids becomes more prevalent, researchers in [30]–[32], have identified a series of significant challenges that must be addressed to ensure the successful deployment and operation of these energy systems. These, among others, are described by Farrokhhabadi et. al and Dragicevic et. al in [27], [33], [34] as follows:

Voltage and Frequency Fluctuations: Microgrids face voltage and frequency fluctuations due to the integration of DERs with varying output. These fluctuations can lead to voltage sags, swells, and frequency deviations, impacting the stability of the microgrid. To mitigate this challenge, advanced voltage and frequency regulation

Table 2.1 Summary of Closely Related Works: Objectives and model

| References | Objectives | Model | | | |
|---------------------|---|-------------|----------|----------------------|----------------|
| | | PV and BESS | VSC Type | Load | Grid Connected |
| [64] | Load scheduling for a reduced bill | ✓ | Average | Active | ✓ |
| [65] | Load scheduling for a reduced bill | ✓ | Average | Active | ✓ |
| [66] | Increase uptime | ✓ | Average | Mixed 1 | ✗ |
| [67] | Load scheduling for a reduced bill | ✓ | Average | Active | ✓ |
| [68] | Demand and supply balance | ✓ | Detailed | Active | ✗ |
| [69] | Demand and supply balance | ✓ | Detailed | Active | ✗ |
| [100] | Demand and supply balance | ✓ | Detailed | Mixed ^{1,2} | ✓ |
| [101] | Demand and supply balance | ✓ | Detailed | Mixed ¹ | ✗ |
| [102] | Demand and supply balance | ✓ | Average | Mixed ¹ | ✓ |
| [103] | Power flow control by day-ahead scheduling | ✓ | Detailed | Mixed ² | ✓ ³ |
| [104] | System stability by treating BESS thermal constraints | ✓ | Detailed | Active | ✗ |
| [94] | System stability in grid-forming applications | ✓ | Detailed | Mixed ² | ✓ |
| The proposed method | Energy preservation during low generation periods | ✓ | Average | Mixed ² | ✓ |

devices, such as smart inverters and grid-forming controllers, are employed to maintain the desired power quality within acceptable limits as described by the researchers [2] in Table 2.1 and Table 2.2. These tables attempt to compare the research that is closely related to this thesis.

Phase Mismatches: Phase mismatches can occur when DERs and loads within the microgrid have different phase angles. This misalignment can result in phase imbalances that affect the overall system performance. The cause lies in the heterogeneous nature of DERs and loads. Mitigation strategies include phase synchronization techniques and the use of power electronic converters to align the phases of different components, ensuring a balanced and synchronized microgrid operation is reiterated in [35].

To achieve this goal, various types of Phase-Locked Loops (PLLs) have been suggested by different researchers to synchronize the injected current with the grid voltage. These methods encompass a range of approaches, including the time delay PLL, inverse park transform PLL, enhanced PLL, and second-order generalized integrators (SOGI)-PLL, among others. Among these options, the SOGI-based PLL stands out, particularly in single-phase applications, due to its ability to reject harmonics effectively, deliver high precision, and respond quickly to changes in the grid [36], [37].

Table 2.2 Summary of Closely Related Works: Control parameters and features

| References | Control parameters and features | | | | Disaster Consideration |
|------------------------|-------------------------------------|-------------------|------------------|-------------------|------------------------|
| | Voltage/Frequency/ Phase Control | Energy Sharing | Load shedding | PV Curtailment | |
| [64] | N/A | ✗ | ✓ | ✓ | ✗ |
| [65] | N/A | ✗ | ✓ | ✓ | ✗ |
| [66] | ✗ | ✗ | ✓ | ✓ | ✗ |
| [67] | N/A | ✓ | ✓ | ✓ | ✗ |
| [68] | ✓ | ✗ | ✓ | ✓ | ✗ |
| [69] | ✓ | ✗ | ✗ | ✗ | ✗ |
| [100] | ✓ | ✗ | ✗ | ✗ | ✗ |
| [101] | ✓ | ✗ | ✗ | ✗ | ✗ |
| [102] | ✓ | ✗ | ✗ | ✗ | ✗ |
| [103] | ✗ | ✗ | ✗ | ✗ | ✗ |
| [104] | ✓ | ✗ | ✗ | ✗ | ✗ |
| [94] | ✓ | ✓ | ✗ | ✗ | ✗ |
| The proposed method | ✓ | ✓ | ✓ | ✓ | ✓ |

However, it's worth noting that the quadrature signal generator (QSG)-SOGI can still exhibit instability when its input signal contains frequency harmonic currents and other harmonic elements, as discussed in [38]. Hence, the authors of this article have introduced the double SOGI-QSG PLL to align the phase angle of the generated current with the prosumer supply voltage. The double QSG configuration is favored for its enhanced ability to reject harmonics while preserving simplicity [39], making it well-suited for rapid responses during switching events and grid fluctuations, which is essential for extended-duration simulations.

Supply-Demand Imbalances: Variability in DER output, load changes, and intermittent renewable energy sources contribute to supply-demand imbalances in microgrids. These imbalances can manifest as overloading or underutilization of energy resources, affecting reliability. Advanced forecasting, real-time monitoring, and demand response programs are essential for managing these imbalances. Energy storage systems also play a vital role in storing excess energy during surplus periods and releasing it during high-demand phases, ensuring a reliable microgrid operation.

Integration of Energy Storage: While energy storage is a key solution to many challenges, its integration introduces challenges of its own, such as battery degradation and limited capacity. These challenges can lead to reduced energy storage system (ESS) efficiency and lifespan. To address this, researchers and practitioners focus on optimizing ESS operation through advanced control algorithms, predictive maintenance strategies, and innovative battery technologies to maximize ESS reliability and longevity as listed in Table 2.1 and Table 2.2.

Islanding Detection: Microgrids should seamlessly transition between grid-connected and islanded modes. However, detecting islanding events accurately remains a challenge. False detection can disrupt power supply, while missed detection can endanger grid workers. The cause of this challenge lies in the need for rapid and precise detection mechanisms. Advanced algorithms, including rate of change of frequency and voltage stability indices, are employed to enhance islanding detection accuracy, ensuring a safer and more reliable microgrid operation.

These challenges and their respective mitigations are pivotal aspects of microgrid deployment and operation, aiming to enhance their reliability, stability, and overall performance.

2.1.3 Resilience in Microgrid Systems

The term "resilience" is defined as a system's ability to be flexible, robust, adaptable, and resourceful, with predictive capabilities [40], [41]. In the context of microgrids, resilience is especially important for preventing system collapse during unplanned outages [42]–[46] such as recorded in Table 2.3, which are increasingly being caused by natural disasters, faults, and cyber-attacks. Researchers in [40], [41], [47], [48], detail the immense losses incurred by the affected communities. In the event of a disaster, these researchers cast light on the lack of resilient power systems characterized by emergency backup systems to grid power supply.

Authors of the international standard in [49] discuss the importance of city service continuity during disasters, particularly focusing on maintaining essential services that rely on electricity. To cope with the loss of grid power during emergencies, organizations need to create Business Continuity Plans (BCP) and Electricity Continuity Plans (ECP). These plans ensure the least disruption in services by outlining backup electricity sources and coordination methods among different organizations.

Table 2.3 Recent Disaster Related Outages Worldwide

| Area | Disaster type | Date | Duration of Restoration |
|----------------------|---------------|----------------|-------------------------|
| South Australia | Tornado | September 2016 | About 26 hours |
| Hawaii (Oahu Island) | Earthquake | October 2006 | About 19 hours |
| Hokkaido, Japan | Earthquake | September 2018 | About 45 hours |
| New Jersey, US | Hurricane | October 2012 | Several weeks |
| Fukushima, Japan | Earthquake | March 2011 | > 1 year |
| Uganda | Flooding | April 2020 | 2 days |

The standard emphasizes that to manage the risks associated with power outages due to calamities, organizations should adopt Business Continuity Plans (BCP). Within these BCPs, a specific focus should be given to Electricity Continuity Plans (ECP). BCPs help organizations prepare for electricity supply disruption by prioritizing crucial services and establishing backup power sources. On the other hand, ECPs are integrated within the BCPs and zero in on the intricacies of sustaining electricity supply.

The BCP might differ from one city to another, depending on their specific needs. For instance, it might only cover a portion of a city, or span a broader area, extending beyond city boundaries. The ECP, on the other hand, provides detailed protocols on how to maintain electricity supply for vital city services during and after disasters such as

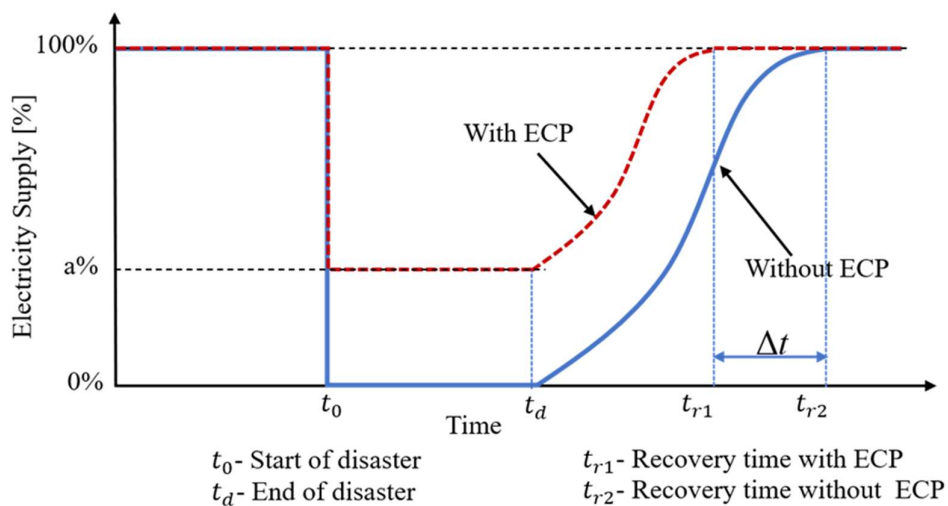


Figure 2.3 The Role of ECP

described in Fig. 2.3. These plans can be tailored for different organizational levels, ranging from an entire city to individual facilities.

Both BCPs and ECPs are instrumental in ensuring that cities can maintain a minimum level of essential services when faced with electrical disruptions due to disasters. These plans provide guidelines for preparing and responding to such scenarios, making sure that both service providers and citizens are well-equipped to handle emergencies.

The resilience of a microgrid is often bolstered by various system components that contribute to the overall reliability of microgrid systems that lie in the following categories:

- **Redundancy and Distributed Generation:** Microgrids incorporate multiple distributed energy resources, such as solar panels, wind turbines, and energy storage systems, ensuring a diversified and redundant energy supply. Commonly BESS's are used to store excess energy for use during periods of high demand or low supply. These systems are critical to the resilience and reliability of a microgrid. The State of Charge (SOC) of a BESS can serve as an indicator for guaranteed output power, which is vital for decision-making in energy management systems within a microgrid.
- **Control and Management Systems:** Advanced control and management systems enable microgrids to autonomously disconnect from the main grid during disruptions, reconfigure energy sources, and balance supply and demand.
- **Communication Infrastructure:** Robust communication networks facilitate real-time monitoring and control of microgrid components, allowing for swift response to disturbances.
- **Grid Interaction:** The ability to switch between grid-connected and islanded modes is essential for microgrid resilience, as it ensures energy supply even when the main grid is compromised.

Despite their potential, microgrid systems face various challenges and vulnerabilities in achieving resilience:

The unpredictable nature of the weather which directly affects renewable energy production is a major source of control challenges, including demand and supply balance

issues as well as system characteristic instabilities. Various researchers have proposed various solutions, some of which are described in Table 2.1 and Table 2.2, to mitigate this challenge that include stochastic optimization, infrastructural adaptation, and machine learning-based solutions among others.

Traditional power grids are generally centrally monitored and controlled. However, the distributed nature of microgrids has resulted in the need for decentralized control systems that are reliant on communication systems if they are to be centrally coordinated. As microgrids become increasingly reliant on digital technologies, they are susceptible to cyber-attacks that can disrupt their operations as noted in [50]. These authors reiterate the need for cybersecurity in grid operations and discuss promising approaches to this effect.

The cost of implementing microgrid systems can also be a barrier to widespread adoption, especially in remote or underserved areas. Additionally, inconsistent regulatory frameworks and policies may hinder the integration of microgrids into existing energy infrastructures. Control strategies are therefore required to mitigate these challenges and are further described in the next section.

2.1.4 Microgrid Control Strategies

Microgrid control strategies play a pivotal role in the efficient and reliable operation of microgrid systems. These strategies encompass a wide array of techniques and approaches designed to manage the generation, distribution, and consumption of electrical energy within a microgrid environment as reviewed by the authors in [51], [52]. As the integration of DERs and renewable energy sources (RES) continues to grow, the importance of robust control strategies becomes increasingly evident. Microgrid control strategies serve several critical functions:

- **Energy Management:** Microgrid control systems are responsible for optimizing the allocation of electrical energy within the system. They decide when and where to generate, store, or distribute energy based on factors such as demand, resource availability, and cost [32], [42]. Optimization techniques are employed to schedule and allocate energy resources efficiently in microgrids. Linear programming, mixed-integer linear programming, and other optimization methods to minimize energy costs, reduce greenhouse gas emissions, and maximize the utilization of renewable energy sources.

-
- **Grid Stability:** Maintaining stable voltage and frequency levels is crucial for the reliable operation of a microgrid. Control strategies that employ algorithms such as proportional-integral-derivative (PID) control, model predictive control (MPC), and fuzzy logic control monitor and adjust these parameters to ensure the quality of electricity supplied to consumers.
 - **Integration of DERs:** Microgrids often incorporate various DERs, including solar panels, wind turbines, and energy storage systems. Control strategies orchestrate the seamless integration of these resources to maximize their utilization.
 - **Grid-Connected and Islanded Modes:** Microgrids can operate in grid-connected mode, relying on the main grid for support, or in islanded mode, operating autonomously. Control strategies enable smooth transitions.
 - **Real-time Monitoring:** Real-time monitoring is crucial for effective energy management in microgrids such as the integration of advanced metering infrastructure, sensor networks, and data analytics techniques to collect and analyze real-time data on energy generation, consumption, and storage. Real-time monitoring enables accurate load forecasting, detection of anomalies, and adaptive control strategies to ensure optimal energy management in dynamic operating conditions.

Despite their significant advantages, microgrid control strategies face several challenges:

- **Complexity:** Microgrids are inherently complex systems with diverse DERs, different operational modes, and varying consumer demands. Developing control algorithms that can handle this complexity while ensuring optimal performance is a significant challenge as expressed in Table 2.1 and Table 2.2.
- **Synchronization:** Coordinating the operation of DERs with different characteristics, such as solar and wind resources, can be challenging. Synchronization control methods are essential to ensure harmonious operation [36], [37].

-
- **Grid-Forming and Grid-Following Control:** Microgrids must seamlessly switch between grid-forming control (operating autonomously) and grid-following control (synchronizing with the main grid). Achieving smooth mode transitions is a critical control challenge.
 - **Cybersecurity and Resilience:** With the increasing digitization of microgrid control systems, cybersecurity threats pose a significant risk. Protecting control systems from cyberattacks and ensuring resilience are ongoing challenges, especially related to rationality between central or distributed control strategies. In accordance with findings presented in [53], it has been noted that interconnected systems present several benefits in comparison to standalone systems. These advantages encompass enhanced resilience and decreased energy losses, resulting in cost savings through resource sharing. Notably, the resilience attribute of Distributed Energy Resources (DERs) plays a pivotal role in averting power system failures, whether they are planned or unplanned, as elucidated in [42].

A summary of related research in Table 2.1 and Table 2.2 shows that researchers and industry experts are actively addressing these challenges through innovative control strategies and technologies. Topology adaptation and advanced control algorithms, including model predictive control (MPC) and hierarchical control schemes, are being developed to manage the complexity of microgrids effectively. Also, Synchronization techniques, such as PLLs and synchronization controllers, are being employed to coordinate the operation of diverse DERs seamlessly. There are also efforts focused on improving grid-forming and grid-following control, enabling microgrids to operate reliably in both connected and islanded modes. Other researchers are proposing robust cybersecurity protocols, intrusion detection systems, and continuous monitoring are being implemented to protect microgrid control systems from potential threats.

2.1.5 The Robust Electricity Supply-Demand Manager (RESDM)

In the quest for resilient and sustainable energy systems, the Electric Power and Energy Systems Laboratory (Hiroshima University) research team has designed an intricate Robust Electricity Supply-Demand Manager (RESDM), as depicted in Fig. 2.4. This RESDM aims to serve as a comprehensive control platform for energy systems ranging from singular building units to isolated island grids. Central to this endeavor are

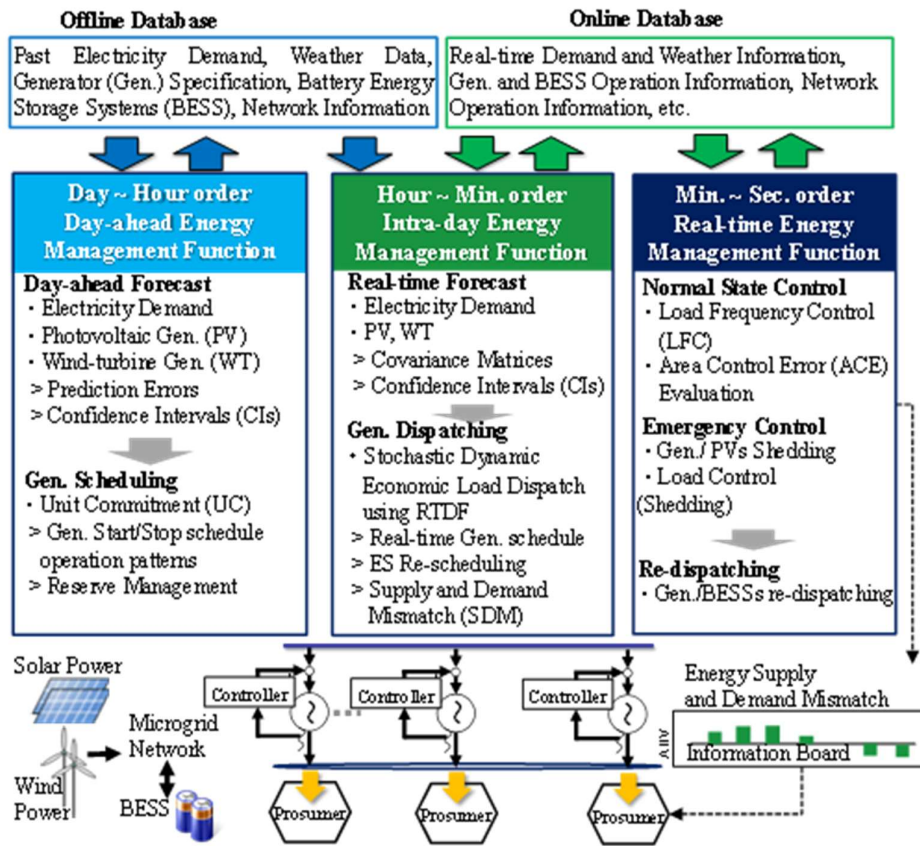


Figure 2.4 The Robust Electricity Supply-Demand Manager (RESDM)

the synergistic applications of Variable Renewable Energies (VREs) such PV and wind turbines, along with BESSs, conventional generators, and diverse load demands. The controller is architecturally structured across a three-tiered control hierarchy, thereby facilitating real-time operations, intra-day adjustments, and day-ahead planning] [8], [54], [55].

The RESDM amalgamates advanced supply-demand control algorithms that are firmly rooted in both real-time monitoring and predictive analytics. Specifically, the system exploits forecasts of VREs, and load demands to adjust the operations of controllable generators and BESSs [8], [54], [55]. A robust and economical grid monitoring mechanism, termed as the Time-sequence Dynamic Feasible Domain (TDF), further augments this adaptive control [56]–[58]. Notably, the RESDM is equipped with an offline database that ensures operational integrity even during online connectivity interruptions by relying on a minimal dataset gleaned from historical information.

Intricately woven into the RESDM's architecture is a localized energy trading model, serving as a micro-electricity market. This market-oriented approach aims to maximize the social welfare of the microgrid while ensuring reliable operations. It opens the avenue for more dynamic, market-based interactions among generators, customers, and prosumers within the networked microgrid environments.

The merits of the RESDM can be encapsulated in several key points:

i) The real-time surveillance of the generator's feasible region enhances the resilience of the system, thereby minimizing the risks associated with power outages

ii) A unique bidding mechanism is integrated into the Microgrid Operator's market operations division. This allows generators to optimize their profits while ensuring that customers and prosumers can secure electricity at economically viable rates [56]–[58].

iii) Utilizing Neural Networks for PV forecasting, the system takes into account uncertainties by incorporating confidence intervals (CIs) that are directly applied to day-ahead and intra-day operations [56].

iv) Economic power generation scheduling and Robust Dynamic Economic Load Dispatch (RDED) are enabled through a TDF region approach, providing an effective countermeasure to potential supply-demand imbalances [57], [58].

In light of the burgeoning trend of prosumer engagement catalyzed by the green energy revolution and emergent energy markets, the RESDM additionally incorporates a peer-to-peer energy management control strategy for networked microgrids operating in off-grid modes. This has been verified through a series of supply-demand simulations conducted on a representative microgrid system, confirming the RESDM's capabilities in advancing reliable and sustainable energy systems.

The multifaceted RESDM thus represents a paradigm shift in how microgrid operators can effectively manage complex energy systems, ensuring a harmonious balance between supply, demand, and social welfare, whilst navigating the challenges and uncertainties inherent in modern energy landscapes. This thesis's scope is a component of this RESDM.

2.2 Renewable Energy and Prosumer Models

As the global community grapples with the challenges of climate change and resource depletion, the traditional paradigms of energy production and consumption are

undergoing a radical transformation [21]. This section delves into two interlinked themes at the forefront of this transformation: the increasing prominence of renewable energy sources and the evolving role of electricity consumers as 'prosumers.' By synthesizing existing literature and building upon key advancements in these areas, we aim to paint a comprehensive picture of the current state and future potential of renewable energy and prosumer models.

2.2.1 The Rise of Renewable Energy

The push towards renewable energy resources, particularly solar, wind, and hydro-electric, has garnered significant attention in recent years. This heightened focus is driven by a variety of factors: government initiatives for reducing carbon footprints, public awareness of climate change, and the advancing technological landscape that has rendered renewable energy systems more efficient and cost-effective [19]–[22]. With increased awareness and technological maturity, renewable energy resources have transitioned from being marginal players to becoming central to many discussions about future energy systems.

2.2.2 Concept of the Prosumer in Renewable Energy Systems

A pivotal advancement in the realm of renewable energy systems is the concept of the "prosumer"—a term amalgamating 'producer' and 'consumer.' Unlike traditional energy consumers who merely consume electricity from the grid, prosumers produce their energy, often using small-scale renewable installations like rooftop solar panels or wind turbines. Prosumers are not just end-users but active participants in the energy landscape, contributing to distributed generation and even selling excess power back to the grid [14], [27], [59].

Various prosumer models have evolved, responding to different community needs, technological availabilities, and economic conditions as described [60], [61]. These models can be broadly categorized into:

- **Residential Prosumers:** Individual households equipped with renewable energy generation capabilities, often solar PV systems.
- **Commercial Prosumers:** Businesses or commercial spaces that produce their electricity, often for internal consumption and occasionally selling surplus power.

-
- **Community-Based Prosumers:** A community-centered model where residents pool resources to establish a larger renewable energy system benefiting the entire community.
 - **Industrial Prosumers:** Large industries that establish renewable energy resources not just to cater to their demand but also to supply to the grid.

It is noteworthy that the existing body of literature on prosumer models predominantly centers on the business and energy trading aspects of the concept, often neglecting critical technical dimensions. Specifically, the focus tends to be skewed towards market operations, economic incentives, and mechanisms for energy exchange, while overlooking the intricate technicalities associated with systems parameter maintenance, such as voltage regulation, frequency stabilization, and grid resiliency. Such an orientation may lead to a gap in understanding the full scope and potential of prosumer models, particularly when it comes to ensuring optimal functionality and reliability of these decentralized energy systems. It thus becomes imperative to extend scholarly attention towards the engineering challenges and solutions inherent to prosumer-based energy systems, in order to provide a more comprehensive, balanced, and actionable framework for both research and practical implementation.

This thesis focuses on delivering a more comprehensive model based on simulation. Simulation models for microgrids often use approximate average value models to mimic real system characteristics [62]. These models assist in resolving common issues related to system installation, such as human errors, inconsistencies, costs, and time factors. Therefore, developing simplified yet accurate models can be extremely beneficial for the design and testing phases.

2.2.3 Literature Review: Renewable Energy and Prosumer Models

In this intricate tapestry of renewable energy and prosumer models, we delve into the pertinent literature that informs our research. Works by various scholars, cited in references [27], [33], [34], provide comprehensive overviews of microgrid architectures, including the widely-accepted single-bus topology, and introduce the prosumer model—often couched in terms like Home Energy Management Systems (HEMS) or residential microgrids. A cross-sectional examination of relevant models, as summarized in Tables 1 and 2, offers valuable insights into research closely aligned with our objectives, typologies, and critical control parameters.

An insightful work by Arani et al. [63] accentuates the growing significance of residential prosumer models within the context of low and medium-voltage distribution networks. Such observations substantiate our research's emphasis on a single-phase approach for inverter and load modeling. Existing literature, as encapsulated in Tables 1 and 2, often overlooks single-phase models, preferring to focus on more complex three-phase systems. This gap in the literature lends credence to our chosen methodological approach.

Furthermore, our review highlights the limited attention given to complex load model designs, specifically those incorporating mixed and partitioned loads for refined load management strategies. While some researchers, cited in references [64], [65], do integrate load shedding within their algorithms, only Michaelson et al. [66] provide a nuanced load-shedding strategy that segregates loads into critical and non-critical categories. However, the practical applicability of their model remains debatable due to their reliance on arbitrary load profiles.

Interestingly, our analysis reveals that the objectives driving various research projects often pre-determine the design of their microgrid and prosumer models. Studies in references [64], [65], [67], geared towards minimizing electricity costs, often neglect important system characteristics, thereby compromising the accuracy of their control algorithms. Such oversights are particularly evident in works featuring Voltage Source Controllers (VSCs) [68], [69] and those focused on long-duration pricing models that disregard inherent system characteristics.

Lastly, we observe a noticeable gap in the literature concerning the integration of energy sharing and disaster preparedness within prosumer model designs [67]. With the rise of community energy markets and the increasing frequency of natural disasters, these aspects are no longer peripheral but central to any robust and resilient prosumer model. Therefore, our proposed model aims to address these overlooked areas by incorporating advanced load management techniques, comprehensive control mechanisms, and considerations for quick disaster recovery.

2.3 Solar Power Prediction Techniques

Solar power prediction has become an indispensable part of grid management and energy planning, especially with the increasing contribution of renewable energy

resources [70]–[73]. Accurate forecasting techniques are essential for operational scheduling, grid reliability, and integrating solar energy into utility systems.

2.3.1 Basics of Solar Power and Its Predictability

Solar power, harnessed from the sun's rays, is a clean, renewable energy source. Photovoltaic cells, often assembled in panels, capture sunlight and convert it into electricity. The amount of electricity generated is contingent on the intensity of sunlight, which varies due to several factors:

- Daily solar cycles
- Seasonal changes
- Local weather conditions, including cloud cover, temperature, and humidity.

Predicting the generated power is essential for efficient microgrid operation, ensuring stability, and optimizing energy storage and distribution.

While various forecasting methods exist, summarized in Fig. 2.5, machine learning-based strategies, weather-based clustering feedforward neural networks commonly known as wavelet fuzzy neural networks (WFNNs), and iterative pruning techniques have proven to be highly promising. This section delves into these advanced approaches, examining their relevance to microgrid systems and larger grid operations.

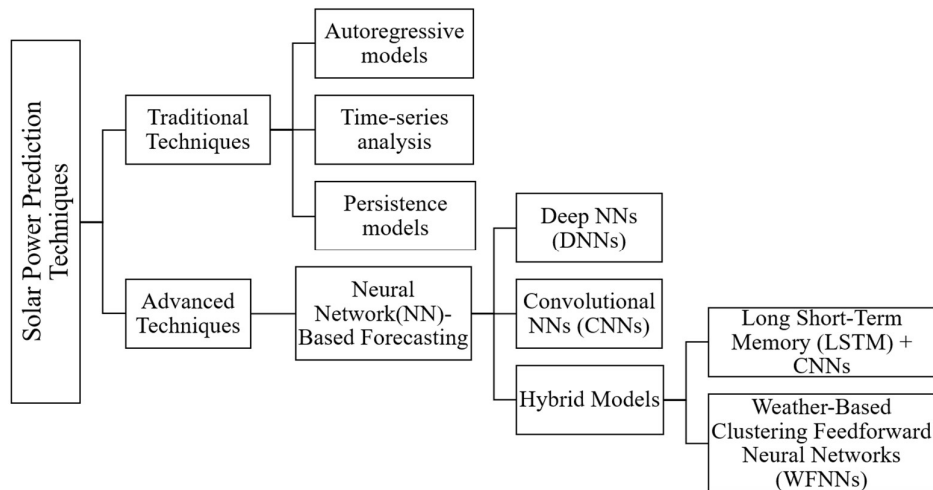


Figure 2.5 Summary of the Solar Power Prediction Techniques

2.3.2 Traditional Techniques and Their Limitations

Before focusing on machine learning-based strategies, it's important to acknowledge the existence of traditional techniques like autoregressive models, time-series analysis, and persistence models. While effective to some extent, authors in [74] contend that these traditional methods often fall short in capturing the non-linear relationships between weather variables and solar power output.

Autoregressive models leverage past values to predict future data points. These models are statistically rigorous and have been useful in capturing temporal trends. However, their primary limitation is their linear assumption, which often fails to capture the nonlinear interactions between various factors affecting solar power generation, such as solar irradiance, cloud cover, and temperature.

Time-series analysis is another well-established method that generally employs historical data to forecast future values. Techniques like ARIMA (Autoregressive Integrated Moving Average) are commonly used [75]. The strength of time-series analysis lies in its capability to model seasonal trends and other temporal structures. Nevertheless, its predictive accuracy diminishes with abrupt changes in environmental conditions, such as unexpected weather events, making it less reliable for short-term solar power forecasting in dynamic settings.

Persistence models serve as perhaps the simplest form of solar power prediction, where the power output at a future time is assumed to be the same as the most recent observation. While these models are computationally inexpensive and straightforward to implement, they are often considered naive approaches. Their limitation is glaringly evident when there are rapid fluctuations in power output due to changing weather conditions, making them unsuitable for anything beyond very short-term forecasts.

Each of these traditional methodologies has its merits, but they are constrained by the complexities and the highly dynamic nature of solar power generation. They tend to struggle with abrupt changes, nonlinearity, and the influence of multiple interacting variables, shortcomings that machine learning techniques are increasingly being designed to address. Therefore, while traditional models offer valuable insights and have served as stepping stones in the evolution of forecasting methodologies, there is a growing consensus on the need to transition toward more sophisticated techniques capable of capturing the nuanced factors affecting solar power output [75].

2.3.3 Neural Network-Based Forecasting

Neural network-based forecasting methods, particularly deep neural networks (DNNs) [76], [77] and convolutional neural networks (CNNs) [78], mark a significant advancement in the domain of solar power output prediction [74], [75]. These architectures excel at capturing the complex, nonlinear relationships between variables, something that traditional models often fail to achieve. Hybrid models that integrate CNNs with long short-term memory networks (LSTMs) applied in [79], [80] have further pushed the boundaries, demonstrating unprecedented accuracy in solar power forecasting.

However, this performance comes at the cost of computational complexity. DNNs comprise multiple layers of interconnected nodes, necessitating a large number of parameters to be trained. The training process involves iterative optimization algorithms that adjust these parameters based on loss functions, which can be computationally expensive. CNNs, tailored for image and sequence data, employ multiple filters and pooling layers, further adding to the complexity. In hybrid models combining CNNs and LSTMs, the intricacies multiply. LSTMs are designed to remember patterns over long sequences, which involves complex transformations and the maintenance of a cell state across sequences. This results in an increase in the number of computations needed for both the forward and backward passes during training and inference.

The necessity for extensive computational resources becomes particularly challenging for real-time forecasting applications. Real-time prediction demands low-latency, high-throughput computational performance, which may be compromised by the time-consuming calculations required by advanced neural networks. Consequently, the computational intensity of these models becomes a limiting factor, particularly in settings where rapid decision-making is paramount or where computational resources are constrained.

2.3.4 Weather-Based Clustering Feedforward Neural Networks (WFNNs)

Weather-Based Clustering Feedforward Neural Networks (WFNNs) present an innovative methodological development in the realm of solar power prediction, particularly offering advantages over both traditional statistical models and more general neural network-based approaches. The WFNNs model capitalizes on the idea of

segmenting weather conditions into distinct categories—such as sunny, cloudy, and rainy—and then employs specialized feedforward neural networks (FNNs) tailored for each category [3], [4], [56], [75].

A WFNN is an artificial neural network in which connections between nodes are weighted. It's primarily utilized for prediction tasks. The formula representing the WFNN is:

$$y = f(W \times x + b) \quad (2.1)$$

Where:

- y is the output.
- W represents the weight matrix.
- x is the input.
- b is the bias.
- f is an activation function.

For solar power prediction, the input can be historical solar power data, weather conditions, and other relevant parameters. The network learns from this data, adjusts its weights and biases to minimize prediction error, and can then forecast future solar power outputs.

2.3.5 Advantages Over Traditional Methods

The most notable advantages of WFNNs over traditional approaches include:

- 1) **Enhanced Accuracy:** One of the primary shortcomings of traditional methods, such as time series analysis and autoregressive models, is their limited capacity to account for nonlinear and abrupt changes in weather conditions. By clustering weather conditions, WFNNs are capable of addressing this limitation. The specialized FNNs can be intricately tuned to the peculiarities of each weather condition, thereby enhancing predictive accuracy.
- 2) **Domain-Specific Adaptability:** While traditional models often rely on generalized assumptions and linear approximations, the WFNN approach allows for domain-specific customizations that can capture the complex, nonlinear dynamics unique to each weather condition.

-
- 3) **Data Efficiency:** Traditional models can suffer from data inefficiency when they attempt to generalize across diverse weather conditions. WFNNs, by contrast, allow for more effective utilization of available data by segmenting it into meaningful categories.

2.3.6 Advantages Over General Neural Network-Based Approaches

The most notable advantages of WFNNs over NN-based approaches include:

- 1) **Computational Efficiency:** Compared to complex architectures like DNNs, CNNs, and hybrids like CNN-LSTM, feedforward neural networks are generally less computationally intensive. By segmenting weather conditions and using specialized but simpler FNNs, WFNNs can offer a compromise between computational cost and predictive power.
- 2) **Interpretability:** General neural network models, especially deep architectures, are often criticized for being "black boxes" that offer limited insights into their decision-making processes. In contrast, the simpler architecture of FNNs and the logic of weather-based clustering make WFNNs more interpretable, facilitating easier model validation and troubleshooting.
- 3) **Real-time Forecasting:** One of the key challenges with advanced neural network models is their computational intensity, which hinders their applicability in real-time forecasting scenarios. The relatively simpler FNNs used in WFNNs are quicker to train and deploy, thus offering an advantage in real-time, low-latency applications.
- 4) **Model Specialization:** The use of specialized FNNs for each weather condition allows for fine-tuned model performance, making it possible to capture subtleties and nuances that generalized models might overlook.

In summary, WFNNs offer a balanced and innovative approach to solar power forecasting by effectively bridging the gap between traditional statistical models and advanced neural network-based methods. They leverage the strengths of neural networks for capturing complex patterns while addressing some of their limitations, such as computational intensity and lack of interpretability [3], [4], [56]. This makes WFNNs a compelling alternative that merits further exploration and validation in the continually evolving landscape of solar power forecasting methodologies.

2.4 Optimization Techniques in Microgrids

The optimization of energy systems, particularly in microgrids, is an essential subject that has attracted significant attention in the last decade. The increased adoption of renewable energy sources like PV systems and the growing need for resilience against disasters have necessitated more sophisticated methods of energy management. However, the effectiveness of a microgrid's operation hinges on its optimization techniques, which should address critical areas like energy cost, power security, and operational resilience. This section will delve into existing optimization techniques in microgrids. A summary of reviewed optimization techniques is presented in Fig. 2.6.

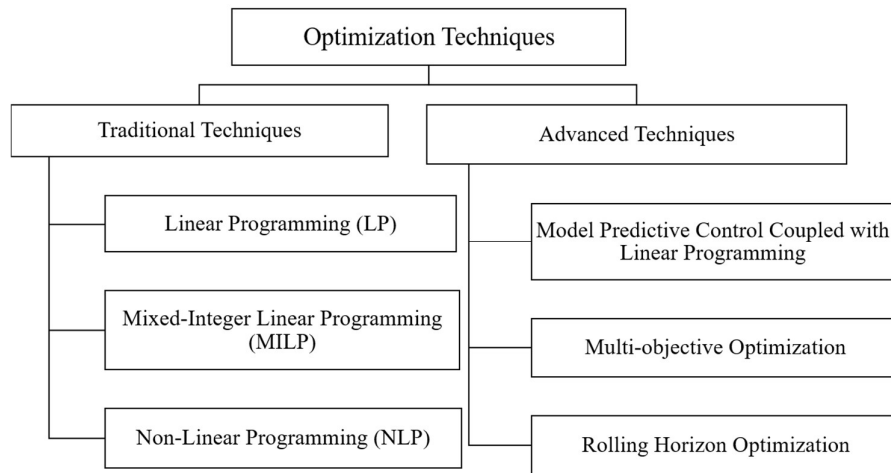


Figure 2.6 Summary of the Reviewed Optimization Techniques

2.4.1 Traditional Optimization Techniques

2.4.1.1 Linear Programming (LP)

LP is one of the earliest optimization techniques applied to microgrids. It involves linearizing all the objective functions and constraints to simplify models [81], [82]. The technique is computationally efficient, making it suitable for systems where the optimization variables exhibit linear behaviors. However, the linearization process can lead to approximations that are not representative of the true system dynamics, particularly for systems that incorporate renewable energy sources which have non-linear characteristics [83].

2.4.1.2 Mixed-Integer Linear Programming (MILP)

An extension of LP, MILP incorporates integer variables to handle scenarios such as unit commitment, where the decision variable is either on or off [84]. While MILP is powerful and can represent more complex systems than LP, it suffers from high computational loads as observed by the authors in [85], making it unsuitable for real-time or near-real-time optimization scenarios.

2.4.1.3 Non-Linear Programming (NLP)

Non-Linear Programming is used when the objective function or any of the constraints are non-linear. NLP is advantageous when dealing with complex system behaviors like those involving PV and BESS. However, the complexity comes at a cost: NLP algorithms require higher computational resources and are prone to getting stuck in local optima, failing to find the global optimum [82].

Traditional optimization techniques, although robust for certain applications, exhibit shortcomings when employed in dynamically changing microgrids with a high penetration of renewable resources. These techniques often require perfect or near-perfect forecasts of energy demand and supply. In the context of increasingly frequent and unpredictable disasters, these methods are particularly weak, lacking the agility to adapt to rapidly changing scenarios.

2.4.2 Need for Advanced Techniques

The limitations of traditional methods have given rise to advanced optimization techniques that can adapt to real-time changes and forecast uncertainties. They emphasize the need for methods that can provide more reliable and flexible solutions. Thus, there is a shift towards using predictive approaches like Rolling Horizon Optimization and Model Predictive Control, which not only manage the complexity of the system but also handle uncertainties in a more robust way [82], [86].

2.4.2.1 Model Predictive Control Coupled with LP

Model Predictive Control (MPC) operates by utilizing a model of the system to predict its future behavior over a certain horizon. The control inputs are then optimized using LP to meet a set of objectives while adhering to constraints. The most significant advantage of MPC is its ability to handle multi-variable systems and constraints explicitly. The method calculates optimal control inputs in real-time, enabling the system to adapt dynamically to varying conditions. The concept explanation follows:

Let:

- $x(t)$ be the state of the system at time t
- $u(t)$ be the control input at time t
- $y(t)$ be the output of the system at time t
- N be the prediction horizon
- J be the objective function to minimize, often a quadratic cost function
- A , B , and C be matrices that describe the system dynamics

Usually, the system dynamics are given by a state-space representation:

$$x(t + 1) = Ax(t) + Bu(t) \quad (2.2)$$

$$y(t) = Cx(t) \quad (2.3)$$

The objective function J is defined to quantify how well the system is performing. It is often a quadratic function of states and control inputs over the prediction horizon N :

$$J = \sum_{k=0}^{N-1} (y(t+k|t) - r(t+k))^2 + \lambda u(t+k|t)^2 \quad (2.4)$$

Here, $r(t+k)$ is the reference signal, and λ is a weighting factor that determines the trade-off between control effort and tracking performance.

In the context of LP, the objective function and the constraints are written in a linear form. If the system is linear and the cost function can be approximated as linear, then the optimization problem can be defined as:

$$\text{Minimize } J \quad (2.5)$$

Subject to: Subject to:

$$Ax(t+k|t) + Bu(t+k|t) = x(t+k+1|t) \quad (2.6)$$

$$y(t+k|t) = Cx(t+k|t) \quad (2.7)$$

Constraints on $u(t+k|t)$ and $x(t+k|t)$

Here, $x(t+k|t)$ and $u(t+k|t)$ are the predicted state and control input at time $t+k$ given the information available at time t .

The resulting algorithm is as follows:

1. Measure the current state $x(t)$

-
2. Solve the LP optimization problem to minimize J
 3. Apply the first element of the optimal control sequence $u^*(t)$
 4. Update $t \rightarrow t+1$
 5. Repeat

By using LP, the computational burden is often reduced, making real-time application feasible. Additionally, constraints can be explicitly incorporated into the optimization problem, allowing for more robust control.

Therefore, LP within the MPC framework serves to simplify the optimization problem, making it computationally more efficient. When coupled with MPC, LP allows for the integration of system constraints directly into the optimization problem. This provides a more accurate and reliable solution, as compared to traditional methods that often involve post-optimization adjustments to meet system constraints.

2.4.2.2 Multi-objective Optimization

The complexity of microgrid management necessitates consideration of multiple, often conflicting, objectives like cost efficiency, resilience, and power security. Multi-objective optimization employs techniques such as Pareto optimality to find a set of solutions that satisfy these objectives to the greatest extent possible, without overly compromising any single one. This is especially valuable when preparing for or responding to varying or unforeseen conditions such as natural disasters [82].

The concept of the multi-objective optimization follows:

- Let x be the decision variables, which could include parameters like the amount of energy to buy/sell, generator output levels, etc.
- Let $f_i(x)$ be the i^{th} objective function that maps the decision variables to a real-valued outcome. For example, $f_1(x)$ might represent cost, $f_2(x)$ might represent resilience, and $f_3(x)$ might represent power security.

The objective is function requires maximization or minimization which in vector form, this can be represented as:

$$\frac{\text{Minimize}}{\text{Maximize}} \mathbf{F}(x) = [f_1(x), f_2(x), \dots, f_m(x)] \quad (2.8)$$

Here, m is the number of objectives. An important that some objectives may need to be minimized while others maximized, which complicates the problem.

The solver intends to find a solution x^* , considered Pareto optimal if there's no other x such that $f_1(x)$ is better than $f_i(x^*)$ for all i , without making at least one $f_j(x)$ worse. Mathematically, x^* is Pareto optimal if:

$$\nexists x: f_i(x) \leq f_i(x^*), \forall i \text{ and } f_j(x) \leq f_j(x^*), \exists j \quad (2.9)$$

Constraints $g(x)$ and $h(x)$ can also be added to ensure feasibility:

$$g(x) \leq 0 \quad (2.10)$$

$$h(x) = 0 \quad (2.11)$$

The Multi-objective Optimization solver algorithm follows the following steps to obtain the optimal solution.

1. Define the objective functions than $f_i(x^*)$ and constraints $g(x)$, $h(x)$.
2. Choose an optimization algorithm suited for the problem.
3. Run the algorithm to find a set of Pareto optimal solutions.
4. The result is a Pareto front, a set of policies x from which a decision can be made based on the current situation and objectives.

In practice, multi-objective optimization often employs algorithms that can consider various objectives in the same optimization run. These algorithms can use LP, mixed-integer programming, or even more complex methods like genetic algorithms and neural networks. The outcome is a set of optimized policies that can be adapted based on the current situation and objectives.

2.4.2.3 Rolling Horizon Optimization

Rolling horizon optimization (RHO) is a dynamic optimization technique particularly useful for systems with non-stationary or uncertain parameters. Unlike traditional optimization methods that make decisions based on a fixed planning horizon, RHO continuously updates the planning horizon as new data becomes available. This "rolling" mechanism enables the system to adapt to new information and changes in the environment, thereby enhancing its flexibility and responsiveness [86].

In the context of microgrid management, RHO can be especially useful for optimizing parameters like energy storage levels, supply schedules, and demand-side management strategies [87], [88]. The rolling horizon allows for real-time adjustments based on actual energy generation and consumption data, making it more robust against uncertainties like sudden changes in weather conditions affecting renewable energy generation or unexpected fluctuations in demand.

Mechanically, RHO solves an optimization problem over a specified horizon but only implements the decision for the first period. After advancing time by one period and obtaining updated data, the model then re-optimizes over a new horizon that "rolls" forward by one period. This process is repeated continuously, ensuring that decisions are always based on the most up-to-date information.

Below the explanation of the concept of the rolling horizon optimization technique:

- **Definitions**

- Let $x(t)$ be the state of the system at time t
- Let $u(t)$ be the control input at time t
- Let N be the length of the optimization horizon
- Let $J(t)$ be the objective function to minimize at time t , often a cost function
- Let A, B, C be matrices describing the system dynamics

Similar to earlier models, the system dynamics can be described as:

$$x(t + 1) = Ax(t) + Bu(t) \quad (2.12)$$

$$y(t) = Cx(t) \quad (2.13)$$

The objective function $J(t)$ is typically defined over a finite horizon N and needs to be minimized:

$$J(t) = \sum_{k=0}^{N-1} f(x(t+k|t), u(t+k|t)) \quad (2.14)$$

Here, f could be any function representing the cost or utility of the system, which can change with time.

The RHO algorithm would function as follows:

1. **Initialization:** Start at $t = 0$ and measure the initial state $x(0)$

2. **Optimization:** At each time t :

- Solve the optimization problem over the horizon $[t, t + N]$ to minimize $J(t)$

$$\text{Minimize } J(t) \quad (2.15)$$

Subject to:

$$Ax(t + k | t) + Bu(t + k | t) = x(t + k + 1 | t) \quad (2.16)$$

where $k = 0, 1, \dots, N - 1$

- Additional constraints (if any) on x and u

$$g(x(t + k | t), u(t + k | t)) \leq 0 \quad (2.17)$$

$$h(x(t + k | t), u(t + k | t)) = 0 \quad (2.18)$$

3. **Implementation:** Apply only the first control input $u^*(t)$ from the optimal sequence found.
4. **Update:** Increment t by one period and update the state $x(t)$ based on new data.
5. **Repeat:** Go back to the Optimization step and solve the new problem over the updated horizon $[t, t + N]$.

Through continuous updates to the optimization problem with a rolling horizon, RHO allows the system to be more responsive and adaptive to changes and uncertainties in the environment.

RHO offers the following advantages over traditional optimization methods.

- 1) **Adaptability:** The rolling horizon allows the model to adjust its optimization strategies as new data becomes available, making it highly adaptable to changing conditions.
- 2) **Precision:** By using the most recent data, RHO can be more accurate in its predictions and, consequently, its optimization results.
- 3) **Resilience:** The continuous updating mechanism allows RHO to be responsive to sudden changes, such as unforeseen disasters, providing an additional layer of resilience to the microgrid system.

-
- 4) Computational Efficiency: While it might seem that RHO would be computationally intensive due to its iterative nature, the optimization over a limited horizon makes the individual problems more tractable than solving a single, large-scale optimization problem.

Therefore, in the context of microgrid management, this mathematical framework enables you to continually update energy storage levels, supply schedules, and demand-side management strategies based on real-time data, enhancing robustness against uncertainties like fluctuating renewable energy generation and demand.

2.4.3 Justification for Chosen Approaches

The advanced techniques discussed above, namely Model Predictive Control, multi-objective optimization, and rolling horizon optimization, collectively present a compelling toolkit for microgrid optimization. These methods are particularly well-suited for complex, uncertain, and dynamically changing environments commonly found in disaster-prone areas.

Both MPC [55], [89] and RHO [86], [87] offer high degrees of adaptability, allowing for real-time adjustments based on current data. This feature is critical for optimizing microgrid operations, especially when encountering unforeseen changes or disasters. Additionally, the use of LP in MPC and the iterative nature of RHO bring about a higher level of precision in optimization results, as well as computational efficiency. These advanced methods contribute to the microgrid's resilience, making them robust against uncertainties in both supply and demand scenarios. The ability to effectively address multiple objectives—such as minimizing cost while maximizing resilience and power security—makes these techniques stand out as holistic solutions for complex microgrid management problems.

Thus, the selected approaches not only individually offer advantages over traditional methods but also synergize well when used together, providing a multifaceted framework for optimizing microgrid operations.

2.5 Gaps in the Current Literature

In this section, we identify key limitations and gaps in the existing body of literature related to the comprehensive design for enhancing resilience in prosumer-based microgrid operations. The thesis endeavors to bridge crucial gaps in the current literature,

primarily focusing on three significant areas for enhancing resilience in prosumer-based microgrid operations.

2.5.1 Modeling for Resilience

One of the significant gaps in the literature pertains to the absence of comprehensive modeling approaches tailored to the unique characteristics of prosumer-based microgrid operations. Existing models often overlook the dynamic nature of prosumer behavior, the integration of diverse energy sources, and the real-time interactions between consumers and producers within microgrids. Our thesis contributes to filling this modeling gap by introducing an advanced prosumer model [2], [11], [14], [17]. This model incorporates crucial elements, including PV generation, BESS, and partitioning of loads for more efficient load management in the implemented Flexible load switching (FLS) function, allowing it to adapt dynamically to supply and demand conditions. Furthermore, it integrates specific characteristic functions, such as PV curtailment (PVC) and DC bus voltage control, improving its accuracy and reliability.

Effective decision support systems tailored to prosumer-based microgrids are often underrepresented in the existing literature. Current tools may not fully integrate real-time data, advanced analytics, and user-centric interfaces, limiting the ability of operators to make informed decisions. To address this gap, our thesis focuses on designing and implementing a real-time monitoring, observation, and alert warning system, featuring a color-coding scheme for each operating mode. These systems provide operators with actionable insights, enabling proactive responses to challenges and uncertainties and ultimately enhancing microgrid resilience.

Furthermore, a noticeable gap in the literature concerns the integration of energy sharing and disaster preparedness within prosumer model designs [67]. With the rise of community energy markets and the increasing frequency of natural disasters, these aspects are no longer peripheral but central to any robust and resilient prosumer model. Therefore, our proposed model aims to address these overlooked areas by incorporating advanced load management techniques, comprehensive control mechanisms, and considerations for quick disaster recovery.

Current studies often fall short in considering the intricate interdependencies between technical, and economic factors that profoundly influence resilience. The inclusion of FLS and NCLS in the EMS Simulator construction allows for improved operational

control in the incidence of grid connections and disconnections while maintaining system stability [2].

2.5.2 PV Forecast Methodology

Existing forecasting methods generally apply a "one-size-fits-all" approach without considering variations in weather conditions. This limitation affects the accuracy of the predictions, especially under fluctuating weather conditions. The thesis delves into the development and validation of Weather-Based Clustering Feedforward Neural Networks (WFNNs). These specialized networks segment weather conditions into distinct categories (e.g., sunny, cloudy, rainy) and optimize prediction models for each, thereby enhancing forecasting accuracy [3].

Although neural networks offer enhanced predictive capabilities, they often suffer from high computational costs, making them less viable for real-time applications or constrained computational resources. For example, despite their effectiveness, WFNNs are computationally intense, making them resource-intensive. This is particularly problematic for microgrid systems that require real-time prediction capabilities. This thesis explores the use of iterative pruning techniques to selectively eliminate less useful neurons in the network. The aim is to reduce computational load without compromising the accuracy of the model, thereby enhancing its utility in real-time applications [4]. A number of researchers have investigated improvement of the learning computation efficiency by using pruning method [90]–[92].

Many existing studies neglect the problem of overfitting, which leads to poor model generalization. Additionally, there is a limited focus on assessing the reliability of these models, especially in a microgrid setting. The thesis investigates the use of regularization terms (L1 and L2) and Confidence Intervals (CIs) to improve the model's robustness and provide a metric for assessing the reliability of the predictions, particularly beneficial for energy management in microgrids.

2.5.3 Optimization Methodology

The existing literature on microgrid optimization exhibits a notable gap in real-time adaptability, resilience, and multi-objective optimization, particularly in environments with dynamic changes in energy supply and demand. While traditional methods such as linear and mixed-integer LP have their merits, they often fall short in fluctuating and disaster-prone conditions. These methods struggle to balance multiple objectives like

cost minimization, power security, and system resilience, especially in the wake of unpredictable events like natural disasters. Additionally, current research either focuses on predictive accuracy or optimization, rarely marrying the two into a comprehensive EMS.

This thesis bridges these gaps by introducing advanced optimization techniques including Model Predictive Control (MPC), multi-objective optimization, and Rolling Horizon Optimization (RHO) that leverage PV prediction data for more accurate day-ahead planning. The proposed EMS is centered around a prosumer model for grid-connected microgrids, which can also function autonomously in the event of grid failures. Through the use of a predictive LP algorithm, the EMS generates an initial SOC that both secures power for critical loads and optimizes the costs involved, thereby achieving a multi-objective balance [93].

The integration of RHO with PV prediction data offers the system an even greater level of adaptability and precision. This is especially invaluable in disaster-prone environments, as it provides the system with the resilience required to adapt to rapidly changing conditions. The predictive approach ensures the microgrid can adapt to real-time changes in supply and demand, optimizing for various objectives without compromising on any.

2.6 Conclusion

As the energy landscape continues to evolve, renewable energy systems and prosumer models stand as vital components of a sustainable future. While challenges remain, the ongoing research, technological innovations, and policy initiatives point toward an increasingly decentralized, democratized, and sustainable energy system.

This thesis aims to make substantial contributions by addressing several critical gaps in the existing literature on microgrid operations and solar power prediction. By developing an optimized, weather-segmented neural network model, a comprehensive prosumer model, and an adaptable resilience assessment framework, the research provides advanced decision support systems for microgrid management. These elements are integrated using advanced optimization techniques and predictive elements, thereby advancing the understanding and implementation of resilient, efficient, and robust prosumer-based microgrid operations in volatile and unpredictable environments.

The work offers a balanced framework that marries accuracy with computational efficiency, making it particularly applicable for both solar power prediction and microgrid management.

Chapter 3: A Resilient Prosumer Model for Microgrids

3.1 Introduction

In recent years, the traditional centralized electrical generation system has faced numerous challenges, including inefficiencies, reliability issues, and environmental concerns. A growing body of research, including the authors' previous works [1], [2], [5]–[8], [10]–[12], [14], [15], [17], points toward decentralized energy systems as a viable solution. These prosumer models, where consumers can also produce energy, are at the forefront of this paradigm shift. This chapter introduces a robust and flexible prosumer model designed for seamless integration into microgrids. The primary motivation is to enhance sustainability, energy security, and economic viability in energy systems.

3.2 The Prosumer Model and Control Scheme

Fig. 3.1 illustrates the configuration of the prosumer model that has been adopted for this research. The setup comprises a PV system equipped with maximum power point

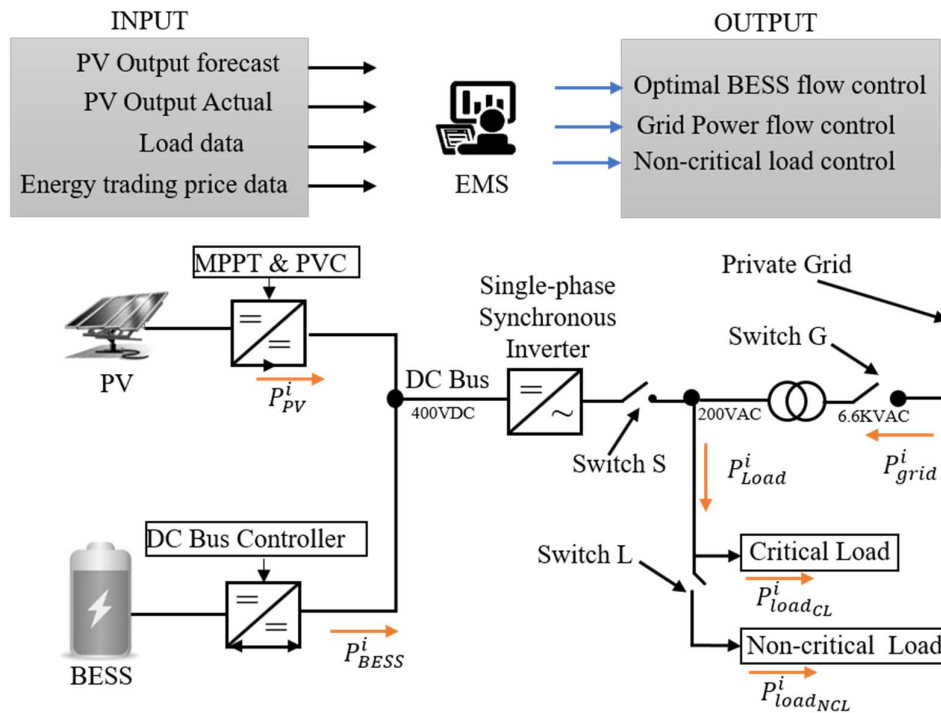


Figure 3.1. The Prosumer Model Configuration

tracking (MPPT) control, serving as the primary power source. In addition, there is a battery energy storage system (BESS) designed to store surplus energy and maintain the DC bus voltage at a consistent 400 Vdc reference level, to which both the PV system and BESS are connected. The diagram in the figure shows the inclusion of various converters to facilitate these functions.

Initially, a unidirectional DC-DC converter of the boost type is employed to elevate the voltage produced by the PV system to match the 400 Vdc reference voltage of the DC bus. A bidirectional DC-DC converter, using a buck-boost configuration, allows for two-way power flow between the BESS and the system.

The conversion of the DC bus voltage, set at 400 Vdc, to an output of 200 Vac at a frequency of 60Hz is achieved through a single-phase voltage source converter (VSC) synchronous inverter, as documented in reference [94]–[97]. This voltage is then used to supply a customizable single-phase load, which can be divided into non-sheddable critical loads and sheddable non-critical loads using switch L, corresponding to the NCLS function.

Furthermore, the proposed prosumer model has the capability to connect with other prosumers through a private line or grid, allowing for bidirectional sharing of energy via an ideal transformer. The functionality of switch S implements the FLS function, enabling the flexibility to satisfy demand either locally or from the private line, depending on the operational mode. Meanwhile, switch L continues to execute the NCLS function as described.

3.2.1 Battery Energy Storage System (BESS)

BESS's act as the cornerstone of the prosumer model. They allow for the storage of excess energy generated from renewable sources for later use, enhancing the grid's resilience and reliability. In this study, we introduce a BESS which consists of the battery, its bidirectional DC-DC converter, and a DC bus controller. The DC bus governed by a Proportional Integrator (PI) controller that effectively regulates the DC bus voltage, ensuring optimal charging and discharging cycles.

3.2.1.1 Battery Model Adopted by BESS

The battery model is adopted from MATLAB/Simulink. This MATLAB Simulink model represents the behavior of a lead-acid battery, a common energy storage device,

for use in various applications. The model accounts for both discharge and charge dynamics and includes an accurate SOC tracking mechanism.

The voltage model of the lead acid battery is modelled as follows:

- Discharge Model ($i^* > 0$):

$$V_{batt_{dch}} = E0 - K * \left(\frac{Q}{Q-it}\right) * i^* - K * \left(\frac{Q}{Q-it}\right) * it + Laplace^{-1}\left(\frac{Exp(s)}{Sel(s)*0}\right) \quad (3.1)$$

- Charge Model ($i^* < 0$):

$$V_{batt_{ch}} = E0 - K * \left(\frac{Q}{it + 0.1 * Q}\right) * i^* - K * \left(\frac{Q}{Q-it}\right) * it + Laplace^{-1}\left(\frac{Exp(s)}{Sel(s)*\frac{1}{s}}\right) \quad (3.2)$$

In these equations:

- $V_{batt_{dch}}$ and $V_{batt_{ch}}$ represent the battery voltage during discharge and charge, respectively, in volts (V).
- $E0$ is the constant voltage, in V.
- $Exp(s)$ is the exponential zone dynamics, in V.
- $Sel(s)$ represents the battery mode. $Sel(s) = 0$ during battery discharge, $Sel(s) = 1$ during battery charging.
- K is the polarization constant, in V/Ah, or polarization resistance, in Ohms.
- i^* is the low-frequency current dynamics, in A.
- i is the battery current in amperes (A)
- it is the extracted capacity, in Ah.
- Q is the maximum battery capacity, in Ah.

The battery SOC is updated according to:

$$SOC_{t+1} = SOC_t - \frac{(i * dt)}{Q} \quad (3.3)$$

Where:

- SOC_{t+1} represents the updated SOC, which is a fraction of the battery's maximum capacity.
- SOC_t is the previous SOC.

- dt is the time step, typically measured in seconds (s).

The above SOC update equation relates to a single battery. When all the batteries are aggregated to form the BESS, the BESS SOC SOC_{BESS}^i at time t for prosumer i is defined by;

$$SOC_{BESS}^i(t + 1) = SOC_{BESS}^i(t) + \Delta P_{BESS}^i(t) / BESS_{Cap}^i \quad (3.4)$$

Where:

- $SOC_{BESS}^i(t + 1)$ represents the updated SOC, which is a fraction of the battery's maximum capacity $BESS_{Cap}^i$ in kW.
- $SOC_{BESS}^i(t)$ is the previous BESS SOC.
- $\Delta P_{BESS}^i(t)$ is the change in the BESS Power, either through charging, or discharging the BESS.

3.2.1.2 DC Bus Control Scheme in BESS

The BESS is connected to the DC bus through a bidirectional DC-DC converter. A PI controller is integrated into the BESS system to manage the DC bus voltage dynamically. This configuration allows the BESS to either charge or discharge, thus either supplying power to the DC bus or drawing power from it to maintain the 400V DC reference voltage. The PI controller continuously measures the voltage on the DC bus and compares it with the reference voltage to generate an error signal. This signal then drives the control actions. This controller minimizes voltage fluctuations, enabling a more stable and reliable operation.

A typical PI controller can be represented by the following mathematical equation:

$$U(t) = K_p \cdot e(t) + K_i \int_0^t e(\tau) d\tau \quad (3.5)$$

Where $U(t)$ is the control signal, $e(t)$ is the error signal, K_p and K_i are the proportional and integral gains, respectively.

In MATLAB Simulink, the PID Controller block can be configured to operate as a PI controller by setting the derivative gain to zero. This block can be connected to measure the DC bus voltage and compute the control signal to manage the charging and discharging operations of the BESS through the bidirectional DC-DC converter.

Various performance metrics such as settling time, overshoot, and steady-state error can be analyzed to demonstrate the effectiveness of the PI controller in maintaining the DC bus voltage close to its reference value. By fine-tuning the proportional and integral gains, the controller can be optimized for fast response and minimal steady-state error, thus ensuring the robustness and reliability of the overall system.

The PI controller is an effective tool for managing the complex interactions between various components connected to a DC bus in a hybrid energy system. In this thesis, the PI controllers employed are tuned arbitrarily to achieve optimum operation setting.

3.2.2 Photovoltaic System Architecture and Control Algorithms

This section describes the PV system architecture and control algorithms the includes the MPPT function as well as the PV curtailment whose control algorithm depicted by Fig. 3.2.

3.2.2.1 Modeling of the PV Array

In this study, a PV array model developed in MATLAB/Simulink is employed to investigate its I-V characteristics based on varying environmental parameters such as temperature and solar irradiance. The model accepts input data at a granularity of five minutes, which is then interpolated to yield more detailed one-minute intervals for simulation purposes. Structurally, the array comprises three parallel-connected modules, with each of these modules containing a series arrangement of 13 individual units. This configuration results in an output characterized by an instantaneous voltage V_{pv}^i and a current I_{pv}^i . The total rated output capacity of this array setup is approximately 7.5 kW.

The PV output power $P_{pv}^i(t)$ is defined by the function:

$$P_{pv}^i(t) = f(Irradance(t), Temperature(t)) \quad (3.6)$$

3.2.2.2 MPPT Controller and the Incremental Conductance Algorithm

A Maximum Power Point Tracking (MPPT) controller is integrated within the PV system to optimize the energy output. This controller employs the incremental conductance algorithm to determine the maximum power point on the I-V curve. The fundamental idea of this algorithm rests on the notion that at the Maximum Power Point (MPP), the slope of the PV array's I-V characteristic curve is zero. Mathematically, this is represented in equation 3.7.

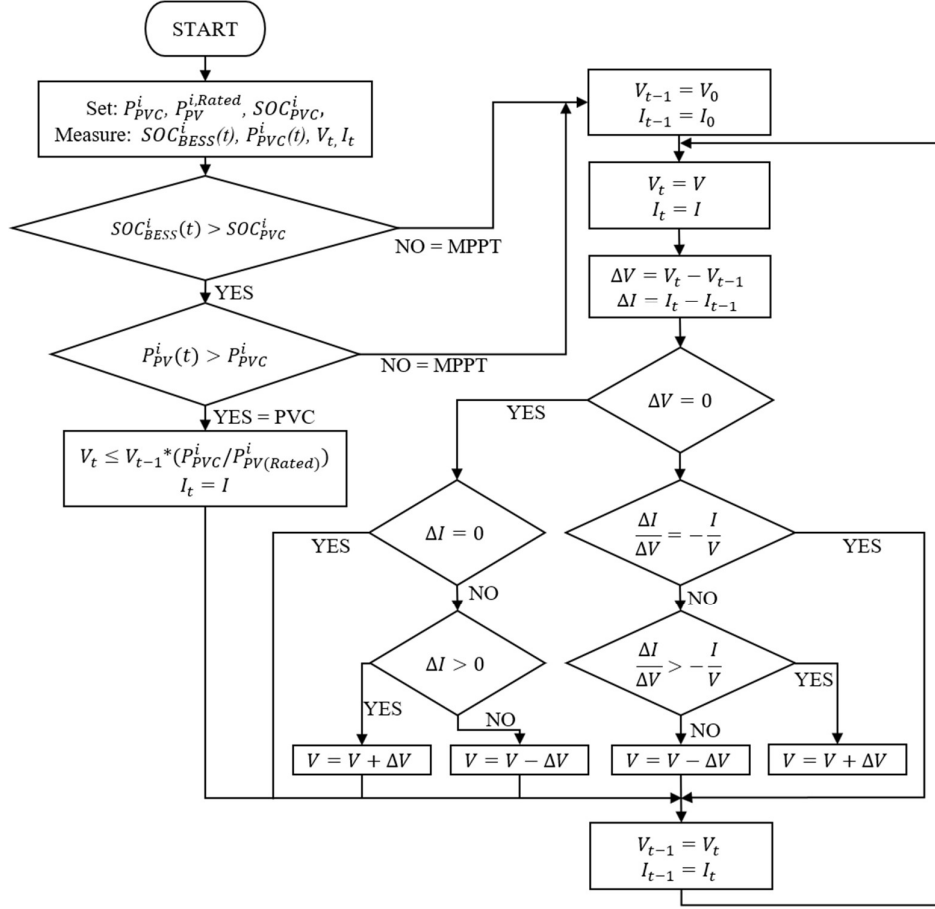


Figure 3.2. Algorithm for MPPT and PV Curtailment

$$\frac{dI_{pv}^i(t)}{dV_{pv}^i(t)} = -\frac{I_{pv}^i}{V_{pv}^i} \quad (3.7)$$

In practical implementation, the incremental conductance algorithm computes the duty cycle required to control the output of a boost DC-DC converter, which then feeds into the DC bus. The converter utilized is of the average-value type, consisting of controlled current and voltage sources.

3.2.2.3 PV Output Limitations

The constraints on the PV output are specified to prevent over-generation or under-generation of power. These limitations are mathematically defined by:

$$0 \leq P_{PV}^i(t) \leq P_{PV}^{i,max} \quad (3.8)$$

3.2.2.4 PV Curtailment Control (PVC) Method

In addition to relying on the MPPT controller for managing the DC-DC converter's output, this research introduces a Photovoltaic Curtailment (PVC) strategy as an

L, illustrated in Fig. 3.3. The state of this circuit breaker is governed by commands from the EMS through a specialized function known as the Non-Critical Load Shedding (NCLS). For simulation in this research, an idealized switch available in MATLAB/Simulink is used.

3.2.3.2 Load Modeling and External Inputs

The proposed load model receives externally generated demand data in the form of temperature and irradiance data, which is then used to create a reference current I_{ref} . This reference current is generated through a controlled current source block available within the MATLAB/Simulink environment.

3.2.3.3 Active and Reactive Power Components

In electrical systems, power is not just a simple scalar quantity; it has both active and reactive components. Active power, often represented as P , is the portion of electricity that does actual work, such as lighting a bulb or running a motor. Reactive power, denoted as Q , is a component orthogonal to active power and is responsible for maintaining the voltage levels and magnetic fields in the system. Both these components combine to form what is known as apparent power (\bar{S}), mathematically represented as $S = P + jQ$.

The model considers both active and reactive power elements, and ensures that the generated current is phase-matched with the supply AC voltage. This phase-matching is crucial, especially when the source of supply alternates between a private line and a local prosumer source. This is imperative for several reasons:

- 1) **Power Factor Optimization:** Phase matching is essential for achieving a high power factor. A high power factor indicates efficient utilization of electrical power.
- 2) **Voltage Regulation:** Accurate phase alignment aids in maintaining a stable voltage level across the electrical system, which is crucial for the effective operation of electrical devices and machinery.
- 3) **Reduced Harmonics:** Phase-matching helps in minimizing harmonic distortions, which can be detrimental to the power quality.

A lack of phase matching can introduce several issues that can destabilize the system as follows;

-
- a) **Harmonic Resonance:** Phase mismatches can introduce harmonic components that resonate within the electrical system, causing unexpected voltage and current spikes.
 - b) **Inefficient Power Transfer:** When the voltage and current waveforms are out of phase, the system cannot effectively transfer power from the source to the load.
 - c) **Increased Losses:** Phase mismatches often result in increased resistive losses in transmission lines and transformers, leading to inefficient operation and even possible equipment failure over time.
 - d) **Complex Control Scenarios:** A mismatched phase makes it challenging for control systems like EMS to optimize energy utilization effectively, introducing additional computational complexity and potential for error.

After combining the active and reactive loads—designated as critical and non-critical loads, respectively—an impedance calculation is performed. This calculation provides an aggregate representation of the total power requirement.

3.2.3.4 Current Reference Generation

The consolidated load is then fed into the current reference generator, depicted in Figure 4. Additional inputs to this generator include the AC voltage V_{AC} and the phase angle θ' . These variables are obtained from the double Quadrature Signal Generator (QSG) Second Order Generalized Integrator Phase Locked Loop (SOGI-PLL) [35], [98]. The open-loop transfer function of the QSG SOGI-PLL proposed in [39], is formulated as:

$$GI(s) = k_1 k_2 \omega'^2 s^2 / ((s^2 + k_2 \omega' s + \omega'^2)(s^2 + \omega'^2)) \quad (3.12)$$

The parameters for this function are defined by the following equations:

$$\omega_n = 4.4 / \zeta t_s \quad (3.13)$$

$$k_1 = \omega_n / \omega' \zeta \quad (3.14)$$

$$k_2 = 4\zeta \omega_n / \omega' \quad (3.15)$$

Where t_s is the selected settling time, ζ represents the damping ratio, and ω' is the centre frequency. The resulting Voltage, V_{rms} and phase angle, θ' are used in the current reference generator to produce I_{ref} , which drives the controlled current source block.

3.2.3.5 Limitations of the NCLS Mechanism

The operational boundaries of the NCLS feature which enables FLS via Switch L are mathematically expressed as:

$$P_{Load}^i(t) = P_{CL}^i(t) + P_{NCL}^i(t) \quad (3.16)$$

$$P_{load_{CL}}^i(t) \leq P_{Load}^i(t) \leq P_{load_{CL}}^i(t) + P_{load_{NCL}}^i(t) \quad (3.17)$$

$$0 \leq SOC_{PV}^i(t) \leq SOC_{L1}^i \quad (3.18)$$

Where $P_{Load}^i(t)$ denotes the active load demand in kW, $P_{CL}^i(t)$ is the critical electric load in kW, and P_{NCL}^i represents the non-critical load in kW

The load model thus ensures a stable and efficient interaction with the Energy Management System, thereby enabling flexibility in the energy distribution for diverse load scenarios.

3.2.4 The Single-Phase Synchronous Inverter (SSI): Principles and Operational Mechanics

The Single-Phase Synchronous Inverter (SSI) is a specific type of inverter that operates based on the average value concept. Structurally, it comprises two core components: a regulated current source on the Direct Current (DC) side, and a modulated voltage source on the Alternating Current (AC) side.

3.2.4.1 Basic Principle

At its most fundamental level, the SSI serves as an interface between a DC electrical system and an AC electrical system. It plays a pivotal role in executing bidirectional energy conversion by leveraging a controlled duty ratio using the pulse width modulation (PWM) technique. This ratio is essentially a calculated parameter that governs the operational behavior of the inverter, controlling the magnitude of its output voltage.

3.2.4.2 Input and Output Specifications

For this model, the DC side accepts an input with a reference voltage level of 400Vdc, while the AC side delivers an output with a reference voltage level of 200Vac at a

frequency of 60Hz. These specific voltage and frequency parameters are critical because they establish the conditions under which the inverter operates optimally.

3.2.4.3 Duty Ratio Calculation

The duty ratio is computed using the AC output and DC input voltage levels, in conjunction with their respective reference voltage values. This ratio serves as the control parameter for the bidirectional energy transfer between the DC and AC sides. It ensures that the energy conversion process is carried out in a manner that preserves the integrity and efficiency of the overall system. In the model used for this simulation, the DC side is modeled as a controlled current source while the AC is modeled as a controlled voltage source.

3.2.4.4 Adoption from Prior Research

It is noteworthy that the design and operational principles of this SSI model in Fig. 3.4 are based on in-house research carried out by Yorino and colleagues [33]. Their research focuses on replicating the dynamic attributes of synchronous machines. This is achieved by directly incorporating the swing equation into the inverter model, which thereby allows the SSI to emulate the behavior of traditional synchronous machines in a highly accurate manner.

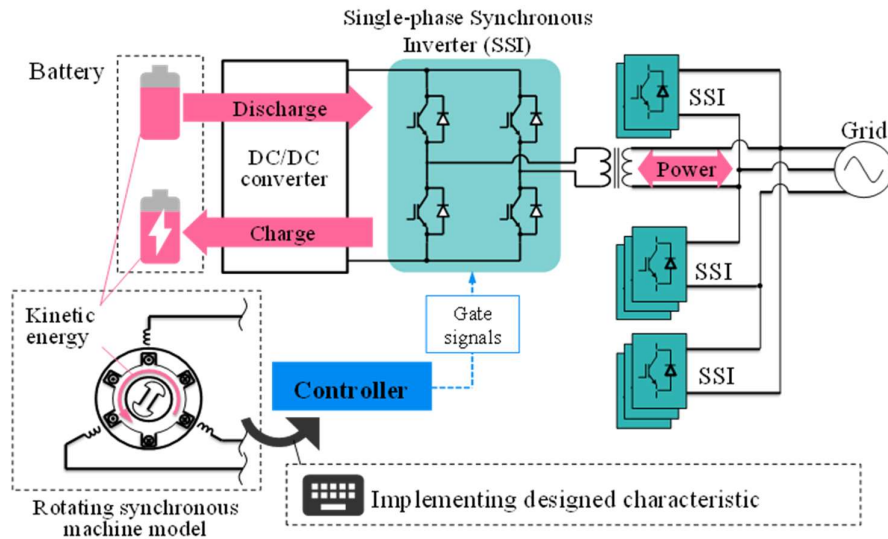


Figure 3.4. Single-phase Synchronous Power Inverter

3.2.5 The proposed Energy Management System (EMS) Simulator

The proposed EMS Simulator is constructed to operate in a real-time dynamic environment. It serves as the operational hub, coordinating the prosumer model's various

components. It aims to maintain system stability and energy balance through controlling power flow within the prosumer components while ensuring that critical loads are supplied with power for extended periods. Specifically, the system has been configured to maintain critical loads for up to three days ($T=3$ days), a duration generally considered adequate to avail initial emergency relief services in the event of an outage.

Among its core functions are:

- Flexible Load Switching (FLS): The EMS can switch the load source from local generation to external suppliers in emergency scenarios, all within predefined BESS limitations.
- Non-Critical Load Shedding (NCLS): The EMS can shed the non-critical load to maintain power balance, thus ensuring power security for the critical load.
- Real-time Monitoring and Alert System: An innovative color-coded scheme is used to monitor different operational modes. This enables immediate identification of system status and timely alerts.

FLS and NCLS are the core resilience hardening functions included within the prosumer model and its resulting EMS.

3.2.5.1 Operating Principles of the EMS Simulator

1) **Mathematical Foundation:** One of the primary operating principles of the EMS Simulator is encoded in an objective function, outlined below. This function aims to maintain an energy balance, giving priority to the uptime of non-critical loads.

$$\sum_{t=0}^T P_{CL}^i(t) = \sum_{t=0}^T (P_{PV}^i(t) + P_{BESS_{dch}}^i(t) - P_{BESS_{ch}}^i(t) + (t) - P_{NCL}^i(t)) \quad (3.19)$$

This foundation equations is limited within the operation limits of the system components including the maximum and maximum instantaneous BESS power that can be drawn or used to charge it that include:

$$P_{BESS_{dch}}^{i,min} \leq P_{BESS_{dch}}^i(t) \leq P_{BESS_{dch}}^{i,max} \quad (3.20)$$

$$P_{BESS_{ch}}^{i,min} \leq P_{BES_{ch}}^i(t) \leq P_{BESS_{ch}}^{i,max} \quad (3.21)$$

The power purchase from the grid is limited to serve only the critical load and is defined by:

$$0 \leq P_{grid}^i(t) \leq P_{critical}^i \quad (3.22)$$

Where $P_{grid}^i(t)$: Net power from the private line (kW), $P_{PV}^{i,max}$: PV maximum output (kW), $P_{BESS_{dch}}^{i,min}$: BESS discharging minimum output (kW), $P_{BESS_{dc}}^{i,max}$: BESS discharging maximum output (kW), $P_{BESS_{ch}}^{i,min}$: BESS charging minimum output (kW), $P_{BESS_{ch}}^{i,max}$: BESS charging maximum output (kW).

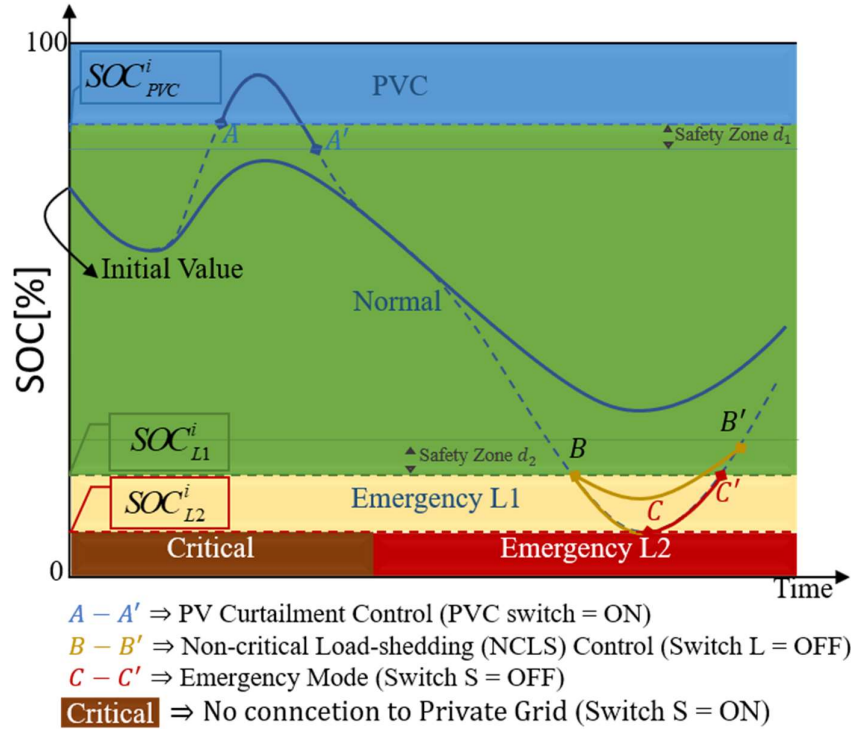


Figure 3.5. BESS SOC Operation Area Definition

- 2) **Definition of SOC Operational Ranges:** The second key operating principle centers on the State of Charge (SOC) operational areas defined for the BESS. These areas are color-coded in Fig. 3.5 and serve as alert thresholds for executing specific control actions. These predefined SOC regions set the framework for the system's decision-making process. In this figure, the SOC operation area of a battery is assumed to be 0 to 100%. However, due to the limitations in predicting the operation of batteries in extreme conditions, this area is further reduced to 0 – 90% operation area for the experimental applications of this study.

3.2.5.2 Algorithmic Control and Operational Modes

The control algorithm in Fig. 3.6 makes dynamic decisions based on the SOC of the BESS and other system variables. It considers the aforementioned mathematical equation

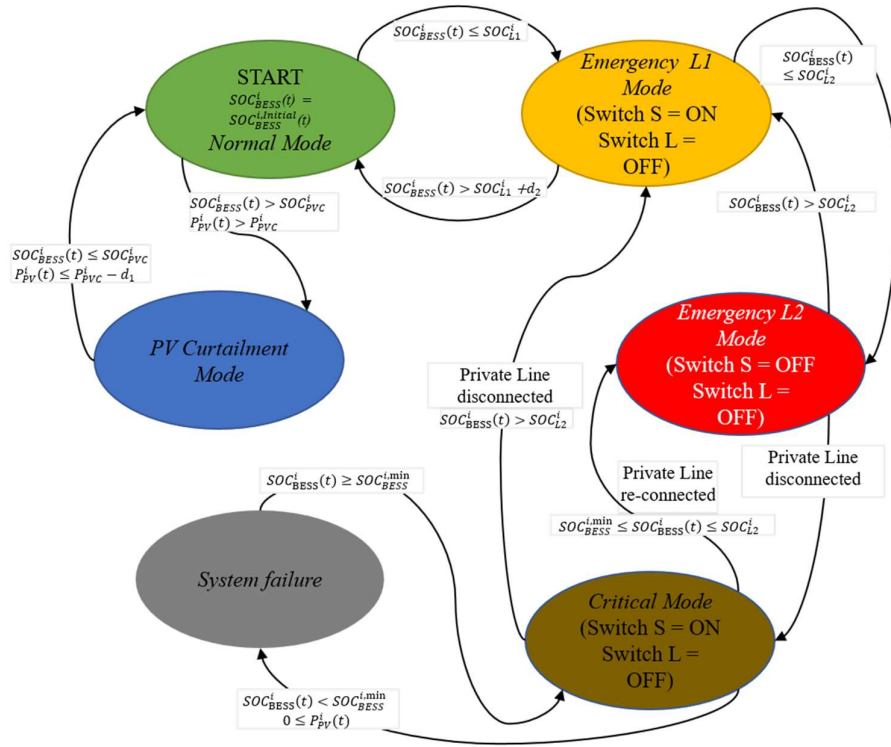


Figure 3.6. EMS simulator Control Algorithm.

and SOC operational ranges to execute actions that keep the system within optimal operating conditions. Normal Mode (Green): Under optimal conditions, the algorithm ensures the battery operates within the normal zone. Power needs are mainly met through PV and BESS resources. Excess energy can also be routed to a private electrical line.

- **PV Curtailment Mode (Blue):** Should PV production exceed demand, a Photovoltaic Curtailment (PVC) function is activated to limit PV output, thereby averting system instability. The control system transitions back to the normal mode through a PI-controlled PVC function.
- **Emergency L1 Mode (Orange):** Triggered when BESS SOC falls below the SOC_{L1}^i limit, this mode activates a Non-Critical Load Shedding (NCLS) mechanism, preserving only the critical load.
- **Emergency L2 Mode (Red):** When the BESS SOC falls below the SOC_{L2}^i limit, other networked prosumers are engaged to meet the critical power demand.
- **Critical Mode (Brown):** Engaged during private line outages, this mode runs on residual BESS SOC until Emergency L1 is restored.

-
- **System Failure (Grey):** This represents a catastrophic failure scenario where the PV output is null and BESS SOC is fully depleted.

As delineated in 3.6, the EMS Simulator interfaces seamlessly with components across individual prosumer units, including but not limited to the PV and BESS units. This integration is not just restricted to hardware; it also extends to the control algorithms employed in these systems. Specifically, the EMS Simulator complements the PV system's PVC and MPPT methods, as well as the BESS's PI controller for the DC Bus. The EMS Simulator thus leverages these existing control methods to implement its operating principles more effectively. It also utilizes the flexibility afforded by the integration of smart switches in the system to implement its layered control strategies.

This feature is pivotal for the realization of interconnected, cooperative microgrid systems. Notably, the simulator accomplishes this level of integration and functionality without requiring direct inter-prosumer communication. This not only enhances the system's resilience against communication failures but also introduces potential avenues for cost-saving in microgrid deployments, thereby elevating both the economic efficiency and operational robustness of the system. Additionally, this SOC area definition not only defines the battery operation area but also provides the color-coding scheme that is used to monitor the state of the charge and can be used as an alert system basis for microgrid operators.

3.3 Case Studies

This simulation case's purpose is to evaluate the relative improvement in the suggested Flexible Load shedding (FLS) and Non-Critical Load Shedding (NCLS) functions regarding improving the power security resilience of the proposed prosumer model.

3.3.1 Simulation Set-up and Conditions

We assume a simple test case including two prosumers, X and Y as portrayed in Fig. 3.7. The design for each prosumer features identical hardware components, including a PV system rated at 7.5 kW and a 40 AH lead-acid BESS characterized by a 5-hour discharge rate, a nominal voltage of 48V, and a discharge current rated at 17.4 A/unit.

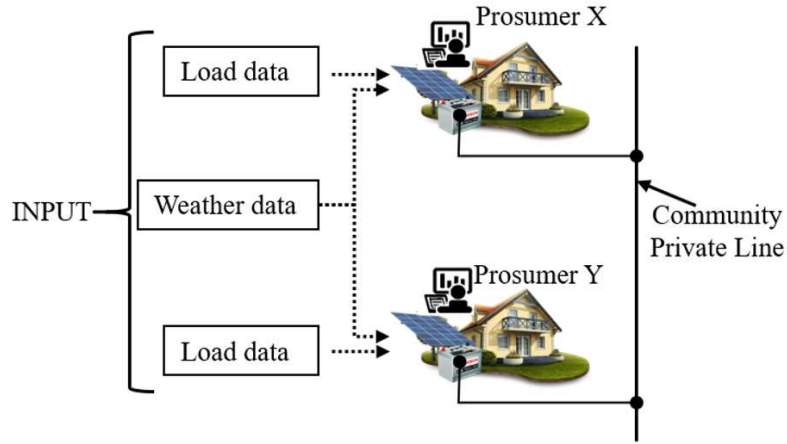


Figure 3.7. Interconnected Case Simulation setup.

Both the PV and BESS setups employ the models available in MATLAB/Simulink. The PVC Controller value, denoted as P_{PVC}^i , was configured to 5 kW, while the parameters d_1 and d_2 shown in Figure 5 were established at 1% of the peak BESS State of Charge (SOC). The system functions at a frequency of 60 Hz and the simulation is modeled to represent a post-disaster scenario.

The BESS configurations for each prosumer are detailed in Table 3.1 and were selected randomly to illustrate the capabilities of the developed prosumer and its EMS. Prosumer X is designed to mimic installations that necessitate high levels of BESS SOC for backup, whereas Prosumer Y is modeled after installations with minimal backup needs and a focus on energy trading. To aid simplicity in simulation, considerations related to energy trading and the associated financial tariffs were omitted.

Table 3.1 SOC Settings for Each Prosumer

| Prosumer | Initial Value [%] | PVC Value [%] | SOC_{L1}^i | SOC_{L2}^i |
|----------|-------------------|---------------|--------------|--------------|
| | | | Value [%] | Value [%] |
| X | 80 | 80 | 65 | 60 |
| Y | 50 | 80 | 45 | 40 |

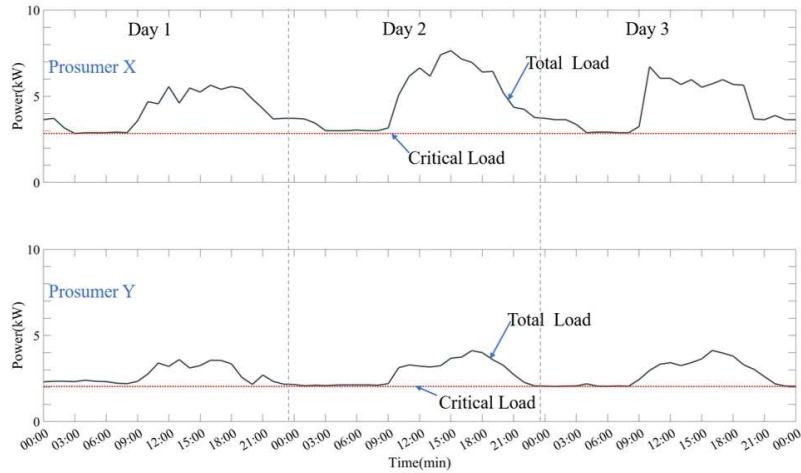


Figure 3.8. Prosumer Load Profiles.

Fig. 3.8 presents the demand profiles for both prosumers under study. The data, based on the proposed load model, displays varying non-critical loads and constant critical loads that serve as the input. This load information was sourced from various levels of the Electric Power and Energy Systems Laboratory building at Hiroshima University, thereby reflecting a standard research facility usage pattern.

The weather data was gathered from sensors located on the building’s rooftop during the summer months. This data is presented in Fig. 3.9. To ensure consistent outcomes, both prosumers depicted in Fig. 3.7 were simulated under the same meteorological conditions.

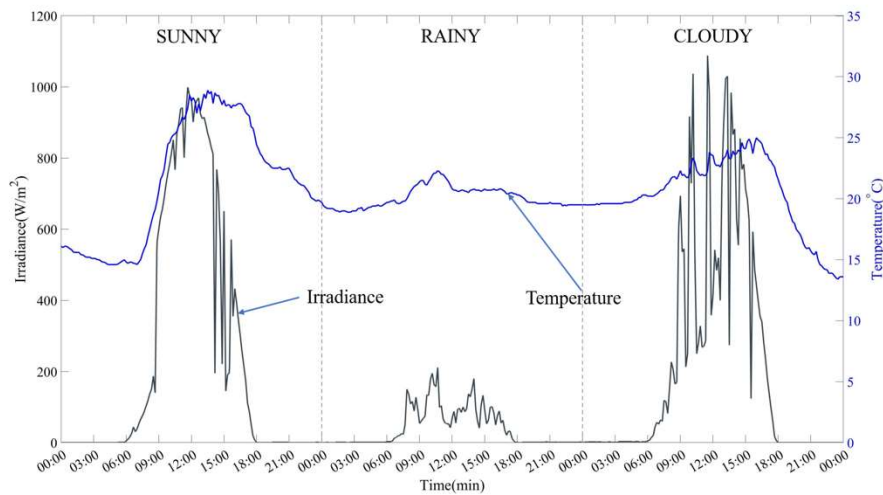


Figure 3.9. Three-day weather data.

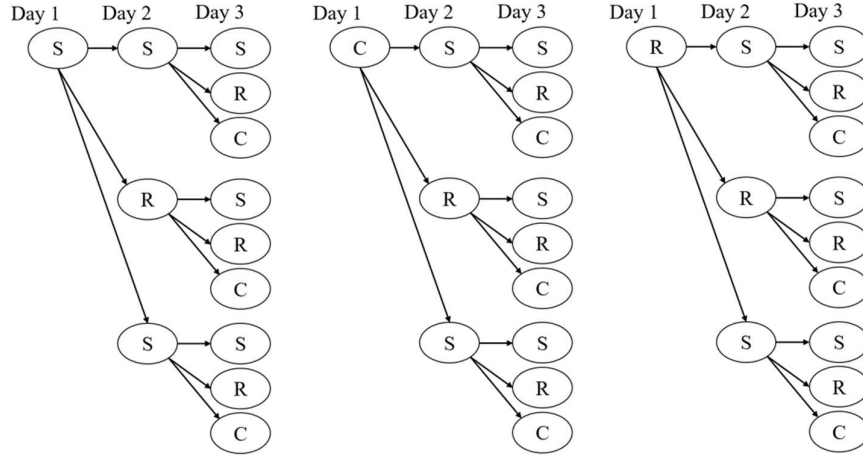


Figure 3.10. Three-day weather pattern possibilities.

Multiple weather patterns spanning three days were designed based on Fig. 3.10, which integrates the sunny (S), rainy (R), and cloudy (C) day data from Fig. 3.9. These weather patterns were then used for the simulation. The data for temperature and solar radiance from this figure served to formulate the respective PV generation curves using the PV system block of the developed simulation model. When the simulation employed the rainy day setting for day one, as found in the third tree, it was unsuccessful because the total demand surpassed the combined output of the PV generation and the energy reserved in the BESS, thus contravening the conditions specified in equation 3.19 for power balance. As a result, the most unfavorable yet feasible scenario chosen for the simulation was a cloudy-rainy-rainy sequence from the second tree.

Table 3.2 Summary of test cases

| Test Scenario | Connection status | Prosumer X | | | Prosumer Y | | |
|----------------|-------------------|------------|------|-----|------------|------|-----|
| | | PVC | NCLS | FLS | PVC | NCLS | FLS |
| 1 | disconnected | ✓ | ✗ | NA | ✓ | ✗ | NA |
| 2 | disconnected | ✓ | ✓ | NA | ✓ | ✓ | NA |
| 3 | Connected | ✓ | ✗ | ✗ | ✓ | ✗ | ✗ |
| 4 | Connected | ✓ | ✓ | ✗ | ✓ | ✓ | ✗ |
| 5 ¹ | Connected | ✓ | ✓ | ✓ | ✓ | ✓ | ✓ |

¹ The proposed method

3.3.2 Simulation Scenarios

A set of five test scenarios, outlined in Table 3.2, were conducted for comparative analysis. These tests considered both disconnected configurations and configurations where Prosumers X and Y were interlinked. FLS was not applicable when the prosumers were disconnected, as no external power source was involved. Test scenarios 1 and 3

acted as baseline scenarios for each connection status, where both the NCLS and the FLS (in case 3) functionalities were deactivated. Test scenarios 2 and 4 examined situations where only the NCLS was operational. Finally, test scenario 5 scrutinized the efficacy of the proposed prosumer model and its EMS by enabling all control features: PVC, NCLS, and FLS. For every test scenario, the PVC functionality remained active.

3.3.3 Results of the Simulated Test Scenarios

Fig.11 to Fig. 3.20 present the outcomes of the three-day simulations for the five test scenarios concerning the resilience hardening of Prosumers X and Y. Each figure is organized in a top-to-bottom manner. The top part of the figure contains the power flow and DC Bus voltage curves while the lower figure contains BESS SOC which is color-coded as explained in Section 3.2.5 about the alert warning system.

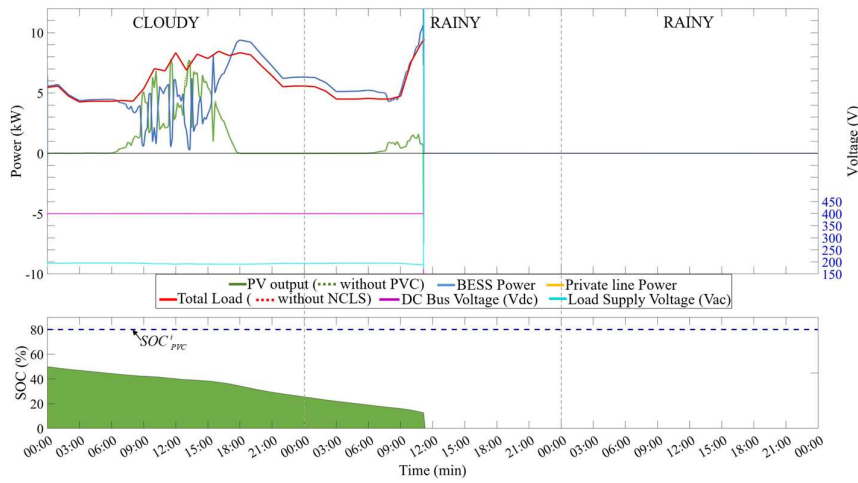


Figure 3.11. Test Scenario 1 (Disconnected): Performance of prosumer X.

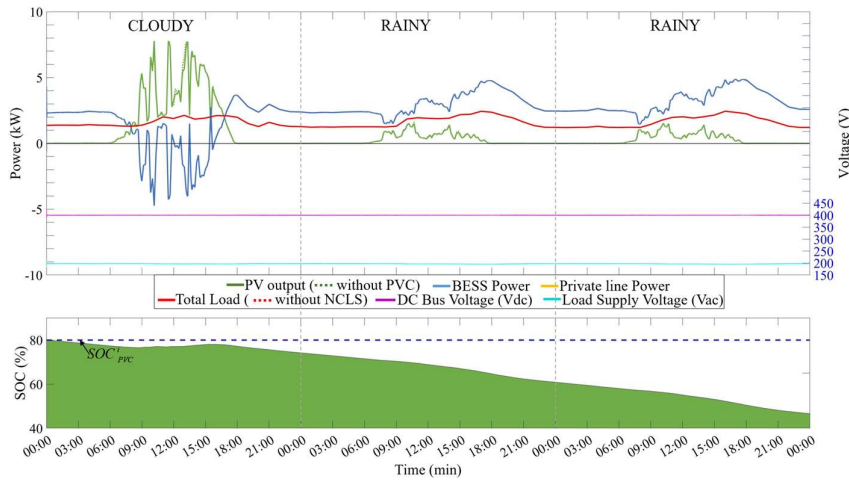


Figure 3.12. Test Scenario 1 (Disconnected): Performance of prosumer Y.

In these figures, a positive BESS power value in the power flow curve signifies discharge, while a negative value indicates BESS charging. Similarly, positive power values on the private line represent power flowing away from the prosumer and towards the private line, while negative values indicate the reverse. The included legend decodes the top half of the figure.

For the disconnected Test scenario 1, Prosumer X's SOC, shown in Fig. 3.11 dropped to 0% on the second day, primarily due to its initially low SOC, coupled with high demand and suboptimal power flow control. Consequently, the system became unstable since the PV generation during the rainy day was insufficient to meet demand. Conversely, Prosumer Y for this Test scenario 1 in Fig. 3.12 completed the simulation by utilizing almost half of its BESS storage along with the generated PV power.

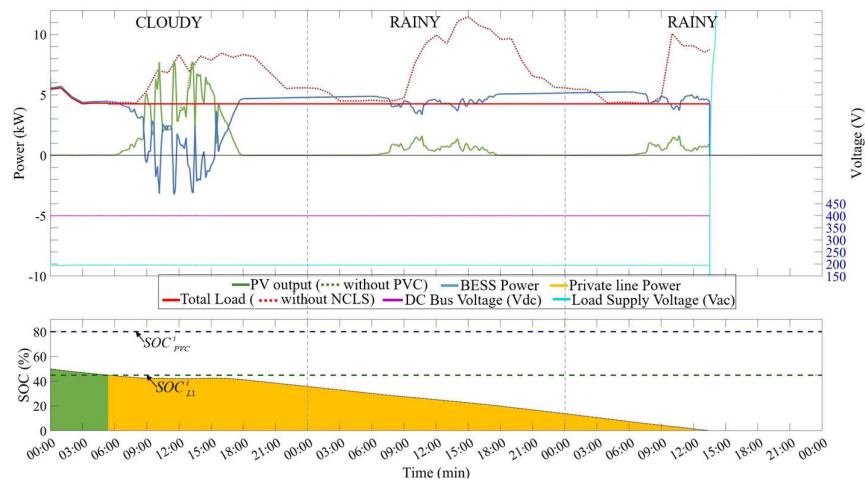


Figure 3.13. Test Scenario 2 (Disconnected): Performance of prosumer X.

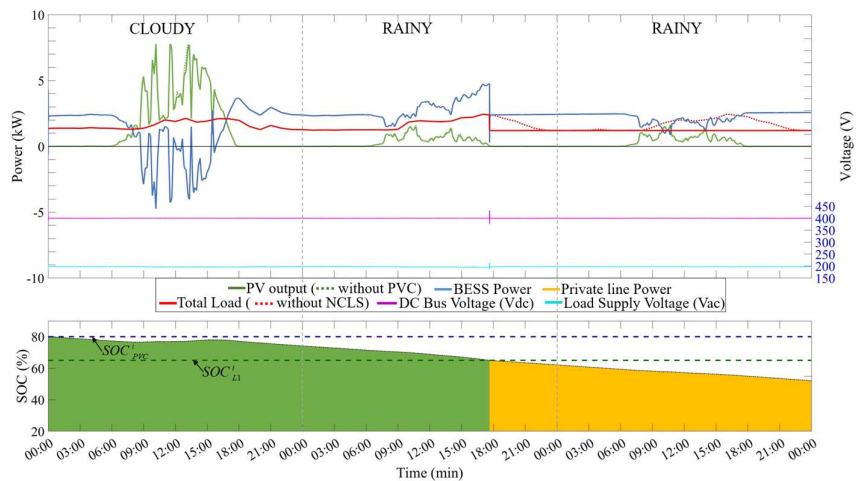


Figure 3.14. Test Scenario 2 (Disconnected): Performance of prosumer Y.

In Fig. 3.13 and Fig. 3.14, which represent disconnected Test Case 2 where NCLS is implemented, both Prosumers X and Y show better performance in terms of remaining BESS SOC after the simulation period. All systems exhibited steady DC bus voltages and uninterrupted operation for the entire simulation period; an improvement attributed to extended non-critical load shedding for both prosumers.

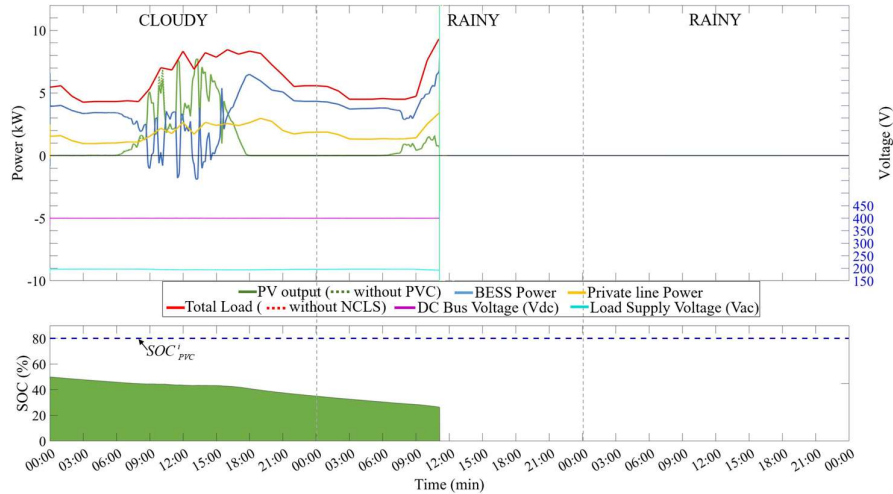


Figure 3.15. Test Scenario 3 (Connected): Performance of prosumer X.

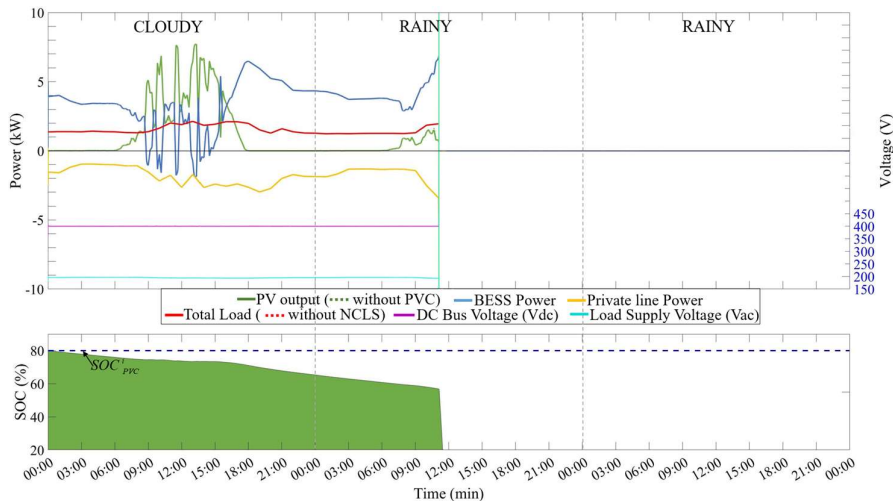


Figure 3.16. Test Scenario 3 (Connected): Performance of prosumer Y.

Fig 3.15 and Fig. 3.16 for the connected Test scenario 3 without NCLS and FLS implemented reveal that, even with power flows between the two prosumers, the system falters on the second day due to the absence of demand and supply control mechanisms such as the proposed resilience hardening functions. At the point of failure, neither prosumer could satisfy the total demand, resulting in system instability.

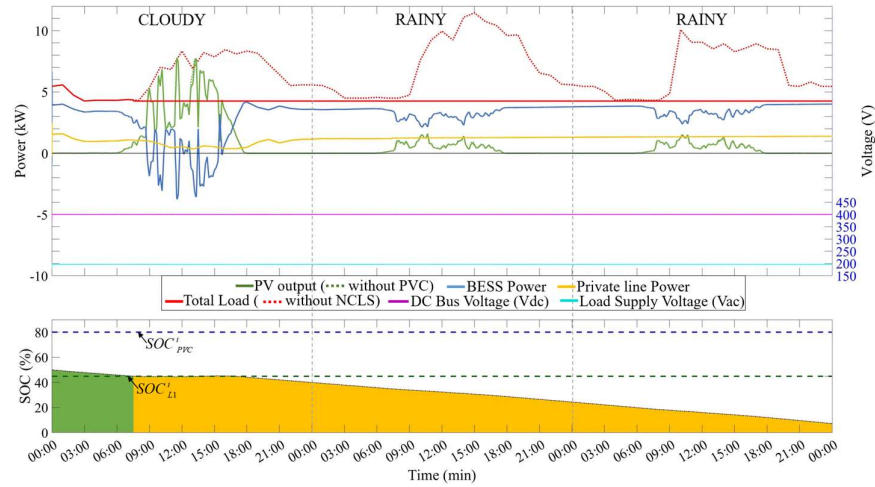


Figure 3.17. Test Scenario 4 (Connected): Performance of prosumer X.

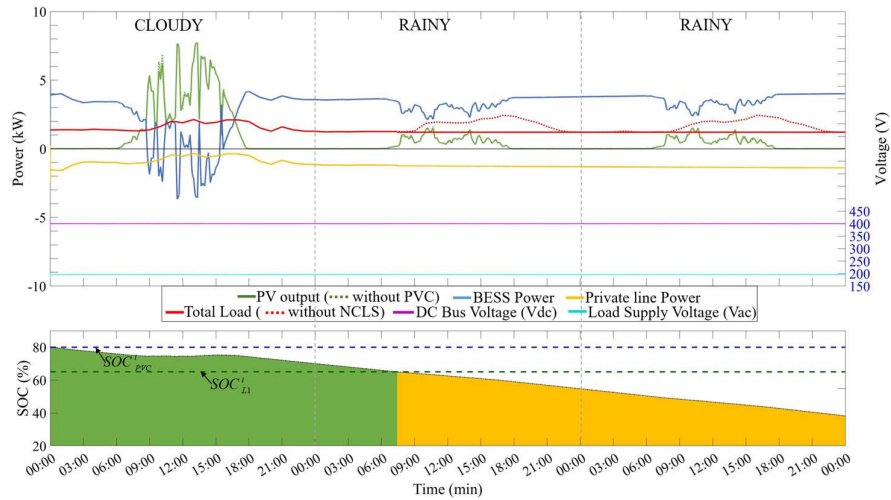


Figure 3.18. Test Scenario 4 (Connected): Performance of prosumer Y.

In contrast, Fig. 3.17 and Fig. 3.18 (Test Case 4), where only NCLS is enabled, shows a more stable system due to the power exchanges between the prosumers. However, it should be noted that the SOC for Prosumer X (Fig. 3.17) remained well below the proposed lower limit of $SOC_{L1}^i = 45\%$, despite prolonged load shedding and

the consistent power contributions from Prosumer Y. The final scenario, portrayed in Fig. 3.19 and Fig. 3.20, illustrates the efficacy of the proposed prosumer model and its associated EMS.

This set-up has both FLS and NCLS enabled, together with PVC. This setup led to increased power flows from Prosumer Y (Fig. 3.19) to Prosumer X (Fig. 3.20), consequently reducing the need for non-critical load shedding when compared with Test Case 4. As a result, Prosumer X was able to maintain its SOC close to the initial levels throughout the simulation. While the PV Conversion Controller (PVC) was active in all scenarios, it was not visibly impactful due to the worst-case weather conditions.

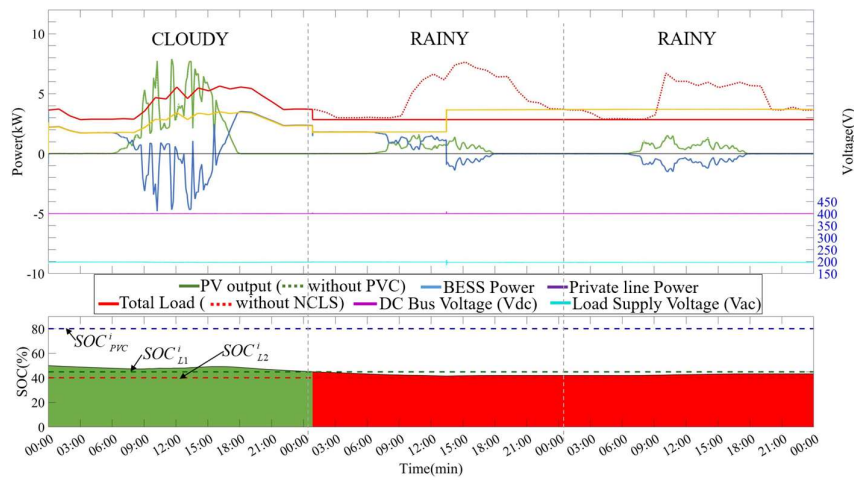


Figure 3.19. Test Scenario 5 (Connected): Performance of prosumer X.

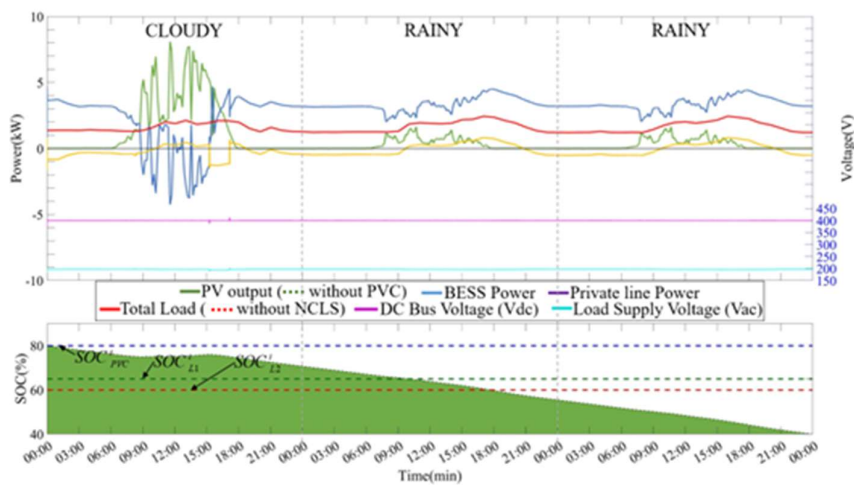


Figure 3.20. Test Scenario 5 (Connected): Performance of prosumer Y.

Table 5 provides a summary of the simulation results from Fig. 3.11 to Fig. 3.20. Upon comparative evaluation, it becomes evident that the proposed integrated prosumer model, complete with its EMS, offers the most reliable performance by sustaining Prosumer X's SOC at a comparatively high level at the conclusion of the three-day

Table 3.3 Summary of results.

| Test case | Prosumer | Initial SOC (%) | Final SOC (%) | Result of Simulation |
|----------------|----------|-----------------|---------------|----------------------|
| 1 | X | 50 | NA | Unstable (day 2) |
| | Y | 80 | 46.7 | Stable |
| 2 | X | 50 | NA | Unstable (day 3) |
| | Y | 80 | 52.10 | Stable |
| 3 | X | 50 | NA | Unstable (day 2) |
| | Y | 80 | NA | Unstable (day 2) |
| 4 | X | 50 | 7.3 | Stable |
| | Y | 80 | 38.3 | Stable |
| 5 ¹ | X | 50 | 42.7 | Stable |
| | Y | 80 | 40 | Stable |

¹The proposed method

simulation.

3.3.4 Discussion of Findings

In this section, we delve into an in-depth discussion of the findings from our simulations and analyses, spanning from the initial conditions and their impact on the system's performance to the various trade-offs and control mechanisms that contribute to system stability. We also explore the economic aspects of energy sharing among prosumers and conclude with future directions for research.

- Initial State of Charge (SOC) and Weather Impact:** The initial SOC for each prosumer affects the performance curve but doesn't impact the system's stability significantly during favorable weather days, as previously noted in [44]. However, scenarios with rainy weather on the first day led to system failure, mainly if Prosumer X had a low initial SOC. Therefore, maintaining a higher pre-disaster SOC is advisable for enhanced post-disaster resilience.

-
- **System Stability and Trade-offs:** The proposed model effectively maintains system stability across a three-day span, even under less-than-ideal weather conditions. Achieving this level of system stability comes with trade-offs, including the curtailment of non-essential loads and the potential financial costs of buying extra power. For this study, the financial aspects are omitted, assuming that both prosumers prioritize system uptime above costs.
 - **Prosumer Behavior and Role:** Prosumer X, ideally representing crucial services such as hospitals, can support critical loads for an additional day due to its high SOC. Prosumer Y, representing non-essential services like offices, also sustains essential operations by using its stored BESS energy.
 - **Energy Trading and Economic Viability:** Significant power exchanges between prosumers, as indicated in Fig. 3.20, hint at the potential for monetizing energy sharing. An economic feasibility study is highly recommended, as this could defray the setup costs of prosumer microgrids and accelerate the adoption of renewable energy, aligning with global sustainable development goals.
 - **Control Mechanisms and Future Directions:** Various control mechanisms like energy trading, PVC, and FLS ensure system stability, irrespective of the initial SOC. The proposed alert system allows for real-time monitoring and supports disaster recovery planning. The ultimate aim is to integrate these features into a future centralized control system for enhanced efficiency and waste management.
 - **Cooperative Energy Sharing:** The system's performance heavily depends on interconnected prosumers being willing to share energy cooperatively. Scenarios where prosumers are disconnected pose a risk to system stability. Our proposed model minimizes these risks by reducing load shedding and keeping the SOC at safe levels, thereby providing a buffer for an extra day in case of adverse conditions.

3.3.5 Limitations

This study provides valuable insights into prosumer microgrids' functioning, particularly their performance under diverse weather conditions and post-disaster scenarios. However, several limitations should be acknowledged for a comprehensive understanding of the research. For instance, the weather scenarios used, although diverse, are not exhaustive and may not cover all the complex weather patterns that could

potentially affect the system. Likewise, the study does not explore various disaster types and their differing impacts on the prosumers.

Financial factors related to energy trading have not been considered, which leaves questions regarding the economic feasibility of the prosumer systems. Additionally, the current study assumes a willingness among prosumers to share energy, an assumption that may not hold universally in real-world applications.

The study's scale, limited to two prosumers, also warrants caution when generalizing the findings. Expanding the study to include a more extensive network of prosumers may yield different outcomes, presenting challenges that have not been explored here.

It is worth noting that the initial SOC of each prosumer's BESS has been considered arbitrary, which as we observe in [14], can impact performance during adverse weather conditions, especially on the first day of a simulation run. This aspect as well as optimal control methods based on prediction and modern optimization techniques are further investigated in a subsequent Chapter 5, which introduces an approach for setting the initial SOC and explores optimal control methods based on predictive analytics and modern optimization techniques.

3.4 Conclusion

This study makes a significant advancement in our understanding of interconnected prosumer microgrids, with a particular focus on enhancing system stability and optimizing energy management. The proposed model skillfully balances operational uptime with factors like minimizing non-critical load curtailment and optimizing energy trading expenditures. It excels in sustaining high State of Charge (SOC) levels in critical facilities, thereby bolstering resilience in scenarios of post-disaster recovery.

Moreover, the model's adaptability and robustness pave the way for incorporating cutting-edge control mechanisms, including machine learning-based strategies and predictive optimization. These enhancements promise to elevate the model's efficiency in power flow scheduling, along with its accuracy and dependability, particularly in contemporary business contexts where disaster incidences are on the rise. The model's inherent flexibility also supports the integration of diverse renewable energy sources, contributing significantly to climate change mitigation efforts through its scalable and adaptable architecture.

Chapter 4: An Enhanced Solar Power Prediction Model

4.1 Introduction

Following the limitations presented in Chapter 3 regarding the need for a prediction method to minimize PV curtailment and improve scheduling, this chapter enhances our earlier methodology for day-ahead photovoltaic (PV) forecasting by integrating weather-based clustering Feed-Forward Neural Networks (WFNNs) from [56] and an Iterative Pruning (IP) algorithm from [3], [4]. The proposed model's advantage lies in its capacity to leverage minimal meteorological data, available through sources like the Japan Meteorological Agency (JMA) and significantly reduce the computational burden. The model can forecast day-ahead PV output and assess Confidence Intervals (CIs), which are integral to energy management strategies. The outcome of this solar prediction method is applied to Chapter 4.

4.2 Solar Power Prediction Using Iterative Network Pruning Technique for Microgrid Operation

4.2.1 Overview

The predictive accuracy of the proposed model is highly adequate for Microgrid (MG) system operations. The model is exceptionally adaptive to publicly available weather data, making it highly applicable to MGs with an EMS, as demonstrated in Figure 1. The model's efficacy is validated using historical meteorological information made publicly available. The prediction operates at 30-minute intervals and serves as a robust tool for system operators in MGs. This subsection will delve into the intricacies of the prediction model, discussing the underlying algorithms, feature sets, and the methodologies applied.

4.2.2 Pre-processing of Weather Data and Feature Extraction

Before feeding the data into our weather-focused feedforward neural networks (WFNNs), the raw data is pre-processed. The JMA provides this data on an hourly basis. However, past datasets from the same source are available at 3-hour intervals, including temperature (T), wind velocity (v), and precipitation (p). For the scope of this paper, we resample the data to 30-minute intervals using linear interpolation.

$$X_{rs}(t) = X(t_0) + X(t_1) - X(t_0) \times \frac{t-t_0}{t_1-t_0}, \quad t_0 \leq t \leq -t_1 \quad (4.1)$$

Where $X_{rs}(t)$ is the resampled data, $X(t_0)$ and $X(t_1)$ are the original data points and t is the re-sampled time.

We utilize three key features: temperature T , wind velocity v , and precipitation p . Temperature is taken in degrees Celsius, wind velocity in meters per second (m/s), and precipitation is categorized into two levels: 'Observed' (1) and 'Not Observed' (0) as defined by JMA. The categorization of wind velocity into four levels is based on its speed in m/s as below.

- Level 1: $0.0 \leq v < 3.0$ m/s
- Level 2: $3.0 \leq v < 6.0$ m/s
- Level 3: $6.0 \leq v < 10.0$ m/s
- Level 4: $v \geq 10.0$ m/s

The choice of data based on these parameters is based on previous inhouse research from [58] that investigates the correlation between insolation and these parameters.

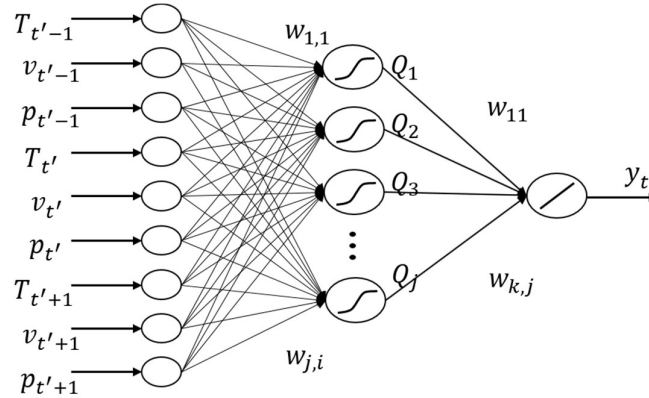


Figure 4.1. Basic structure of a WFNN

4.2.3 Weather Clustering and Construction of WFNNs

This section delineates the weather-based clustering approach employed in WFNNs. Given the variability of insolation intensity with different weather conditions, past weather data is classified into three clusters: sunny, cloudy, and rainy. Based on these classifications, specific FNNs are constructed for each weather condition. This

categorization helps in creating weather-specific FNNs, thus improving the model's predictive accuracy.

The FNNs are constructed as in Fig. 4.1 at 3-hour intervals for each weather condition. If, for instance, the public weather forecast indicates rain, the prediction will employ the WFNN trained specifically for rainy data. The training data for these networks is based on temperature T , wind velocity v , and precipitation p considering the values three hours before ($t' - 1$) the target time t' , and three hours ($t' + 1$) after t' . The backpropagation method is used for the computation of hidden-layer outputs.

4.2.4 Confidence Intervals and Local Energy Management

The calculated CIs play a crucial role in enhancing the resilience of MG system operations against uncertainties. The CIs are derived after the training process of WFNNs and provide upper and lower bounds on prediction accuracy, determined by the standard deviation (σ) of the error data between the predicted and measured values. The setting CIs is based on the solar prediction process from [58] which sets them based on historical data analysis of the accumulated stochastic distribution. Specifically, the CIs shown in Fig. 4.2 are fixed at intervals of $\pm\sigma$ and $\pm2\sigma$, centered around the arithmetic mean of the error values. The implementation of these CIs serves as an instrumental tool in optimizing the operational efficacy of Microgrid (MG) systems. It should be noted that the allocation of the comprehensive meteorological dataset is distributed in an 8:1:1 ratio for the training, testing, and validation phases, respectively.

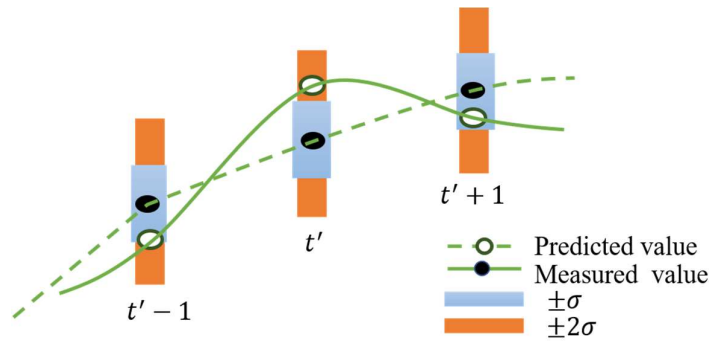


Figure 4.2. Confidence Interval Setting

4.2.5 Feedforward Calculations and Activation Functions in Neural Networks

In this section, we delve into the computational mechanics of neural networks, focusing specifically on the feedforward calculations and the activation functions

employed in the hidden and output layers. We provide mathematical formulations for calculating the weighted sums and activations for each neuron in the hidden layer, followed by similar calculations for the neurons in the output layer. Additionally, we discuss the choice of activation function for the hidden layer, elucidating its properties and its role in the network's performance.

Firstly, the feedforward calculation for the hidden layer is presented:

$$f_j = \sum_{i=1}^D w_{j,i} \cdot x_i + b_j^H \quad (4.2)$$

Here, f_j is the weighted sum for the j^{th} hidden neuron. D is the number of input features, $w_{j,i}$ is the weight between the i^{th} input and the j^{th} hidden neuron, x_i is the i^{th} input feature, and b_j^H is the bias for the j^{th} hidden neuron.

The activation function for the hidden layer neurons is defined by the sigmoid function:

$$z_j = \frac{1}{1+e^{-f_j}} \quad (4.3)$$

This function is used to transform f_j to the j^{th} hidden neuron's output z_j . It is chosen for its properties of bounding the output between 0 and 1, and its differentiability which is essential for backpropagation.

The feedforward calculation for the output layer is defined by:

$$y_k = \sum_{j=1}^M w_{k,j} \cdot z_j + b_k^O \quad (4.4)$$

Where, y_k is the output of the k^{th} neuron in the output layer. M is the number of hidden layer neurons, $w_{k,j}$ is the weight between the j^{th} hidden neuron and the k^{th} output neuron, z_j is the output from the j^{th} hidden neuron, and b_k^O is the bias for the k^{th} output neuron.

4.2.6 Evaluation and Regularization techniques

4.2.6.1 Evaluation methods

The mean absolute error (MAE) which is a common statistical measure used to assess the accuracy of a predictive model or a forecasting technique is mathematically calculated as

$$MAE = \frac{1}{n} \sum_{i=1}^n |g_i - y_i| \quad (4.5)$$

It quantifies the average of the absolute differences between the predicted values and the actual observed values. where n is the number of data points, g_i represents the observed value, and y_i represents the predicted value for each data point i . The MAE provides a straightforward and easily interpretable metric, making it useful for comparing different models or methods. A lower MAE indicates a more accurate model, while a higher MAE suggests less accuracy.

The root mean square error (RMSE) measures the model's performance by calculating the square root of the average squared differences between the actual (g_i) and predicted (y_i) solar power output. Lower RMSE values indicate better model performance. It is represented by:

$$RMSE = \sqrt{\frac{1}{n} \sum_{i=1}^n (g_i - y_i)^2} \quad (4.6)$$

4.2.6.2 Regularization Techniques

Regularization methods, such as L1 and L2, are adopted to mitigate overfitting issues in neural networks. Specifically, L1 regularization based on MAE is employed, which sets the coefficients of less critical variables to zero. We set the MAE of the NNs with the highest accuracy from 100NNs created with 20 units of the hidden layer as MAE^{20} .

In this study, we assess different methods for establishing repetition criteria by employing two specific techniques. The first technique is known as Fixed Value Addition (FVA), which is mathematically represented as $MAE^{20} + \rho$. In this equation, MAE^{20} is a given measure of accuracy, and ρ is an additional fixed value. Specifically, $\rho = 0.1$ was determined through a process of trial and error to optimize the criteria.

The second technique is called Fixed Value Multiplication (FVM). In this method, the repetition criteria are calculated using the formula $MAE^{20} \times \alpha$. Here, α is a multiplication factor that varies depending on the specific version of the FVM method being used: $\alpha = 1.1$ for FVM₁, $\alpha = 1.2$ for FVM₂, and $\alpha = 1.3$ for FVM₃.

The effectiveness and suitability of these two techniques—FVA and FVM—are then compared and evaluated through a series of simulations presented in the case study of this chapter.

4.2.7 Implementation of the Iterative Pruning (IP) Algorithm

The pruning method applied to WFNNs is aimed at enhancing the computation of the learning process. The IP algorithm judiciously removes neurons from the neural network

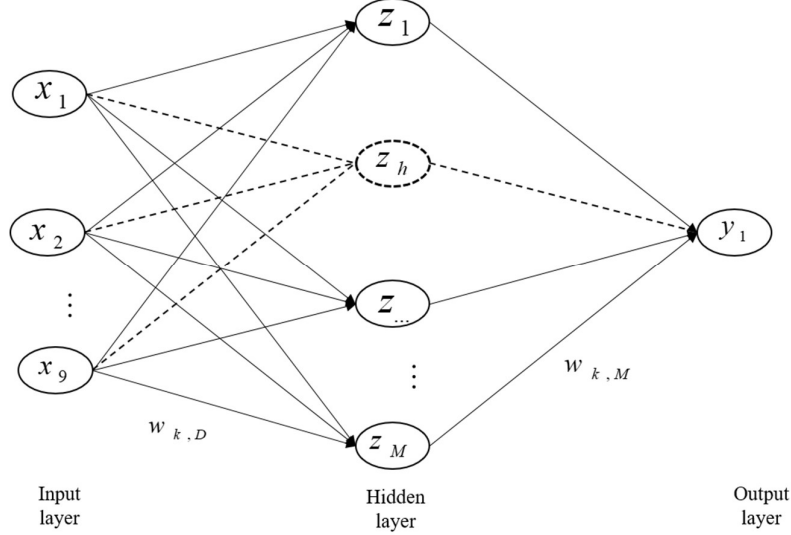


Figure 4.3. Iterative Pruning Illustration

as illustrated by Fig. 4.3, reducing computational burden while maintaining predictive performance. This section elaborates on the mathematical formulations used in the IP algorithm, including the computation of new variables and weight updates.

A description of the structured sequence of steps, encapsulating the heart of the iterative pruning algorithm is detailed as follows:

- **Step 1:** Determine the Unit h to remove

Before pruning, the algorithm identifies which hidden unit h should be removed. It chooses the one that has the least impact on the network's performance. This is performed using the equation:

$$h = \arg \min \sum_{k \in P_h} w_{k,h}^2 \sqrt{(z_h^1)^2 + \dots + (z_h^S)^2} \quad (4.7)$$

where h identifies the neuron to prune, $w_{k,h}$ is the weight from neuron h to the output neuron k and z_h^i is the output value of the training samples i for neuron h .

Here, P_h represents the set of hidden units that will be determined by unit h . The equation seeks to minimize the contribution of h to the output, measured by a weighted sum of its output values z_h^i .

- **Step 2:** Calculate recalibration factor δ

After identifying h , the algorithm computes a new variable δ using Equation:

$$\delta = w_{k,h} z_h Z^{-1} \quad (4.8)$$

This δ serves as a recalibration factor for adjusting the remaining weights and output values once h is removed. Here, Z is the inverse of the sum of all z values from the hidden units.

The equation below is used for recalculating the output value after removing the hidden unit h from the set M of all hidden units.

$$\sum_{j \in M} w_{k,j} z_j = \sum_{j \in M - \{h\}} (v_{k,j} + \delta_{k,j}) z_j \quad (4.9)$$

Then this equation calculates what the output value would be if h were removed.

$$v_{k,h} z_h = \sum_{j \in M - \{h\}} \delta_{k,j} z_j \quad (4.10)$$

- **Step 3:** Update the Weight from the hidden layer to the output layer

The weight from the hidden layer to the output layer, denoted $w_{k,M}^{new}$, is updated using Equation (8):

$$w_{k,M}^{new} = \{w_{k,M}^{old} + \delta_{k,M}\} \quad (4.11)$$

This equation ensures that the removal of h minimally impacts the network's output by recalibrating the remaining weights.

- **Step 4:** Calculate the New Output Value $y_{k,M}^{new}$

The output value $y_{k,M}^{new}$ is then calculated by taking into account the pruned hidden unit and the updated weights.

- **Step 5:** Evaluate MAE and compare it with the IP Criteria

The algorithm then calculates the MAE using the new output values. This MAE is compared against the predefined Iterative Pruning (IP) criteria.

- **Decision Point:** Should Iterative Pruning Continue?

-
- If MAE is larger than the IP criteria, the iterative pruning process breaks, signalling that further pruning would adversely affect the model's performance.
 - If MAE is smaller than the IP criteria, the algorithm updates the weights $v_{k,M}$, removes the hidden unit h , and continues to the next iteration (back to Step 1).

- **Special Case:** When the Number of Hidden Units is One

If only one hidden unit remains, the iterative pruning process stops regardless of MAE, as the network cannot function with zero hidden units.

Iterative Pruning offers a nuanced yet structured methodology for optimizing neural networks by using a systematic approach encapsulated in the algorithm and reinforced with mathematical formulations. It balances the trade-offs between complexity and performance, providing an efficient pathway for network optimization.

4.3 Case study

4.3.1 overview

The focus of our case study was on the predictive capabilities of our solar power prediction model using Iterative Pruning (IP) for August 2015. We utilized a half-hour period for unit commitment, with learning data spanning from July 2012 to July 2015, encompassing sunny and cloudy weather at 3-month intervals, and rainy weather data from January 2012 to July 2015.

The input data for the model included temperature, precipitation, and wind speed, with the amount of insolation serving as the teaching data. The model employed backpropagation as its learning method and linear interpolation for data processing.

4.3.2 Simulation and Results and Discussion

4.3.2.1 Iterative Pruning Implementation

We adopted a detailed iterative pruning strategy, as depicted in Fig. 4.4 and Table 0.1 in Appendix A, focusing on MAE across various hidden units. This approach involved two iterative pruning criteria: FVA and FVM.

Our simulations compared three methods:

- Method I (without IP)

- Method II (FVA with $\rho = 0.1$)
- Method III (FVM with $\alpha = 1.1, 1.2, 1.3$)

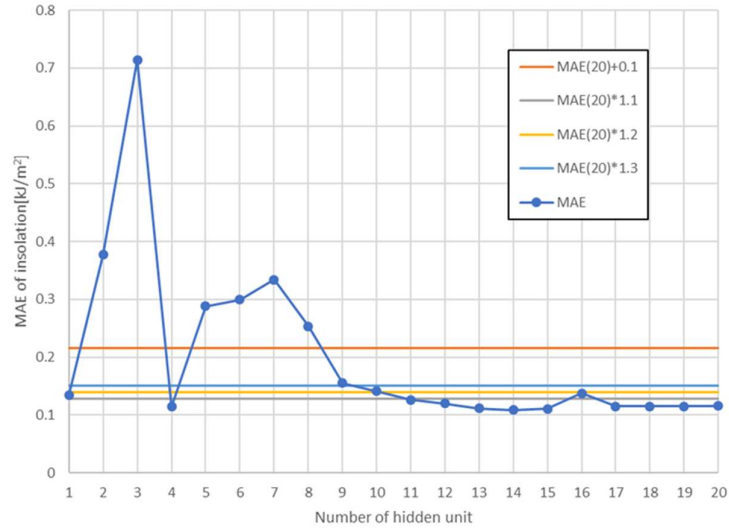


Figure 4.4. Iterative Pruning Strategy

In the sunny weather case depicted in Fig. 4.4 and Table 0.1, the initial setup included 20 hidden units, where the MAE was recorded at 0.1158. With the implementation of Method II, the pruning process continued until the number of hidden units was reduced to 9, where the MAE increased beyond the IP criteria of 0.2158. In contrast, Method III (Fixed Value Multiplication) concluded with 11 hidden units, with the MAE exceeding its IP criterion of 0.1389. The conventional Method I, without IP, resulted in the lowest MAE of 0.1088 with 14 hidden units, indicating the effectiveness of the pruning process in maintaining accuracy while reducing model complexity.

4.3.2.2 Sunny Weather Prediction

In the analysis of sunny weather conditions, the application of Iterative Pruning (IP) demonstrated a significant impact on both the efficiency and accuracy of solar irradiance prediction. The findings are summarized in Table 4.1 and illustrated by Fig. 4.5, comparing the outcomes of three different methods.

Method I in Fig. 4.5(a) serves as the baseline scenario without the use of IP. In this method, the simulation time was recorded at 65118 seconds, with a corresponding RMSE of 33.05 W/m². This sets the standard for evaluating the impact of IP in the methods II and III that follow.

Method II in Fig. 4.5(b), which incorporates an IP strategy, showed a remarkable decrease in simulation time, down to 5928 seconds. This represents a time ratio of 0.091, indicating a substantial improvement in computational efficiency compared to Method I. However, this efficiency came with a notable increase in RMSE, which rose to 52.19 W/m². This significant jump in RMSE suggests that while Method II is highly effective in reducing simulation time, it compromises the accuracy of the predictions more substantially than Method I.

Method III in Fig. 4.5(c), representing a different approach to IP, further decreased the simulation time to 5286 seconds, achieving a time ratio of 0.085. This makes it the

Table 4.1 Summary of Results for Sunny Weather Prediction

| Method | Simulation time [s] | Time ratio | RMSE[W/m ²] |
|------------|---------------------|------------|-------------------------|
| Method I | 65118 | 1 | 33.05 |
| Method II | 5928 | 0.091 | 52.19 |
| Method III | 5286 | 0.085 | 36.47 |

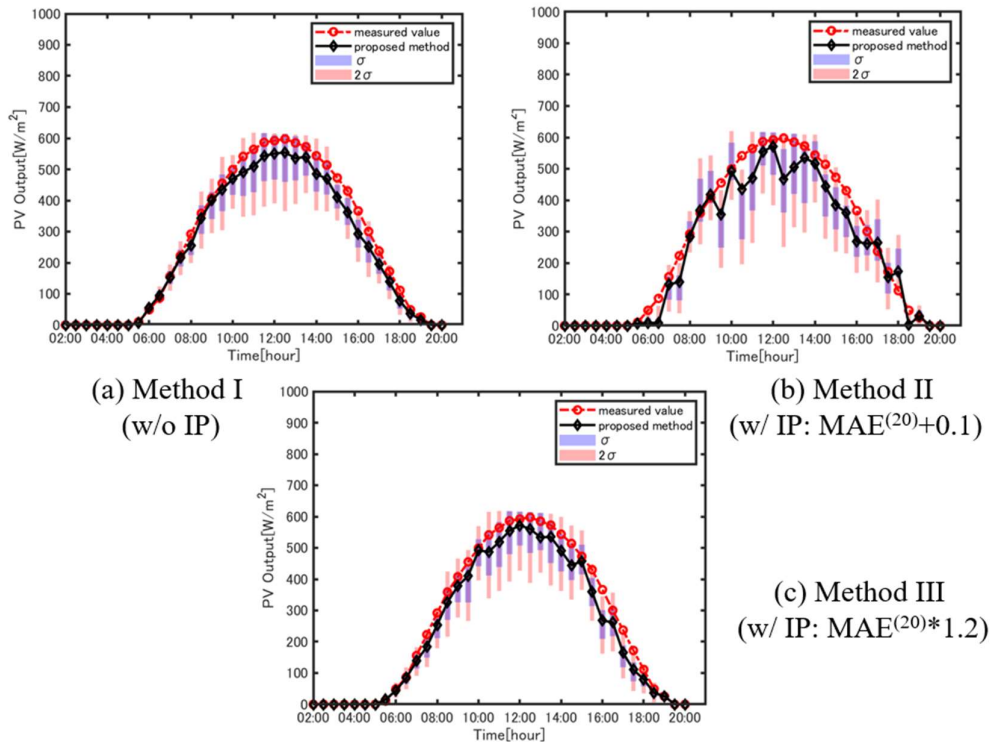


Figure 4.5. Sunny Weather Prediction Result

most time-efficient method among the three. More importantly, Method III exhibited an RMSE of 36.47 W/m², which, while higher than the baseline (Method I), is markedly lower than that of Method II. This indicates that Method III not only enhances time efficiency but does so with a relatively smaller sacrifice in prediction accuracy.

In summary, the application of IP in sunny weather prediction highlights the trade-off between computational efficiency and prediction accuracy. Method II offers the greatest reduction in simulation time but at the cost of significantly higher RMSE. Method III, on the other hand, provides a balanced approach, offering substantial improvements in time efficiency while keeping the increase in RMSE relatively modest. This positions Method III as a potentially more favorable choice when considering both aspects - efficiency and accuracy - in solar irradiance prediction under sunny conditions.

4.3.2.3 Cloudy Weather Prediction

In the examination of cloudy weather predictions, the implementation of Iterative Pruning (IP) again played a crucial role, particularly in terms of enhancing computational efficiency while assessing its impact on the model's accuracy, measured in terms RMSE. The performance data under different methods are elucidated in the results in Table 4.2 and Fig. 4.6.

Method I in Fig. 4.5(a), which did not incorporate IP, established the baseline performance metrics. It required the longest simulation time of 65118 seconds, which is used as the standard time ratio of 1. This method achieved an RMSE of 105.54 W/m², setting a benchmark for the accuracy of solar power prediction in cloudy conditions without the influence of IP.

When IP was introduced with Method II (Fixed Value Addition IP) in Fig. 4.6(b), there was a notable reduction in simulation time. The time taken for simulation was significantly cut down to 5285 seconds, corresponding to a time ratio of 0.095. However,

Table 4.2 Summary of Results for Cloudy Weather Prediction

| Method | Simulation time [s] | Time ratio | RMSE[W/m ²] |
|------------|---------------------|------------|-------------------------|
| Method I | 65118 | 1 | 105.54 |
| Method II | 5285 | 0.095 | 122.26 |
| Method III | 5286 | 0.097 | 103.10 |

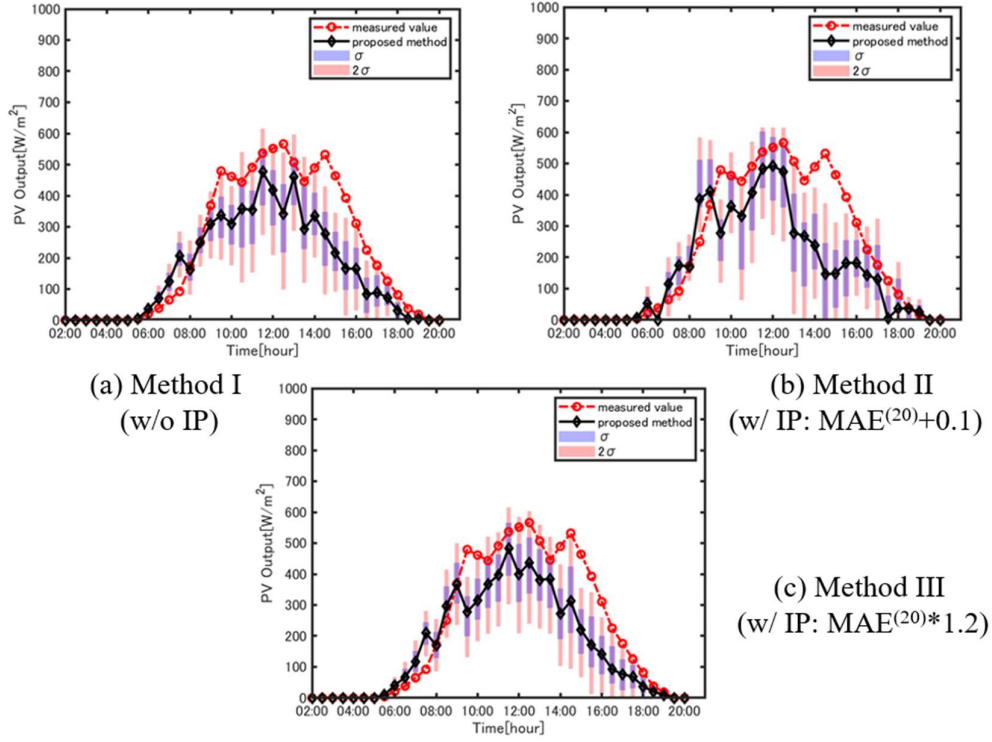


Figure 4.6. Cloudy Weather Prediction Result

this gain in time efficiency was accompanied by an increase in RMSE, which escalated to 122.26 W/m². This indicated that while Method II was highly efficient in terms of computation time, it compromised on the accuracy of the prediction to a certain extent.

Method III in Fig. 4.6(c), employing the Fixed Value Multiplication approach of IP, showed an interesting balance between time efficiency and prediction accuracy. The simulation time was marginally reduced further compared to Method II, standing at 5286 seconds, with a time ratio of 0.097. Notably, Method III was able to maintain a closer RMSE to the baseline, recording a value of 103.10 W/m². This RMSE, while slightly higher than that of Method I, was considerably lower than that of Method II, illustrating that Method III provided a more balanced approach between reducing computational demands and maintaining a relatively high level of prediction accuracy.

The findings from the cloudy weather prediction case underscore the nuanced efficacy of IP. It reveals that while significant reductions in simulation time can be achieved through IP, the choice of IP method (Method II vs. Method III) plays a pivotal role in determining the trade-off between computational efficiency and prediction accuracy. Method III emerges as a particularly effective strategy, offering substantial

time savings while ensuring the RMSE remains within a relatively close range to the baseline established by the non-IP Method I.

4.3.2.4 Rainy Weather Prediction

In the study of rainy weather prediction, the application of IP demonstrated notable improvements in time efficiency, while also influencing the accuracy of the predictions. The results of this study are encapsulated in Table 4.3, which presents a comparative analysis of three distinct methodologies.

Table 4.3 Summary of Results for Rainy Weather Prediction

| Method | Simulation time [s] | Time ratio | RMSE[W/m ²] |
|------------|---------------------|------------|-------------------------|
| Method I | 65119 | 1 | 23.42 |
| Method II | 5925 | 0.091 | 35.52 |
| Method III | 5286 | 0.081 | 29.76 |

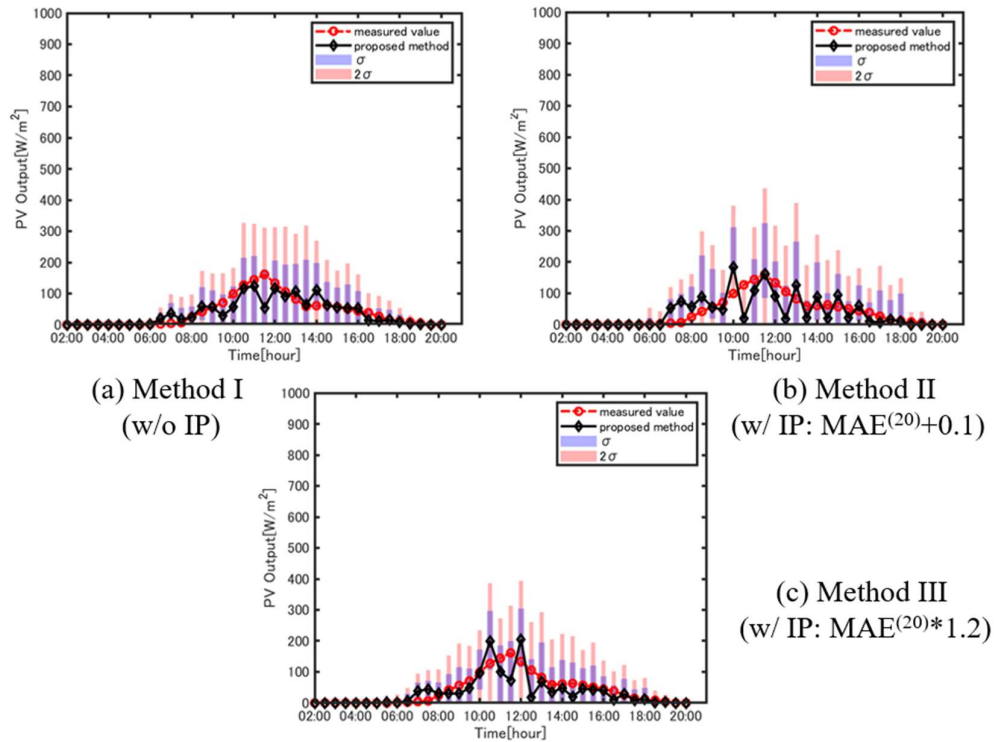


Figure 4.7. Rainy Weather Prediction Result

Method I in Fig. 4.7(a), which does not utilize IP, established a baseline for performance with an RMSE of 23.42 W/m² and required a significant simulation time of

65119 seconds. This method, while accurate, highlighted the need for a more time-efficient approach.

Transitioning to Method II in Fig. 4.7(b), which incorporates the Fixed Value Addition approach of IP, there was a marked reduction in the simulation time, brought down to 5925 seconds. This decrease in time, corresponding to a 0.091 time ratio, however, came with an increased RMSE, rising to 35.52 W/m². This indicates that while Method II is more efficient in terms of time, it does so at the expense of a slight decrease in prediction accuracy.

Method III, implementing the Fixed Value Multiplication strategy of IP in Fig. 4.7(c), further optimized the process. The simulation time was reduced to 5286 seconds, reflecting a time ratio of 0.081, making it the most time-efficient method among the three. Intriguingly, Method III also succeeded in maintaining a relatively lower RMSE of 29.76 W/m² when compared to Method II. This result suggests that Method III strikes a better balance between reducing computational demands and maintaining the accuracy of the predictions.

The exploration of IP in rainy weather conditions thus reveals a nuanced relationship between time efficiency and prediction accuracy. While each method significantly reduces the time required for simulation, the choice between Method II and III depends on the priority given to time efficiency versus the acceptable level of prediction accuracy. Method III emerges as a particularly compelling option, providing a substantial reduction in simulation time while keeping the increase in RMSE relatively moderate.

4.4 Conclusion: Implications and Future Prospects

4.4.1 Conclusion

The study's exploration of Iterative Pruning (IP) across sunny, rainy, and cloudy weather conditions has demonstrated its significant impact on solar power prediction models. In all cases, IP notably enhanced computational efficiency by reducing simulation times. However, this efficiency often came with varied impacts on prediction accuracy, as measured by RMSE. Method III consistently emerged as a balanced approach, offering substantial time savings while maintaining RMSE within an acceptable range. These findings underscore the potential of IP as a powerful tool for optimizing neural network-based solar power forecasting models, especially in applications where both time efficiency and accuracy are critical.

4.4.2 Practical Implications

The application of IP in solar power prediction models carries several practical implications. For operational solar power plants, the ability to predict power output quickly and accurately under varying weather conditions is crucial for grid management and energy allocation. Implementing IP can lead to more efficient use of computational resources, enabling faster decision-making processes. Moreover, the nuanced understanding of the trade-offs between computational efficiency and prediction accuracy can guide operators in selecting the most suitable IP method based on their specific operational requirements and environmental conditions.

4.4.3 Future Works

Looking forward, several areas warrant further investigation to optimize the application of IP in solar power prediction:

- **Optimizing IP Criteria:** Refining the criteria for IP could lead to better balances between accuracy and computational efficiency. Experimenting with different IP thresholds and strategies could yield more optimal models tailored to specific weather conditions.
- **Expanding Weather Condition Analysis:** While the current study focused on sunny, rainy, and cloudy conditions, extending the analysis to include more diverse weather patterns could enhance the model's robustness and applicability.
- **Integration with Real-Time Data:** Investigating the integration of IP models with real-time weather data and forecasting could further enhance the practicality of solar power prediction, allowing for more dynamic and responsive energy management.
- **Exploring Additional Parameters:** Including other relevant meteorological or environmental parameters in the training data, like the incorporation of relative humidity, could provide a more comprehensive understanding of the factors influencing solar power output.
- **Long-Term Performance Assessment:** Assessing the long-term performance and stability of IP-enhanced models over extended periods and under varying operational conditions would provide deeper insights into their practical efficacy and sustainability.

Chapter 5: Forecast-Driven Optimization Strategy for Efficient Microgrid Management

5.1 Introduction

In the contemporary energy landscape, a seismic shift is underway as the focus moves away from centralized generation towards more distributed and interactive systems. Microgrids have materialized as a cornerstone in this paradigm shift, offering not just local energy production but also the promise of increased reliability and resilience, particularly in disaster-prone regions. Within this context, the challenge of optimally coordinating operations among interconnected prosumers—a topic thoroughly investigated in our literature review in Chapter 2—takes on heightened importance. This complexity is further exacerbated by the intrinsic uncertainties of renewable energy generation and volatile energy market prices.

In Chapter 3, we introduced a prosumer model aiming to harness these advantages, though it fell short in addressing the following challenges: Firstly,

- The study omits the costs associated with energy trading by assuming that each prosumer prioritizes uptime over cost.
- The initial SOC for each prosumer is arbitrarily set. Our investigation from [14] demonstrates that the initial SOC can affect a prosumer's performance.
- Energy is wasted through the PV curtailment function and yet the BESS SOC of other prosumers on the private grid is not at maximum capacity. This is due to the uncoordinated, suboptimal operation.

This chapter aims to rectify these shortcomings by diving deeper into this multifaceted challenge, introducing a comprehensive optimal control strategy employing novel predictive optimization techniques for enhanced precision. The resulting optimizer in Fig. 5.1 utilizes the output of the IP-based PV prediction method we propose in Chapter 4. The output of the optimizer is used to improve the energy management system proposed to control the energy flow in the prosumer model elucidated in Chapter 3 by improving the decisions on charging and discharging the BESS, grid transactions and load shedding.

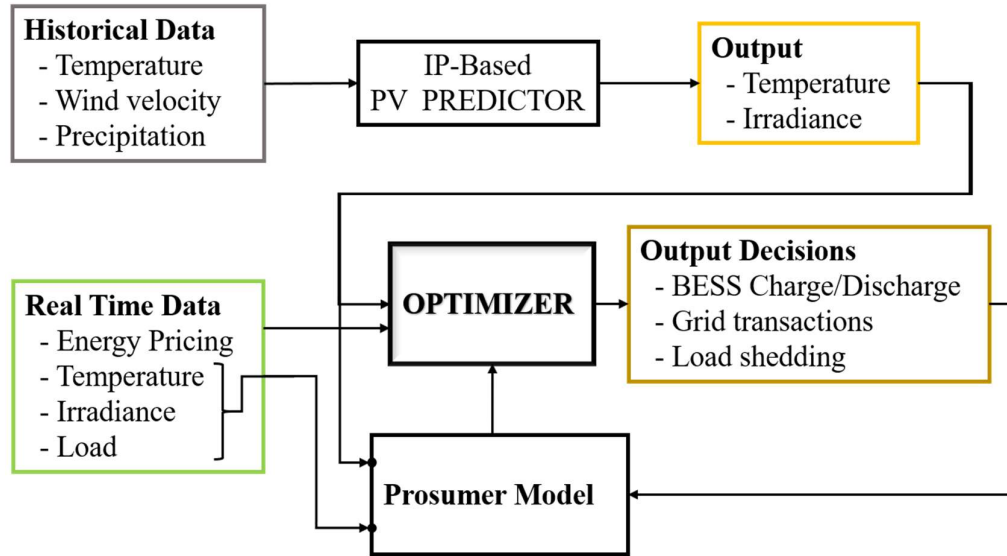


Figure 5.1. The Proposed Optimizer’s Role

In the sections that follow, the chapter will feature case studies and simulation results to substantiate the proposed methodologies. The overall goal is to provide a coherent roadmap for implementing an optimal, resilient, and economical microgrid system.

5.2 SOC Estimation with Optimal Operation of Grid-Connected Microgrid Prosumers

5.2.1 Introduction

The goal of this optimization is to ensure that the interconnected prosumers can engage in energy transactions at the least cost while maintaining energy security for the next day. This is achieved by leveraging the predicted PV output and energy trading prices to calculate a cost-optimal initial SOC for the BESS. Guaranteeing the initial BESS SOC improves post-disaster resiliency in contrast to authors in [99] by eliminating this uncertainty which allows for improved power flow scheduling and optimal grid transactions.

To offer a concrete methodology, this chapter is structured as follows: Section 5.2.2 details the optimization approach, broken down into three major steps. It delves into the constraints and objective functions involved in the optimization. Subsequent sections will deal with case studies, sensitivity analysis, limitations, and future directions.

5.2.2 Proposed Optimization Approach

The proposed optimization model aims to address both the cost and supply security for the next day of operation. To achieve this, the model utilizes a day-ahead optimization methodology based on the predicted PV output power and trading prices. The approach comprises three critical steps:

- Estimate the optimal operation for the next day.
- Derive the estimated initial BESS SOC for the next day.
- Manage power flow and non-critical load to achieve the target initial BESS SOC for the next day.

Each step involves its unique set of calculations, constraints, and objectives, which are subsequently outlined.

5.2.2.1 Estimate the Optimal Operation for the Next Day

The first step in the proposed EMS aims to estimate the optimal operation of interconnected prosumers for the next day. This is a crucial step, as it forms the foundation upon which other optimization steps are built. The focus here is to use predicted data for PV output and energy trading prices to come up with an optimal operational plan that minimizes cost while ensuring power balance and critical load supply.

The objective function aims to minimize the overall cost of electricity, including both buying from and selling to the grid, as well as penalties for non-critical load shedding. The equation is expressed mathematically as:

$$\text{Minimize: } \sum_{i=1}^N \sum_{t=1}^T P_{grid_{buy}}^i(t) * C_p^{pred,i}(t) + P_{grid_{sell}}^i(t) * (C_p^{pred,i}(t) - C_s^i) + P_{load_{NCL}}(t) * C_p^i(t) \quad (5.1)$$

$P_{grid_{buy}}^i(t)$ is the power bought from the grid by prosumer i at time t .

$C_p^{pred,i}(t)$ is the predicted cost of grid electricity at time t for prosumer i .

$P_{grid_{sell}}^i(t)$ is the power sold to the grid by prosumer i at time t .

C_s^i is the selling price at which prosumer i sells electricity back to the grid.

$P_{load_{NCL}}(t)$ is the non-critical load shed by prosumer i at time t .

$C_p^i(t)$ is the penalty for shedding the non-critical load at time t for prosumer i .

N is the total number of interconnected prosumers.

T is the total time steps in the simulation for one day.

Constraints: To form a practical optimization problem, several constraints are introduced:

- 1) **Power Balance Constraints:** The power inflow and outflow must be balanced at each time step for every prosumer. This must consider the predicted PV output.

$$P_{Load}^i(t) = P_{PV}^{pred,i}(t) + P_{BESS}^i(t) + P_{grid_{buy}}^i(t) - P_{grid_{sell}}^i(t) \quad (5.2)$$

- 2) **BESS Constraints:** The SOC of BESS should be maintained within permissible limits, and the maximum charging and discharging rates should not be exceeded.

$$P_{BESS_{dch}}^{i,min} \leq P_{BESS_{dch}}^i(t) \leq P_{BESS_{dch}}^{i,max} \quad (5.3)$$

$$P_{BESS_{ch}}^{i,min} \leq P_{BESS_{ch}}^i(t) \leq P_{BESS_{ch}}^{i,max} \quad (5.4)$$

$$SOC_{BESS}^{i,min} \leq SOC_{BESS}^i(t) \leq SOC_{PVC}^i \quad (5.5)$$

- 3) **Load Constraints:** The sum of critical and non-critical load should not exceed the available power and the critical load must always be maintained.

$$0 \leq P_{load_{CL}}^i(t) \leq P_{Load}^i(t) \leq P_{load_{CL}}^i(t) + P_{load_{NCL}}^i(t) \quad (5.6)$$

- 4) **Grid Power Flow Constraints:** Limitations on how much power can be bought or sold to the grid.

$$P_{grid_{buy}}^i(t) \leq P_{PV}^{pred,i}(t) - P_{Load}^i(t) + P_{BESS}^i(t) \quad (5.7)$$

$$P_{grid_{sell}}^i(t) \leq P_{PV}^{pred,i}(t) - P_{Load}^i(t) + P_{BESS}^i(t) \quad (5.8)$$

- 5) **Conditional constraints:**

$$P_{grid_{sell}}^i(t) = 0 \mid P_{PV}^{pred,i}(t) < P_{Load}^i(t) \quad (5.9)$$

$$P_{grid_{buy}}^i(t) = 0 \mid P_{PV}^{pred,i}(t) > P_{Load}^i(t) \quad (5.10)$$

$$P_{BESS_{dch}}^i(t) = 0 \mid P_{PV}^{pred,i}(t) \geq P_{Load}^i(t) \quad (5.11)$$

$$P_{BESS_{ch}}^i(t) = 0 \mid P_{PV}^{pred,i}(t) \leq P_{Load}^i(t) \quad (5.12)$$

- 6) **Voltage Constraints:** To ensure system stability, both DC and AC bus voltages are confined within upper and lower bounds.

$$V_{DC_{min}}^i \leq V_{DC}^i(t) \leq V_{DC_{max}}^i \quad (5.13)$$

$$V_{AC_{min}}^i \leq V_{AC}^i(t) \leq V_{AC_{max}}^i \quad (5.14)$$

Step 1 of the proposed EMS lays the groundwork for optimizing prosumer interactions in a grid-connected setting for the next day. By judiciously using predicted data for PV output and market prices, the method aims to establish an operational plan that fulfills power balance requirements while also minimizing costs.

5.2.2.2 Derive the Estimated Initial BESS SOC for the Next Day

The second step in our proposed EMS is crucial for setting up the groundwork for optimal operation on the following day. Based on the results obtained from Step 1—namely the optimal operational costs and power flows—Step 2 aims to determine the best initial SOC for the BESS at the beginning of the next day. This is often referred to as the target SOC, SOC_{target} .

Objective Function: In Step 2, the objective function focuses on determining SOC_{target} that minimizes the cost of operation for the next day while ensuring the supply for critical loads is met. This is accomplished by using the estimated optimal power flows and costs calculated in Step 1. The objective function can be expressed as:

$$\text{Minimize: } \sum_{i=1}^N C_{day2}^i \left(SOC_{BESS}^i(T) \right) \quad (5.15)$$

Where C_{day2}^i represents the estimated cost of operation for prosumer i on the next day when the system starts with $SOC_{BESS}^i(T)$ at the beginning of the day.

Constraints: The objective function for step 2 is constrained as follows:

- 1) **SOC Range Constraints:** The initial SOC for the next day must be within permissible bounds.
- 2) **Predicted Power Balance:** The power balance for the next day, based on the predicted data, must be maintained.

$$SOC_{BESS}^{i,min} \leq SOC_{target}(t) \leq SOC_{PVC}^i \quad (5.16)$$

- 3) **Predicted BESS Charging and Discharging Rates:** The estimated BESS charging and discharging rates must be within the specified limits.

$$P_{BES\ dch}^{i,min} \leq P_{BESS\ dc}^{pred,i}(t) \leq P_{BESS\ dch}^{i,max} \quad (5.17)$$

$$P_{BESS\ ch}^{i,min} \leq P_{BESS\ ch}^{pred,i}(t) \leq P_{BESS\ ch}^{i,max} \quad (5.18)$$

Step 2 is a bridge between the predictive modeling carried out in Step 1 and the real-time adjustments done in Step 3. Its main role is to find an initial BESS SOC for the next day that would minimize the operational costs based on the forecasts made. By doing so, the EMS sets up a pre-defined state that would ideally result in the least-cost operation, considering the constraints and uncertainties. This becomes the target SOC that Step 3 aims to achieve, ensuring that the EMS operates in a manner that is both economically and operationally optimal.

5.2.2.3 Manage Power Flow and Non-Critical Load for the Current Day

The third step in the proposed EMS is pivotal in establishing the operational feasibility and economic efficiency for the current day. It aims to adjust the day's power flow and non-critical load based on the target SOC for the BESS established in Step 2. This adjustment is done to guarantee the optimal conditions for the next day's operations.

Objective Function: In this step, the objective function seeks to minimize the daily operational cost while steering the BESS to reach the target initial SOC SOC_{target} by the end of the day. Mathematically, the objective function can be formulated as:

$$\begin{aligned} \text{Minimize: } & \sum_{i=1}^N \sum_{t=1}^T P_{grid\ buy}^i(t) * C_p^{act,i}(t) + P_{grid\ sell}^i(t) * (C_p^{act,i}(t) - C_s^i) + \\ & P_{load\ NCL}(t) * C_p^i(t) + \lambda |SOC_{BESS}^i(T) - SOC_{target}| \end{aligned} \quad (5.19)$$

Where:

- $C_p^{act,i}(t)$ is the actual cost of grid electricity at time t for prosumer i .
- λ is a Lagrange multiplier to balance the importance of minimizing the cost versus achieving the target SOC.
- All other terms have been defined in Step 1.

Constraints: The problem in this step is contained as:

- 1) **Power Balance Constraints:** Similar to Step 1, the power balance constraint for each prosumer should be maintained.

- 2) **BESS Constraints:** The SOC must reach the target value SOC_{target} by the end of the day T .

$$SOC_{BESS}^i(T) = SOC_{target} \quad (5.20)$$

Other BESS constraints are maintained as defined in step 1.

- 3) **Power Balance Constraints:** The power inflow and outflow must be balanced at each time step for every prosumer. This must consider the predicted PV output.

$$P_{Load}^i(t) = P_{PV}^{act,i}(t) + P_{BESS}^i(t) + P_{grid_{buy}}^i(t) - P_{grid_{sell}}^i(t) \quad (5.21)$$

- 4) **BESS Constraints:** The SOC of BESS should be maintained within permissible limits, and the maximum charging and discharging rates should not be exceeded.

$$P_{BESS_{dch}}^{i,min} \leq P_{BESS_{dch}}^i(t) \leq P_{BESS_{dch}}^{i,max} \quad (5.22)$$

$$P_{BESS_{ch}}^{i,min} \leq P_{BESS_{ch}}^i(t) \leq P_{BESS_{ch}}^{i,max} \quad (5.23)$$

$$SOC_{BESS}^{i,min} \leq SOC_{BESS}^i(t) \leq SOC_{PVC}^i \quad (5.24)$$

- 5) **Grid Power Flow Constraints:** Limitations on how much power can be bought or sold to the grid.

$$P_{grid_{buy}}^i(t) \leq P_{PV}^{act,i}(t) - P_{Load}^i(t) + P_{BESS}^i(t) \quad (5.25)$$

$$P_{grid_{sell}}^i(t) \leq P_{PV}^{act,i}(t) - P_{Load}^i(t) + P_{BESS}^i(t) \quad (5.26)$$

- 6) **Conditional constraints:**

$$P_{grid_{sell}}^i = 0 \mid P_{PV}^{act,i}(t) < P_{Load}^i(t) \quad (5.27)$$

$$P_{grid_{buy}}^i = 0 \mid P_{PV}^{act,i}(t) > P_{Load}^i(t) \quad (5.28)$$

$$P_{BESS_{dch}}^i = 0 \mid P_{PV}^{act,i}(t) \geq P_{Load}^i(t) \quad (5.29)$$

$$P_{BESS_{ch}}^i = 0 \mid P_{PV}^{act,i}(t) \leq P_{Load}^i(t) \quad (5.30)$$

Other constraints that include the load, conditional and voltage constraints are as stated in step 1.

5.2.3 Optimization Methodology

5.2.3.1 Methodologies for Efficient Prosumer-Based Microgrid Management

The proposed methodology in this research synergistically combines Model Predictive Control (MPC), Linear Programming (LP), and Multi-objective Optimization (MOO) for effective management of prosumer-based microgrids. MPC plays a crucial role in the initial phase, utilizing historical and current data to predict optimal operations for the following day, which enhances the accuracy of day-ahead optimization and improves microgrid resilience.

In contrast, MOO is instrumental in balancing various objectives such as cost minimization and reliability maximization, ensuring that solutions address the interests of different stakeholders. It adeptly navigates between competing goals to find optimal solutions. Meanwhile, LP acts as the computational foundation, efficiently solving large-scale problems in real-time scenarios by transforming complex optimization challenges into manageable linear forms. This combination of approaches forms a robust, comprehensive strategy for the management of microgrids.

5.2.3.2 Solver: MATLAB's linprog Function

The linprog function in MATLAB's Optimization Toolbox chosen for this problem is particularly suited for solving this class of linear optimization problems. It is integrated within the hybrid MPC-LP-MOO framework to provide a systematic and efficient approach to solving the complex optimization problems intrinsic to prosumer microgrids. The function effectively identifies the optimal solution by navigating through the feasible region defined by the linear constraints. Its advantages include computational efficiency, robustness to variations in constraints, and the ability to handle large-scale problems.

5.2.4 Algorithm for Implementing Proposed Steps

The algorithm for implementing the three steps of the two-stage optimizer is presented below.

Input:

- Predicted and actual PV output power
- Predicted and actual trading prices
- Load demands (critical and non-critical)
- BESS parameters (SOC bounds, Charging and Discharging Rate bounds)
- Grid parameters (Voltage and Frequency bounds)

Initialization:

1. Initialize day index, $t = 1$
 2. Initialize N prosumers with given BESS SOC_s
 3. Read the predicted PV output power, and predicted trading prices for the next day
- //Step 1: Estimate the Optimal Operation for the Next Day
4. FOR each prosumer i DO
 - a. Formulate and solve the linear programming (LP) problem for day $t + 1$ using `linprog`
 - b. Calculate the optimal cost, power flows, and SOC for the next day
- END FOR
- // Step 2: Derive the Estimated Initial BESS SOC for the Next Day
5. FOR each prosumer i DO
 - a. Use the results from Step 1 to formulate the objective function for SOC_{target}
 - b. Solve the LP problem for SOC_{target} using `linprog`
 - c. Store SOC_{target} as the initial SOC for the next day
- END FOR
- // Step 3: Manage Power Flow and Non-Critical Load for the Current Day
6. FOR each prosumer i DO
 - a. Formulate and solve the LP problem for day t aiming to reach SOC_{target} by the end of the day
 - b. Execute the calculated optimal power flows and load shedding
- END FOR
7. Update $t = t + 1$ and GO TO Step 3

5.3 A Two-Stage Optimal Control Strategy for Mitigating Uncertainty in Microgrids

5.3.1 Introduction

This study proposes a Two-Stage Optimal Control Strategy to address the inherent uncertainties in microgrid operations, particularly those associated with solar PV systems. The unique aspect of this research is its integration of both day-ahead predictive and real-time data, allowing for dynamic re-optimization to reconcile any discrepancies between anticipated and actual system behaviours.

This section delves into the detailed formulation of this dual-stage strategy, covering its objectives and constraints in optimizing energy trading, storage, and consumption

within a microgrid environment. These elements collectively contribute to enhancing the system's overall robustness and economic efficiency.

5.3.2 Proposed Optimization Strategy

Our proposed strategy is divided into two stages: Predictive Optimization (stage 1) and Re-Optimization (stage 2), as illustrated in Fig. 5.2.

5.3.2.1 Predictive Optimization (Stage 1)

The initial stage involves optimization based on predicted PV output data. The optimization problem is formulated mathematically as:

$$\min \sum_{i=0}^N c_i * A_{pred_i} \quad (5.31)$$

where c_i is the energy trading price in yen/kWh and A_{pred_i} represents the optimal control actions at each time step i based on predicted data which includes power exchanges with the grid and BESS and $\forall i \in [1, N]$.

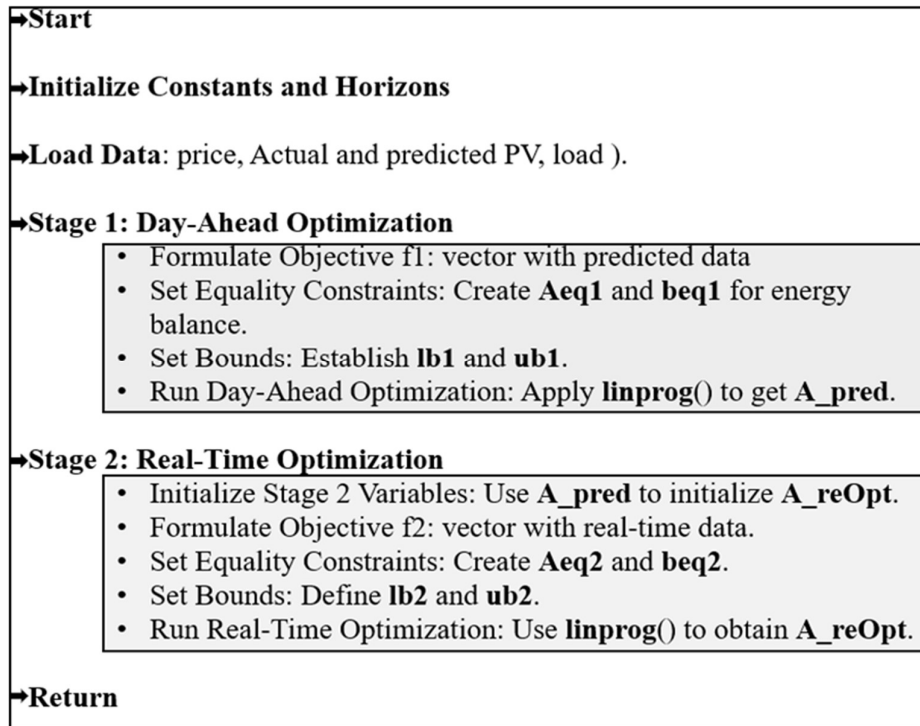


Figure 5.2. The 2-Stage Optimization Algorithm.

5.3.2.2 Re-Optimization (Stage 2)

The second stage accounts for the discrepancy between predicted and actual PV power outputs, fine-tuning the previously determined control actions from the Predictive Optimizer. The objective function at this stage is formulated as:

$$\min \sum_{i=0}^N c_i * A_{reOpt_i} + \lambda \left| A_{reOpt_i} - A_{pred_i} - \delta_i \right| \quad (5.32)$$

where δ_i denotes the deviation between the predicted and actual PV data. λ is a tunable parameter that determines the weight of the absolute deviation term in the objective function and A_{reOpt_i} are the re-optimized control actions. λ is introduced to penalize the absolute deviation between the re-optimized control actions.

5.3.2.3 Objective Function and Constraints

Objective Function: The central objective of this approach is to minimize the overall cost of electricity within the microgrid. The objective function, from which control actions are calculated, can be expressed mathematically as follows for each scenario, adapted from Equation 5.1 in Section 5.1.2.1:

$$\begin{aligned} \text{Minimize: } \sum_{i=1}^N \sum_{t=1}^T P_{gridbuy}^i(t) * C_p^{scenario,i}(t) + P_{gridsell}^i(t) * (C_p^{stage,i}(t) - \\ C_s^i) + P_{load_{NCL}}(t) * C_p^i(t) \end{aligned} \quad (5.33)$$

Where *scenario* is “*pred*” for predicted price data and “*act*” for the for actual/real-time data

Here, “*scenario*” stands for either “*pred*” when referring to predicted price data or “*act*” when referring to actual or real-time price data.

Constraints: The power inflow and outflow must be balanced for each prosumer at each time step, accounting for both predicted and actual PV output across the different scenarios. The constraint can be reformulated as:

$$P_{Load}^i(t) = P_{PV}^{stage,i}(t) + P_{BES}^i(t) + P_{gridbuy}^i(t) - P_{gridsell}^i(t) \quad (5.34)$$

All other constraints remain the same as in section 5.2.2 across both scenarios for this optimization.

5.4 Case Studies

5.4.1 SOC Estimation with Optimal Operation of a Grid-Connected Microgrid Prosumer

5.4.1.1 Simulation Setup

This case study focuses on a grid-connected microgrid prosumer, featuring a PV system of 7.5kW capacity and a 40 AH lead-acid BESS with a 5-hour discharge rate, a nominal voltage of 48V, and a discharge current rated at 17.4 A/unit. The prosumer model, as elaborated in Chapter 3, was utilized within the new structure in Fig. 5.1. Weather data, including temperature and irradiance, were gathered from our laboratory's rooftop to simulate the PV output using MATLAB Simulink. This data, alongside load profiles from the laboratory, were essential for the EMS simulation. The load management allowed the shedding of non-critical loads as part of the optimization strategy. Energy trading prices in Fig. 5.3 were based on data from the JEPX for two contrasting days in August 2019.

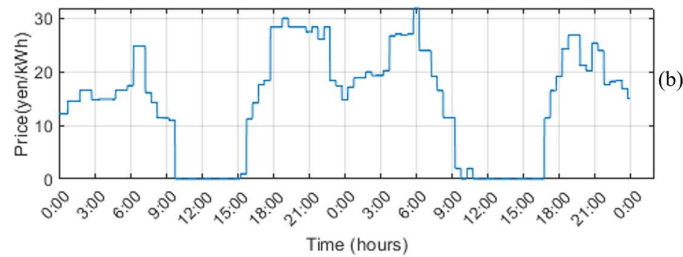


Figure 5.3. Two-day Energy Trading Prices.

5.4.1.2 Simulation Results and Discussion

The simulation aimed to optimize power flow control in a grid-connected system with bi-directional energy trading following the algorithm described in section 5.2.4 for SOC estimation and optimal grid operation. The first phase involves estimating day 2's optimal cost by simulating the system's function using predicted photovoltaic (PV) generation, consumption patterns, and energy trading prices. Here, the EMS optimizes power control by balancing PV power, battery storage, and grid interactions.

The second phase calculates the ideal SOC to initiate day 2, using the optimal cost from the first phase. This step aims to prepare the system for minimizing electricity

expenses for the next day by setting the appropriate initial SOC. A key finding emerged during this step of the simulation where the initial experiments showed that the $\lambda |SOC_{BESS}^i(T) - SOC_{target}|$ term in the optimization function typically gravitates towards a maximum SOC upper limit of 0.9%. Consequently, this term was omitted in the revised optimization function, by setting $\lambda = 0$ and the SOC_{target} was assumed as 45%. This strategic maneuver is crucial as it allows for the demonstration of the proposed algorithm.

With the initial BESS SOC for day 1 set to 25%, the essence of our study is in the 2nd phase, where the EMS executes day 1 transactions to reach the target SOC of 45% by the end of the day, as illustrated in Fig. 5.5. This involves managing the PV system's output, the BESS's charging and discharging, and grid interactions for buying or selling

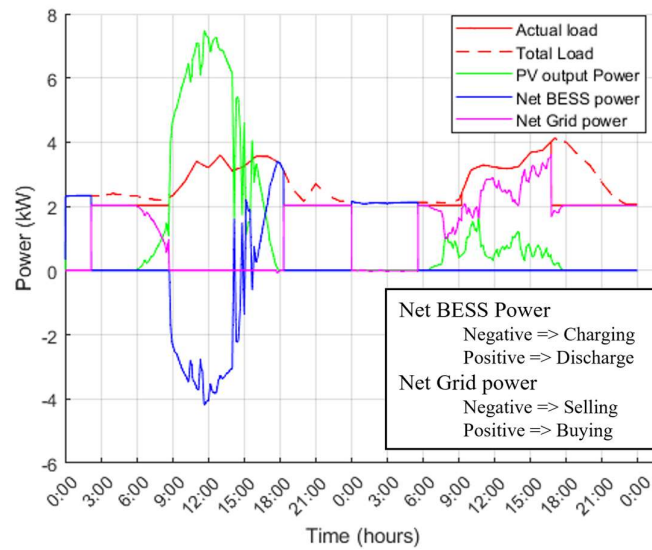


Figure 5.4. 2-day Power Flow Curve.

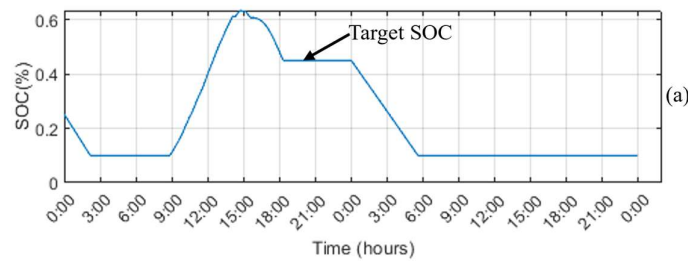


Figure 5.5. BESS SOC Over Time.

power, leading to the outcomes shown in Fig. 5.4. The EMS also controls non-critical loads, shedding them when needed to reduce electricity costs.

By comparing results from Table 5.1, where the SOC_{target} for day 2 is set against a scenario where it is not, we notice a saving of 18.17 yen. This highlights the efficiency of our proposed prosumer structure and the EMS in managing optimal power flow in a grid-connected system with two-way energy trading. The system effectively handles grid power transactions, lowers electricity costs, and maximizes renewable energy utilization. However, the current model has its limitations as it does not accommodate power purchases when PV generation surpasses the load, thus not fully leveraging low-cost periods.

Table 5.1 Optimal Costs

| SOC_{target} NOT set | | SOC_{target} set | |
|-------------------------|-------------------------|-------------------------|-------------------------|
| Day 1 Cost (Yen/kWh) | Day 2 Cost (Yen/kWh) | Day 1 Cost (Yen/kWh) | Day 2 Cost (Yen/kWh) |
| 296.33 | 713.89 | 523.47 | 468.58 |

5.4.2 The Two-Stage Optimal Control Strategy for a Grid-Connected Microgrid Prosumer

5.4.2.1 Simulation Setup

The case study considers a grid-connected prosumer, with a rated PV capacity of 5kW, including a 40 AH lead-acid BESS characterized by a 5-hour discharge rate, a nominal voltage of 48V, and a discharge current rated at 17.4 A/unit. It uses the prosumer model developed in Chapter 3, with modifications that include an optimizer with

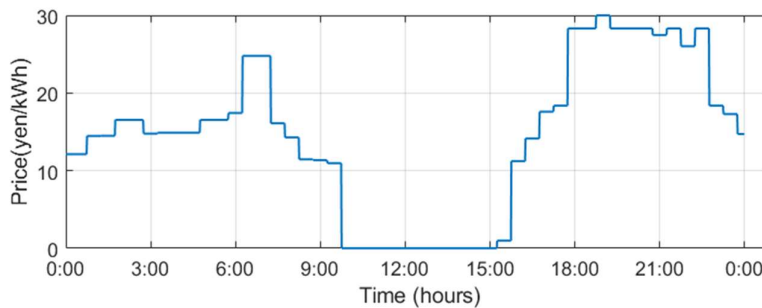


Figure 5.6. One Day Trading Prices.

consideration for both predicted and real-time PV data. The predicted PV data utilized to achieve optimal control is the output of the forecasting method we propose in Chapter 4. This setup is illustrated in Fig. 5.1 and employs the algorithm proposed in Fig. 5.2

The one-day pricing data in Fig. 5.6 is obtained from the JEPX which provides day-ahead pricing data based on their bidding market. They also offer a forward market to resolve unforeseen supply-demand mismatches that may occur in real-time. However, for simplicity, our case study does not consider this pricing adjustment and instead relies on the proposed objective function to account for this discrepancy. The data used

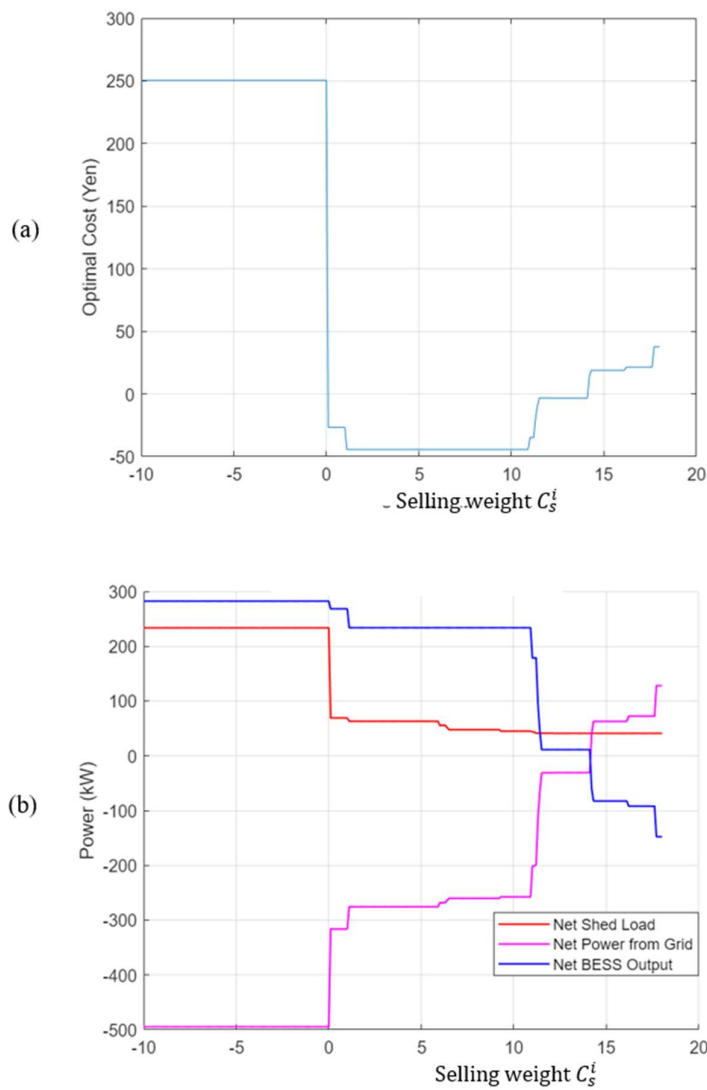


Figure 5.7. (a) Selling Weight vs Optimal Cost, (b) Selling Weight vs 24-hour Net Power Management Strategies

corresponds to the first day of August 2019, a sunny day. The predicted and real-time weather data also correspond to this day.

The simulation assumes a stable grid power supply and focuses on minimizing the cost of power purchased from the grid while ensuring the power security of the critical load. The results of the simulation follow, where the results of stage 1 and stage 2 of the optimization are compared as the penalty λ that represents the deviation between the predicted and actual control actions is varied.

5.4.2.2 Simulation Result and Discussion

Initially, the simulation is run based on Monte Carlo simulations to determine the optimum value of the selling weight, C_s^i which is found to be constant between 1.1 yen and 10.9 yen as can be observed in Fig. 5.7 (a). This figure corresponds to the minimum optimal cost of -44.3 yen as C_s^i is varied. At this constant C_s^i , there is a relatively constant balance among the net BESS output, net Power from the Grid and the Net shed load. A setting outside this range results in a sub-optimal solution as portrayed by Fig. 5.7(b). The proceeding simulations consider the case $C_s^i = 1.1$ Yen.

The Stage 1 Optimization, which is predictive in Fig. 5.8 (a), yielded an optimal cost of 3.07, indicating that the microgrid's initial operation plan based on predicted PV power output is economically sound. This initial stage sets the groundwork for subsequent energy transactions and management within the microgrid.

Transitioning to Stage 2 Optimization in Fig. 5.8 (b), where the actual PV power is considered, the optimal cost plummets to -26.60 , significantly undercutting the Stage 1 cost. This dramatic reduction suggests that the actual PV generation exceeded expectations, or the energy market offered more favorable trading prices than anticipated, allowing the microgrid to operate at a surplus or even turn a profit.

The parameter λ in Fig. 5.9 (a) is observed to exert a noticeable influence on this optimization process. When λ is negative, the system seems to diverge from the predicted course of action, which is likely an adaptation to unexpectedly beneficial conditions, such as a surplus in PV generation or advantageous energy prices. This divergence enables the microgrid to optimize its performance beyond the initial predictions. Conversely, a positive λ imposes a penalty for straying from the predicted actions, compelling the system to stick to the pre-established plan. While this can be beneficial for maintaining

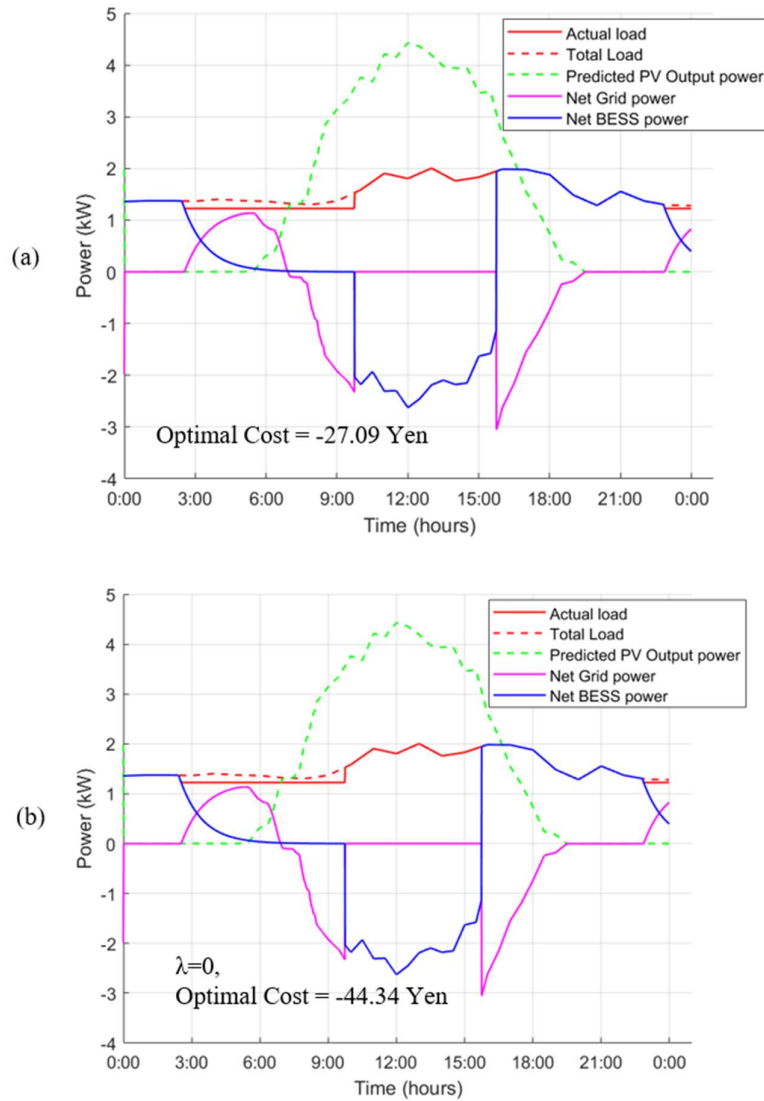


Figure 5.8. (a) The Stage 1 Optimal Result, (b) The Stage 2 Optimal Result

cost-effectiveness and reliability, an overly stringent λ could stifle the system's ability to adapt to potentially favorable unforeseen circumstances.

The intricate relationship between λ and the cumulative microgrid's power management strategies with respect to the energy trading prices over the 24-hour simulation period is exemplified in Fig 5.9 (b). The graph shows that as λ increases from negative to positive, there is a minimum point near $\lambda = 0$ where the optimal cost is at its lowest, suggesting that at this point, the balance between the cost of the solution and the penalty for deviation is optimal. As λ nears zero, we observe significant fluctuations in the net power from the grid and the BESS output. This indicates a dynamic adjustment

process, where the microgrid seeks to reconcile the predicted and actual scenarios to optimize cost outcomes. The insights from this graph can be crucial for determining the appropriate value of λ to use in practice to ensure economic efficiency while maintaining system robustness against the inherent uncertainties of solar PV outputs.

The resulting negative optimal cost from the re-optimization process is particularly striking, as it suggests that the microgrid is not just economically viable but also capable of generating excess energy or financial gain.

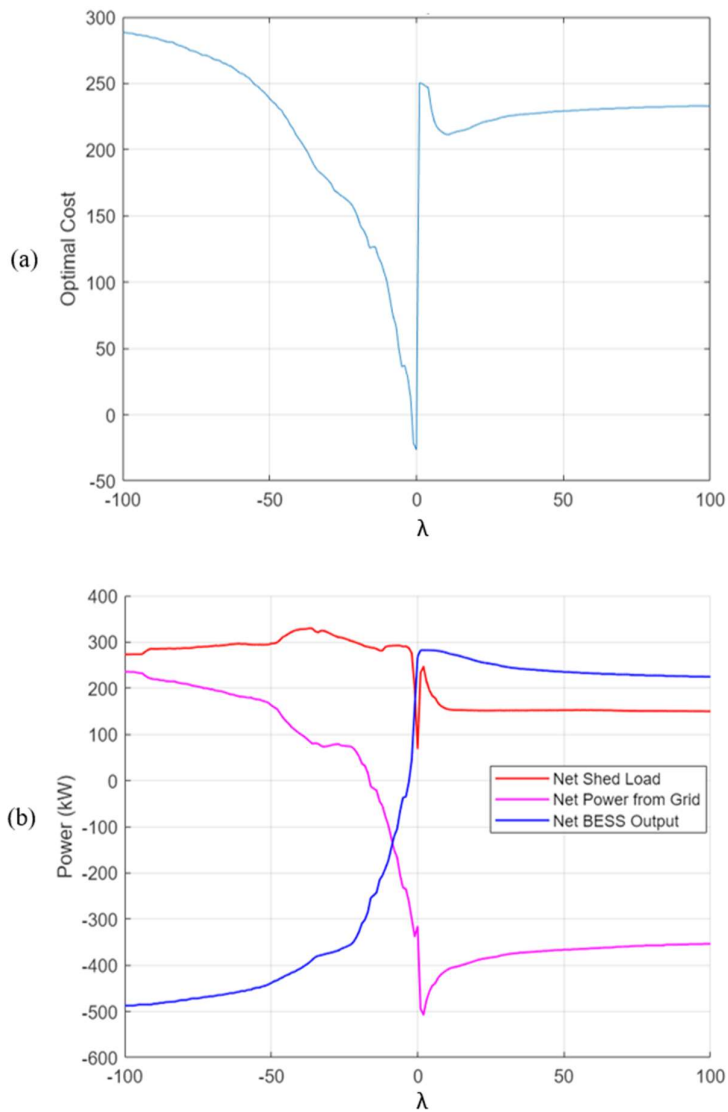


Figure 5.9. (a) λ vs Optimal Cost, (b) λ vs 24-hour Net Power Management Strategies

5.5 Conclusion

The Two-Stage Optimal Control Strategy and SOC Estimation with Optimal Operation of a Grid-Connected Microgrid Prosumer delineated in this research exhibits a robust framework for managing the economic operations of microgrids, particularly those incorporating solar PV systems. The study's findings, encapsulated by the optimal costs derived from predictive and actual PV data, demonstrate a significant enhancement in cost efficiency when transitioning from a predictive model to one that incorporates real-time data. The optimization process, particularly in the re-optimization stage, underscores the value of integrating actual PV output, which can result in optimal costs that not only minimize expenses but potentially yield revenue, as evidenced by the negative optimal cost obtained.

The critical role of the tunable parameter λ in the re-optimization process emerges as a pivotal factor in the strategic operation of the microgrid. Its calibrated manipulation allows the system to adaptively respond to the real-time discrepancies between predicted and actual conditions, optimizing the trade-off between strict adherence to predictions and the flexibility to capitalize on unforeseen advantageous circumstances.

The results of this study offer promising directions for future research, including the exploration of an adaptive λ strategy, further economic impact studies, and the potential for real-world applications. The success of the Two-Stage Optimal Control Strategy in achieving a dynamic and economically viable operation of microgrids significantly contributes to the discourse on renewable energy integration and sustainable power management. As the world moves towards a greater reliance on renewable energy sources, the methodologies and insights gleaned from this research will undoubtedly play an influential role in shaping future energy systems that are both resilient and economically beneficial.

Chapter 6: Conclusion and Future Work

6.1 Summary of Findings

This thesis has made significant strides in advancing the field of prosumer-based microgrid operations, aligning closely with the overarching aim of advancing solar power prediction and microgrid optimization. The development of a comprehensive resilient prosumer model integrates BESS, PV systems, and EMS, optimizing energy usage and storage. This model, particularly effective in disaster scenarios, has proven instrumental in enhancing microgrid resilience, as validated through MATLAB Simulink simulations. The accurate PV power prediction model developed under this research utilizes machine learning algorithms, significantly surpassing existing models in both accuracy and reliability.

6.2 Contributions

The primary contributions of this thesis are as follows:

- **Development of a Comprehensive Resilient Prosumer Model:** Enhanced by its resilience-hardening capabilities, this model innovatively integrates PV curtailment, flexible load switching, and non-critical load shedding that can be integrated with state-of-the-art optimization and machine learning techniques. It represents a substantial leap in simulating dynamic prosumer behavior, providing pragmatic approaches for harmonizing PV generation, BESS, and load management within microgrid frameworks. Specifically designed for microgrid applications, the model is a pivotal contribution to the development of sustainable, resilient, and efficient global energy systems, proving particularly valuable in the context of post-disaster recovery and resilience building.
- **Enhanced Decision Support Systems:** The implementation of real-time monitoring and alert systems revolutionizes how operators interact with and manage microgrid systems, with direct implications for operational efficiency and system reliability.
- **Innovative Solar Power Prediction Methods:** The Weather-Based Clustering Feedforward Neural Networks represent a significant advancement in solar power forecasting, particularly in terms of accuracy and computational efficiency.

which is seen to improve by 91%, making them practical for real-world applications.

- **Optimized Day-Ahead and Real-Time Energy Management:** The introduction of MPC and RHO for optimizing microgrid operations underlines the potential for more resilient and adaptable energy systems in real-time scenarios, balancing optimization with computational burden.

6.3 Practical Implications

The practical implications of our research are extensive and directly relevant to the objectives. Microgrid operators can now manage energy systems more effectively, responding proactively to changes and challenges. Our solar power prediction models offer enhanced accuracy and efficiency, crucial for grid management and energy allocation in operational solar power plants. The optimization techniques we introduced can significantly enhance the economic operations of microgrids, particularly those incorporating solar PV systems. This balance between theoretical advancement and practical applicability underscores the potential for these proposed methods to be implemented in actual microgrid systems, particularly those incorporating solar PV systems. They offer scalable solutions that can be adapted to various real-world scenarios, emphasizing their business potential and relevance in today's energy market.

6.4 Limitations and Future Work

While making substantial contributions, this research also acknowledges its limitations, most have been exhaustively described after each major chapter. Future work should aim to expand on these areas:

- **Broadening Weather Scenarios and Disaster Types:** To further test and enhance the resilience and adaptability of the models.
- **Economic Feasibility Studies:** Conducting in-depth studies on the economic aspects of energy trading and the cost-effectiveness of prosumer models to understand their business potential.
- **Scaling Up the Study:** To include a larger network of prosumers, thereby understanding the dynamics in a more complex system and exploring its business implications.

-
- **Integrating Additional Renewable Energy Sources:** Exploring the coordination of various renewable energy sources with PV systems and BESS for enhanced system resilience. and explore new business opportunities in renewable energy.
 - **Further Optimization Techniques:** Developing more advanced methods and control strategies, focusing on practicality and scalability in real-world applications.

In conclusion, this thesis not only advances the state-of-the-art in solar power prediction and microgrid optimization but also lays a solid foundation for future research and development in the field of renewable energy systems and prosumer-based microgrid operations. It not only pushes the boundaries towards a more sustainable, efficient, and resilient energy future but also opens avenues for practical application and significant business potential.

References

- [1] Y. Tanioka, Y. Sasaki, Y. Matsumoto, K. S. Mumbere, A. Fukuhara, S. Sekizaki, N. Yorino, Y. Zoka, “A Study on Power Sharing Control Considering State of Charge of Prosumers Batteries in Local Community,” *The Transactions of the Institute of Electrical Installation Engineers of Japan*, vol. 41, no. 3, pp. 19–28, 2021.
- [2] K. S. Mumbere, Y. Sasaki, N. Yorino, Y. Zoka, Y. Tanioka, and A. Bedawy, “A Resilient Prosumer Model for Microgrid Communities with High PV Penetration,” *Energies 2023, Vol. 16, Page 621*, vol. 16, no. 2, p. 621, Jan. 2023.
- [3] Y. Sasaki, S. Enomoto, N. Yorino, Y. Zoka, and M. S. Kihembo, “Solar Power Prediction Using Iterative Network Pruning Technique for Microgrid Operation,” in *2021 IEEE PES Innovative Smart Grid Technologies - Asia (ISGT Asia)*, 2021, pp. 1–5.
- [4] S. Enomoto, Y. Sasaki, N. Yorino, Y. Zoka, and M. S. Kihembo, “Solar Power Prediction Using Iterative Network Pruning Technique for Renewable-based Microgrid,” in *2021 IEEE 12th International Workshop on Computational Intelligence and Applications (IWCIA)*, 2021, pp. 1–6.
- [5] S. K. Mumbere, Y. Tanioka, S. Matsumoto, Y. Sasaki, Y. Zoka, and N. Yorino, “Distributed control of Islanded Microgrids Based on Battery SOC in Disaster situations,” in *2020 IEEE PES Innovative Smart Grid Technologies Europe (ISGT-Europe)*, 2020, pp. 1226–1230.
- [6] M. K. Samuel, A. Fukuhara, Y. Sasaki, Y. Zoka, N. Yorino, and Y. Tanioka, “A Novel Energy Management Approach to Networked Microgrids for Disaster Resilience,” in *2021 International Symposium on Devices, Circuits and Systems (ISDCS)*, 2021.
- [7] S. K. Mumbere, A. Fukuhara, Y. Sasaki, A. Bedawy, Y. Zoka, and N. Yorino, “Development of An Energy Management System Tool for Disaster Resilience in Islanded Microgrid Networks,” in *2021 20th International Symposium on Communications and Information Technologies (ISCIT)*, 2021, pp. 97–100.
- [8] K. S. Mumbere, Y. Sasaki, N. Yorino, Y. Zoka, A. Bedawy, and Y. Tanioka, “An Interconnected Prosumer Energy Management System Model for Improved Outage Resilience,” in *2022 IEEE PES/IAS PowerAfrica*, 2022, pp. 1–5.
- [9] Y. Sasaki, M. Ueoka, N. Yorino, Y. Zoka, A. Bedawy, and M. S. Kihembo, “Dynamic Economic Load Dispatch with Emergency Demand Response for Microgrid System Operation,” in *2021 22nd International Middle East Power Systems Conference (MEPCON)*, 2021, pp. 497–502.
- [10] M. K. Samuel, A. Fukuhara, Y. Sasaki, Y. Zoka, N. Yorino, and Y. Tanioka, “Development of An Energy Management Tool for Community Disaster Resilience,” *電気学会研究会資料. PE/電気学会電力技術研究会 [編]*, vol. 2021, no. 1–8, pp. 1–6, 2021.
- [11] K. S. Mumbere, Y. Sasaki, N. Yorino, Y. Zoka, A. Bedawy, and Y. Tanioka, “Prosumers Control Strategy for Microgrid Energy Management System,” *電気学会研究会資料. PE/電気学会電力技術研究会 [編]*, vol. 2022, no. 65-76 · 78-83, pp. 53–57, 2022.
- [12] M. K. Samuel, Y. Tanioka, S. Matsumoto, Y. Sasaki, Y. Zoka, and N. Yorino, “Battery Management System for Microgrid Customers,” *電気学会研究会資料. PE/電気学会電力技術研究会 [編]*, vol. 2019, no. 47-53 · 55-60 · 62-64, pp. 11–16, 2019.

-
- [13] A. Bedawy, N. Yorino, Y. Sasaki, Y. Zoka, K. S. Mumbere, and R. Kubo, "Distributed Agent-Based Voltage Control Approach for Active Distribution Systems," in *Emerging Electronic Devices, Circuits and Systems: Select Proceedings of EEDCS Workshop Held in Conjunction with ISDCS 2022*, 2023, pp. 349–362.
- [14] K. S. Mumbere, Y. Sasaki, N. Yorino, A. Fukuhara, Y. Zoka, A. Bedawy, Y. Tanioka, "Prosumer Control Strategy for A Robust Microgrid Energy Management System," in *2021 IEEE PES Innovative Smart Grid Technologies Europe (ISGT Europe)*, 2021, pp. 1–6.
- [15] S. K. Mumbere, Y. Tanioka, Y. Matsumoto, A. Fukuhara, Y. Sasaki, Y. Zoka, N. Yorino, "A Novel Energy Management Technique for Shared Solar and Storage Resources in Remote Communities," in *2020 IEEE PES/IAS PowerAfrica*, 2020, pp. 1–5.
- [16] Y. Sasaki, M. Ueoka, Y. Uesugi, N. Yorino, Y. Zoka, A. Bedawy, M.S. Kihembo, "A Robust Economic Load Dispatch in Community Microgrid Considering Incentive-based Demand Response," *IFAC-PapersOnLine*, vol. 55, no. 9, pp. 389–394, 2022.
- [17] S. K. Mumbere, Y. Matsumoto, A. Fukuhara, A. Bedawy, Y. Sasaki, Y. Zoka, N. Yorino, Y. Tanioka, "An Energy Management System for Disaster Resilience in Islanded Microgrid Networks," in *2021 IEEE PES/IAS PowerAfrica*, 2021, pp. 1–5.
- [18] A. Bedawy, N. Yorino, Y. Sasaki, Y. Zoka, K. S. Mumbere, R. Kubo, "Distributed Agent-Based Voltage Control Approach for Active Distribution Systems," in *Emerging Electronic Devices, Circuits and Systems*, Springer Nature Singapore, 2023, pp. 349–362.
- [19] R. M. Elavarasan, G. Shafiullah, S. Padmanaban, N.M. Kumar, A. Annam, A.M. Vetrichelvan, L. Mihet-Popa, J.B. Holm-Nielson, "A Comprehensive Review on Renewable Energy Development, Challenges, and Policies of Leading Indian States with an International Perspective," *IEEE Access*, vol. 8, pp. 74432–74457, 2020.
- [20] W. U. Rehman, A.R. Bhatti, A.B. Awan, I.A. Sajjad, A.A. Khan, R. Bo, S.S Haroon, S. Amin, I. Tlili, O. Oboreh-Snapps, "The penetration of renewable and sustainable energy in Asia: A state-of-the-art review on net-metering," *IEEE Access*, vol. 8, pp. 170364–170388, 2020.
- [21] F. R. Alharbi and D. Csala, "GCC Countries' Renewable Energy Penetration and the Progress of Their Energy Sector Projects," *IEEE Access*, vol. 8, pp. 211986–212002, 2020.
- [22] S. Xu, Y. Xue, and L. Chang, "Review of Power System Support Functions for Inverter-Based Distributed Energy Resources- Standards, Control Algorithms, and Trends," *IEEE Open Journal of Power Electronics*, vol. 2, pp. 88–105, Feb. 2021.
- [23] António Guterres, "The Sustainable Development Goals Report," 2023: Special Edition. Accessed: Oct. 12, 2023. [Online]. Available: <https://unstats.un.org/sdgs/report/2023/>
- [24] Y. Kurachi, H. Morishima, H. Kawata, R. Shibata, K. Bunya, and J. Moteki, "Challenges for Japan's Economy in the Decarbonization Process," Jun. 2022. Accessed: Oct. 12, 2023. [Online]. Available: https://www.boj.or.jp/en/research/brp/ron_2022/ron220609a.htm
- [25] World Bank, "Tracking SDG 7: The Energy Progress Report," World Bank Bank Reports. Accessed: Oct. 12, 2023. [Online]. Available: <https://trackingsdg7.esmap.org/time>

-
- [26] D. E. Olivares, A. Mehrizi-Sani, A.H. Etemadi, C.A. Cañizares, R. Iravani, M. Kazerani, A.H. Hajimiragha, O. Gomis-Bellmunt, M. Saeedifard, R. Palma-Behnke *et al.*, “Trends in microgrid control,” *IEEE Trans Smart Grid*, vol. 5, no. 4, pp. 1905–1919, 2014.
- [27] M. Farrokhhabadi, D. Lagos, R.W. Weis, M. Paolone, M. Liserre, L. Meegahapola, M. Kabalan, A.H. Hajimiragha, D. Peralta, M.A. Elizondo *et al.*, “Microgrid Stability Definitions, Analysis, and Examples,” *IEEE Transactions on Power Systems*, vol. 35, no. 1, pp. 13–29, Jan. 2020.
- [28] A. S. Bahaj and P. A. B. James, “Electrical Minigrids for Development: Lessons from the Field,” *Proceedings of the IEEE*, vol. 107, no. 9, pp. 1967–1980, Sep. 2019.
- [29] O. Lavagne d’Ortigue, D. Saygin, J. Skeer, S. Vinci, and D. Gielen, “OFF-GRID RENEWABLE ENERGY SYSTEMS: STATUS AND METHODOLOGICAL ISSUES About IRENA,” 2015.
- [30] A. Bedawy, N. Yorino, K. Mahmoud, and M. Lehtonen, “An Effective Coordination Strategy for Voltage Regulation in Distribution System Containing High Intermittent Photovoltaic Penetrations,” *IEEE Access*, 2021.
- [31] N. Yorino, H. Taenaka, A. Bedawy, Y. Sasaki, and Y. Zoka, “Novel agent-based voltage control methods for PV prosumers using nodal price,” *Electric Power Systems Research*, vol. 213, p. 108407, Dec. 2022.
- [32] Y. Sasaki, N. Yorino, Y. Zoka, and F. Wahyudi, “Robust stochastic dynamic load dispatch against uncertainties,” *IEEE Trans Smart Grid*, vol. 9, no. 6, pp. 5535–5542, Nov. 2018.
- [33] T. Dragicevic, X. Lu, J. C. Vasquez, and J. M. Guerrero, “DC Microgrids - Part I: A Review of Control Strategies and Stabilization Techniques,” *IEEE Trans Power Electron*, vol. 31, no. 7, pp. 4876–4891, Jul. 2016.
- [34] T. Dragičević, X. Lu, J. C. Vasquez, and J. M. Guerrero, “DC Microgrids - Part II: A Review of Power Architectures, Applications, and Standardization Issues,” *IEEE Trans Power Electron*, vol. 31, no. 5, pp. 3528–3549, May 2016.
- [35] M. Ciobotaru, R. Teodorescu, and F. Blaabjerg, “A new single-phase PLL structure based on second order generalized integrator,” *PESC Record - IEEE Annual Power Electronics Specialists Conference*, 2006.
- [36] Y. Yang, L. Hadjidemetriou, F. Blaabjerg, and E. Kyriakides, “Benchmarking of phase locked loop based synchronization techniques for grid-connected inverter systems,” *9th International Conference on Power Electronics - ECCE Asia: “Green World with Power Electronics”, ICPE 2015-ECCE Asia*, pp. 2167–2174, Jul. 2015.
- [37] J. Xu, H. Qian, Y. Hu, S. Bian, and S. Xie, “Overview of SOGI-Based Single-Phase Phase-Locked Loops for Grid Synchronization under Complex Grid Conditions,” *IEEE Access*, vol. 9, pp. 39275–39291, 2021.
- [38] D. Basic, “Input current interharmonics of variable-speed drives due to motor current imbalance,” *IEEE Transactions on Power Delivery*, vol. 25, no. 4, pp. 2797–2806, Oct. 2010.
- [39] Z. Xin, X. Wang, Z. Qin, M. Lu, P. C. Loh, and F. Blaabjerg, “An Improved Second-Order Generalized Integrator Based Quadrature Signal Generator,” *IEEE Trans Power Electron*, vol. 31, no. 12, pp. 8068–8073, Dec. 2016.

-
- [40] M. A. Mohamed, T. Chen, W. Su, and T. Jin, "Proactive Resilience of Power Systems against Natural Disasters: A Literature Review," *IEEE Access*, vol. 7, pp. 163778–163795, 2019.
- [41] Y. Wang, C. Chen, J. Wang, and R. Baldick, "Research on Resilience of Power Systems under Natural Disasters - A Review," *IEEE Transactions on Power Systems*, vol. 31, no. 2, pp. 1604–1613, Mar. 2016.
- [42] Y. Sasaki, T. Tsurumi, N. Yorino, Y. Zoka, A.B. Rehiara, "Real-time dynamic economic load dispatch integrated with renewable energy curtailment," <http://www.tandfonline.com/action/authorSubmission?journalCode=tjee20&page=instructions>, vol. 9, no. 1, pp. 85–92, Jan. 2019.
- [43] H. Masrur, T. Senjyu, M. R. Islam, A. Z. Kouzani, and M. A. P. Mahmud, "Resilience-Oriented Dispatch of Microgrids Considering Grid Interruptions," *IEEE Transactions on Applied Superconductivity*, vol. 31, no. 8, Nov. 2021.
- [44] Y. Wang, A. O. Rousis, and G. Strbac, "On microgrids and resilience: A comprehensive review on modeling and operational strategies," *Renewable and Sustainable Energy Reviews*, vol. 134. Elsevier Ltd, p. 110313, Dec. 01, 2020.
- [45] C. Chen, J. Wang, F. Qiu, and D. Zhao, "Resilient Distribution System by Microgrids Formation after Natural Disasters," *IEEE Trans Smart Grid*, vol. 7, no. 2, pp. 958–966, Mar. 2016.
- [46] "Resilient Distribution System by Microgrids Formation After Natural Disasters - IEEE Journals & Magazine." Accessed: Feb. 24, 2020. [Online]. Available: <https://ieeexplore.ieee.org/document/7127029>
- [47] S. Afzal, H. Mokhlis, H. Azil Lllias, N. Nadzirah Mansor, and H. Shareef, "State-of-the-art review on power system resilience and assessment techniques," *IET Generation, Transmission & Distribution*, vol. 14, no. 25, pp. 6107–6121, Dec. 2020.
- [48] C. Abbey, D. Cornforth, N. Hatzigiorgiou; K. Hirose, A. Kwasinski, E. Kyriakides, G. Platt, L. Reye, S. Suryanarayanan , "Powering through the storm: Microgrids operation for more efficient disaster recovery," *IEEE Power and Energy Magazine*, vol. 12, no. 3, pp. 67–76, 2014.
- [49] "IEC 63152:2020 Smart cities - City service continuity against disasters - The role of the electrical supply," Jul. 2020.
- [50] T. Krause, R. Ernst, B. Klaer, I. Hacker, and M. Henze, "Cybersecurity in Power Grids: Challenges and Opportunities," *Sensors*, vol. 21, no. 18, p. 6225, Sep. 2021.
- [51] S. Ahmad, M. Shafiullah, C. B. Ahmed, and M. Alowaifeer, "A Review of Microgrid Energy Management and Control Strategies," *IEEE Access*, vol. 11, pp. 21729–21757, 2023.
- [52] T. Pamulapati, M. Cavus, I. Odigwe, A. Allahham, S. Walker, and D. Giaouris, "A Review of Microgrid Energy Management Strategies from the Energy Trilemma Perspective," *Energies (Basel)*, vol. 16, no. 1, 2023.
- [53] S. W. Blume, "Interconnected Power Systems," *Electric Power System Basics for the Nonelectrical Professional*, pp. 165–186, Nov. 2016.
- [54] M. Sato, Y. Sasaki, Y. Zoka, and N. Yorino, "Day-ahead Generation Schedule Considering Community Microgrid's Uncertainties," in *2022 IEEE PES Innovative Smart Grid Technologies - Asia (ISGT Asia)*, 2022, pp. 190–194.

-
- [55] W. Wang, N. Yorino, Y. Sasaki, Y. Zoka, A. Bedawy, and S. Kawauchi, "Adaptive MPC-Based Cooperative Frequency Control for Community Microgrid," in *2022 4th International Conference on Smart Power & Internet Energy Systems (SPIES)*, 2022, pp. 1434–1438.
- [56] L. Ma, N. Yorino, Y. Sasaki, Y. Zoka, K. Khorasani, and A. B. Rehiara, "A Simple and Reliable Photovoltaic Forecast for Reliable Power System Operation Control," *IFAC-PapersOnLine*, vol. 51, no. 28, pp. 161–166, 2018.
- [57] N. Yorino, M. Abdillah, Y. Sasaki, and Y. Zoka, "Robust Power System Security Assessment Under Uncertainties Using Bi-Level Optimization," *IEEE Transactions on Power Systems*, vol. 33, no. 1, pp. 352–362, 2018.
- [58] Y. Sasaki, N. Yorino, Y. Zoka, and F. I. Wahyudi, "Robust Stochastic Dynamic Load Dispatch Against Uncertainties," *IEEE Trans Smart Grid*, vol. 9, no. 6, pp. 5535–5542, 2018.
- [59] "IEEE Power & Energy Society Microgrid Stability Definitions, Analysis, and Modeling PREPARED BY THE IEEE PES Power System Dynamic Performance Committee IEEE PES Task Force on Microgrid Stability Analysis and Modeling PES-TR66," 2018.
- [60] J. Parra-Domínguez, E. Sánchez, and Á. Ordóñez, "The Prosumer: A Systematic Review of the New Paradigm in Energy and Sustainable Development," *Sustainability*, vol. 15, no. 13, 2023.
- [61] M. Gržanić, T. Capuder, N. Zhang, and W. Huang, "Prosumers as active market participants: A systematic review of evolution of opportunities, models and challenges," *Renewable and Sustainable Energy Reviews*, vol. 154, p. 111859, 2022.
- [62] J. Hashimoto, T. S. Ustun, M. Suzuki, S. Sugahara, M. Hasegawa, and K. Otani, "Advanced Grid Integration Test Platform for Increased Distributed Renewable Energy Penetration in Smart Grids," *IEEE Access*, vol. 9, pp. 34040–34053, 2021.
- [63] A. A. Khodadoost Arani, G. B. Gharehpetian, and M. Abedi, "Review on Energy Storage Systems Control Methods in Microgrids," *International Journal of Electrical Power & Energy Systems*, vol. 107, pp. 745–757, May 2019.
- [64] A. U. Rehman, Z. Wadud, R.M. Elavarasan, G. Hafeez, I. Khan, Z. Shafiq, H.H. Alhelou,, "An Optimal Power Usage Scheduling in Smart Grid Integrated with Renewable Energy Sources for Energy Management," *IEEE Access*, vol. 9, pp. 84619–84638, 2021.
- [65] A. Singaravelan, K. M., J. P. Ram, G. B., and Y. J. Kim, "Application of Two-Phase Simplex Method (TPSM) for an Efficient Home Energy Management System to Reduce Peak Demand and Consumer Consumption Cost," *IEEE Access*, vol. 9, pp. 63591–63601, 2021.
- [66] D. Michaelson, H. Mahmood, and J. Jiang, "A Predictive Energy Management System Using Pre-Emptive Load Shedding for Islanded Photovoltaic Microgrids," *IEEE Transactions on Industrial Electronics*, vol. 64, no. 7, pp. 5440–5448, Jul. 2017.
- [67] H. T. Dinh, J. Yun, D. M. Kim, K. H. Lee, and D. Kim, "A Home Energy Management System with Renewable Energy and Energy Storage Utilizing Main Grid and Electricity Selling," *IEEE Access*, vol. 8, pp. 49436–49450, 2020.

-
- [68] P. S. Kumar, R. P. S. Chandrasena, V. Ramu, G. N. Srinivas, and K. V. S. M. Babu, "Energy Management System for Small Scale Hybrid Wind Solar Battery Based Microgrid," *IEEE Access*, vol. 8, pp. 8336–8345, 2020.
- [69] P. Mathew, S. Madichetty, and S. Mishra, "A Multilevel Distributed Hybrid Control Scheme for Islanded DC Microgrids," *IEEE Syst J*, vol. 13, no. 4, pp. 4200–4207, Dec. 2019.
- [70] N. Krishnan, K. R. Kumar, and C. S. Inda, "How solar radiation forecasting impacts the utilization of solar energy: A critical review," *J Clean Prod*, vol. 388, p. 135860, 2023.
- [71] K. J. Iheanetu, "Solar Photovoltaic Power Forecasting: A Review," *Sustainability*, vol. 14, no. 24, 2022.
- [72] N. Rahimi, S. Park, W. Choi, B. Oh, S. Kim, Y. Cho, S. Ahn, C. Chong, D. Kim, D.; C. Jin, *et al.*, "A Comprehensive Review on Ensemble Solar Power Forecasting Algorithms," *Journal of Electrical Engineering & Technology*, vol. 18, no. 2, pp. 719–733, 2023.
- [73] H. Ye, B. Yang, Y. Han, and N. Chen, "State-Of-The-Art Solar Energy Forecasting Approaches: Critical Potentials and Challenges," *Front Energy Res*, vol. 10, 2022.
- [74] G. Sahin, G. Isik, and W. G. J. H. M. van Sark, "Predictive modeling of PV solar power plant efficiency considering weather conditions: A comparative analysis of artificial neural networks and multiple linear regression," *Energy Reports*, vol. 10, pp. 2837–2849, 2023.
- [75] F. Petropoulos, D. Apiletti, V. Assimakopoulos, M.Z. Babai, D. K. Barrow, S. Ben Taieb, C. Bergmeir, R.J. Bessa, J. Bijak, J.; J.E. Boylan, *et al.*, "Forecasting: theory and practice," *Int J Forecast*, vol. 38, no. 3, pp. 705–871, 2022.
- [76] R. A. Zemouri, N. Omri, F. Fnaiech, N. Zerhouni, and N. Fnaiech, "A new growing pruning deep learning neural network algorithm (GP-DLNN)," *Neural Comput Appl*, pp. 1–17, 2019, [Online].
- [77] P. Kumari and D. Toshniwal, "Extreme gradient boosting and deep neural network based ensemble learning approach to forecast hourly solar irradiance," *J Clean Prod*, vol. 279, p. 123285, 2021.
- [78] N. Dong, J.-F. Chang, A.-G. Wu, and Z.-K. Gao, "A novel convolutional neural network framework based solar irradiance prediction method," *International Journal of Electrical Power & Energy Systems*, vol. 114, p. 105411, 2020.
- [79] S. M. J. Jalali, S. Ahmadian, A. Kavousi-Fard, A. Khosravi, and S. Nahavandi, "Automated Deep CNN-LSTM Architecture Design for Solar Irradiance Forecasting," *IEEE Trans Syst Man Cybern Syst*, vol. 52, no. 1, pp. 54–65, 2022.
- [80] S. Ghimire, R. C. Deo, D. Casillas-Pérez, S. Salcedo-Sanz, E. Sharma, and M. Ali, "Deep learning CNN-LSTM-MLP hybrid fusion model for feature optimizations and daily solar radiation prediction," *Measurement*, vol. 202, p. 111759, 2022.
- [81] A. Hussain, V.-H. Bui, and H.-M. Kim, "Robust Optimal Operation of AC/DC Hybrid Microgrids Under Market Price Uncertainties," *IEEE Access*, vol. 6, pp. 2654–2667, 2018.
- [82] L. Ahmethodžić, M. Musić, and S. Huseinbegović, "Microgrid Energy Management: Classification, Review and Challenges," *CSEE Journal of Power and Energy Systems*, vol. 9, no. 4, pp. 1425–1438, 2023.

-
- [83] M. Asghari, A. M. Fathollahi-Fard, S. M. J. Mirzapour Al-e-hashem, and M. A. Dulebenets, "Transformation and Linearization Techniques in Optimization: A State-of-the-Art Survey," *Mathematics*, vol. 10, no. 2, 2022.
- [84] C. Li, A. J. Conejo, P. Liu, B. P. Omell, J. D. Sirola, and I. E. Grossmann, "Mixed-integer linear programming models and algorithms for generation and transmission expansion planning of power systems," *Eur J Oper Res*, vol. 297, no. 3, pp. 1071–1082, 2022.
- [85] T. Kannengießer, M. Hoffmann, L. Kotzur, P. Stenzel, F. Schuetz, K. Peters, K.; S. Nykamp, D. Stolten, M. Robinius, "Reducing Computational Load for Mixed Integer Linear Programming: An Example for a District and an Island Energy System," *Energies (Basel)*, vol. 12, no. 14, 2019.
- [86] L. A. L. Zaneti, N. B. Arias, M. C. de Almeida, and M. J. Rider, "Sustainable charging schedule of electric buses in a University Campus: A rolling horizon approach," *Renewable and Sustainable Energy Reviews*, vol. 161, p. 112276, 2022.
- [87] J. Silvente, G. M. Kopanos, E. N. Pistikopoulos, and A. Espuña, "A rolling horizon optimization framework for the simultaneous energy supply and demand planning in microgrids," *Appl Energy*, vol. 155, pp. 485–501, 2015.
- [88] X. Wang, Z. Wang, Y. Mu, Y. Deng, and H. Jia, "Rolling horizon optimization for real-time operation of prosumers with Peer-to-Peer energy trading," *Energy Reports*, vol. 9, pp. 321–328, 2023.
- [89] Z. Zhang , O. Babayomi, T. Dragicevic, R. Heydari, C. Garcia, J. Rodriguez, R. Kennel , "Advances and opportunities in the model predictive control of microgrids: Part I–primary layer," *International Journal of Electrical Power & Energy Systems*, vol. 134, p. 107411, 2022.
- [90] K. Akyol, "Comparing of deep neural networks and extreme learning machines based on growing and pruning approach," *Expert Syst Appl*, vol. 140, p. 112875, 2020.
- [91] G. Castellano, A. M. Fanelli, and M. Pelillo, "An iterative pruning algorithm for feedforward neural networks," *IEEE Trans Neural Netw*, vol. 8, no. 3, pp. 519–531, 1997.
- [92] F. Grimaccia, S. Leva, M. Mussetta, and E. Ogliari, "ANN Sizing Procedure for the Day-Ahead Output Power Forecast of a PV Plant," *Applied Sciences*, vol. 7, no. 6, 2017.
- [93] K. S. Mumbere, N. Yorino, Y. Sasaki, A. Bedawy, Y. Tanioka Y. Zoka, C. Krifa, "Day-Ahead Optimal Resilient Energy Management for Grid-Connected Prosumer Microgrids," Paris, Oct. 2023.
- [94] N. Yorino, S. Sekizaki, K. Adachi, Y. Sasaki, Y. Zoka, A. Bedawy, T. Shimizu, K. Amimoto, "A novel design of single-phase microgrid based on non-interference core synchronous inverters for power system stabilization," *IET Generation, Transmission & Distribution*, 2022.
- [95] S. Sekizaki, Y. Nakamura, Y. Sasaki, N. Yorino, Y. Zoka, and I. Nishizaki, "A development of pseudo-synchronizing power VSCs controller for grid stabilization," in *19th Power Systems Computation Conference, PSCC 2016*, Institute of Electrical and Electronics Engineers Inc., Aug. 2016.
- [96] S. Sekizaki, K. Matsuo, Y. Sasaki, N. Yorino, Y. Nakamura, Y. Zoka, T. Shimizu, I. Nishizaki , "A Development of Single-phase Synchronous Inverter and Integration to

-
- Single-phase Microgrid effective for frequency stability enhancement,” *IFAC-PapersOnLine*, vol. 51, no. 28, pp. 245–250, Jan. 2018.
- [97] S. Sekizaki, Y. Sasaki, N. Yorino, Y. Zoka, Y. Nakamura, and I. Nishizaki, “A development of a single-phase synchronous inverter for grid resilience and stabilization,” *2017 IEEE Innovative Smart Grid Technologies - Asia: Smart Grid for Smart Community, ISGT-Asia 2017*, pp. 1–6, 2018.
- [98] R. Teodorescu, M. Liserre, and P. Rodríguez, “Grid Synchronization in Single-Phase Power Converters,” *Grid Converters for Photovoltaic and Wind Power Systems*, pp. 43–91, Dec. 2010.
- [99] C. L. Bhattar and M. A. Chaudhari, “Centralized Energy Management Scheme for Grid Connected DC Microgrid,” *IEEE Syst J*, pp. 1–11, Jan. 2023.
- [100] L. Ortiz, R. Orizondo, A. Águila, J. W. González, G. J. López, and I. Isaac, “Hybrid AC/DC microgrid test system simulation: grid-connected mode,” *Heliyon*, vol. 5, no. 12, p. e02862, Dec. 2019.
- [101] S. Njoya Motapon, L. A. Dessaint, and K. Al-Haddad, “A comparative study of energy management schemes for a fuel-cell hybrid emergency power system of more-electric aircraft,” *IEEE Transactions on Industrial Electronics*, vol. 61, no. 3, pp. 1320–1334, 2014.
- [102] F. L. Albuquerque, A. J. Moraes, G. C. Guimarães, S. M. R. Sanhueza, and A. R. Vaz, “Photovoltaic solar system connected to the electric power grid operating as active power generator and reactive power compensator,” *Solar Energy*, vol. 84, no. 7, pp. 1310–1317, Jul. 2010.
- [103] S. Aznavi, P. Fajri, A. Asrari, and F. Harirchi, “Realistic and Intelligent Management of Connected Storage Devices in Future Smart Homes Considering Energy Price Tag,” *IEEE Trans Ind Appl*, vol. 56, no. 2, pp. 1679–1689, Mar. 2020..
- [104] Y. Sasaki, Y. Shimamura, Y. Yamamoto, Y. Zoka, N. Yorino, and N. Mayaguchi, “Development of an EMS Simulator for the Purpose of Installation of Photovoltaic Power Generation and Storage Battery in a Customer - Considering Thermal Constraints of Storage Battery,” *The Transactions of the Institute of Electrical Installation Engineers of Japan*, vol. 39, no. 7, pp. 41–49, 2019.

Appendix A: Detailed Description of Iterative Pruning

Table 0.1 MAE for the Iterative Pruning Techniques for a Sunny Day

| Number of Hidden units | MAE | MAE ^{(20)+0.1} (Method B) | MAE ^{(20)*1.2} (Method C) |
|---------------------------|--------|---------------------------------------|---------------------------------------|
| 20 | 0.1158 | 0.2158 | 0.1389 |
| 19 | 0.1149 | ○ | ○ |
| 18 | 0.1153 | ○ | ○ |
| 17 | 0.1149 | ○ | ○ |
| 16 | 0.1374 | ○ | ○ |
| 15 | 0.1109 | ○ | ○ |
| 14 | 0.1088 | ○ | ○ |
| 13 | 0.1114 | ○ | ○ |
| 12 | 0.1196 | ○ | ○ |
| 11 | 0.1266 | ○ | ○ |
| 10 | 0.1412 | ○ | break |
| 9 | 0.1552 | ○ | |
| 8 | 0.2534 | break | |
| 7 | 0.3338 | | |
| 6 | 0.2996 | | |
| 5 | 0.2882 | | |
| 4 | 0.1144 | | |
| 3 | 0.7144 | | |
| 2 | 0.3771 | | |
| 1 | 0.1339 | | |

List of Publications by the Author

A. Transactions/ International Journal Papers

- [1] Y. Tanioka, Y. Sasaki, Y. Matsumoto, K. S. Mumbere, A. Fukuhara, S. Sekizaki, N. Yorino, Y. Zoka, “A Study on Power Sharing Control Considering State of Charge of Prosumers Batteries in Local Community,” *The Transactions of the Institute of Electrical Installation Engineers of Japan*, vol. 41, no. 3, pp. 19–28, 2021.
- [2] K. S. Mumbere, Y. Sasaki, N. Yorino, Y. Zoka, Y. Tanioka, and A. Bedawy, “A Resilient Prosumer Model for Microgrid Communities with High PV Penetration,” *Energies* 2023, Vol. 16, Page 621, vol. 16, no. 2, p. 621, Jan. 2023.

B. International Conference Papers Related to This Thesis

- [1] Y. Sasaki, S. Enomoto, N. Yorino, Y. Zoka, and M. S. Kihembo, “Solar Power Prediction Using Iterative Network Pruning Technique for Microgrid Operation,” in *2021 IEEE PES Innovative Smart Grid Technologies - Asia (ISGT Asia)*, 2021, pp. 1–5.
- [2] S. Enomoto, Y. Sasaki, N. Yorino, Y. Zoka, and M. S. Kihembo, “Solar Power Prediction Using Iterative Network Pruning Technique for Renewable-based Microgrid,” in *2021 IEEE 12th International Workshop on Computational Intelligence and Applications (IWCIA)*, 2021, pp. 1–6.
- [3] S. K. Mumbere, Y. Tanioka, S. Matsumoto, Y. Sasaki, Y. Zoka, and N. Yorino, “Distributed control of Islanded Microgrids Based on Battery SOC in Disaster situations,” in *2020 IEEE PES Innovative Smart Grid Technologies Europe (ISGT-Europe)*, 2020, pp. 1226–1230.
- [4] M. K. Samuel, A. Fukuhara, Y. Sasaki, Y. Zoka, N. Yorino, and Y. Tanioka, “A Novel Energy Management Approach to Networked Microgrids for Disaster Resilience,” in *2021 International Symposium on Devices, Circuits and Systems (ISDCS)*, 2021, pp. 1–5.
- [5] S. K. Mumbere, A. Fukuhara, Y. Sasaki, A. Bedawy, Y. Zoka, and N. Yorino, “Development of An Energy Management System Tool for Disaster Resilience in Islanded Microgrid Networks,” in *2021 20th International Symposium on Communications and Information Technologies (ISCIT)*, 2021, pp. 97–100.
- [6] K. S. Mumbere, Y. Sasaki, N. Yorino, Y. Zoka, A. Bedawy, and Y. Tanioka, “An Interconnected Prosumer Energy Management System Model for Improved Outage Resilience,” in *2022 IEEE PES/IAS PowerAfrica*, 2022, pp. 1–5.
- [7] Y. Sasaki, M. Ueoka, N. Yorino, Y. Zoka, A. Bedawy, and M. S. Kihembo, “Dynamic Economic Load Dispatch with Emergency Demand Response for Microgrid System Operation,” in *2021 22nd International Middle East Power Systems Conference (MEPCON)*, 2021, pp. 497–502.

-
- [8] K. S. Mumbere, N. Yorino, Y. Sasaki, A. Bedawy, Y. Tanioka Y. Zoka, C. Krifa, “Day-Ahead Optimal Resilient Energy Management for Grid-Connected Prosumer Microgrids,” Paris, Oct. 2023.
- [9] K. S. Mumbere, Y. Sasaki, N. Yorino, A. Fukuhara, Y. Zoka, A. Bedawy, Y. Tanioka, “Prosumer Control Strategy for A Robust Microgrid Energy Management System,” in 2021 IEEE PES Innovative Smart Grid Technologies Europe (ISGT Europe), 2021, pp. 1–6.
- [10] S. K. Mumbere, Y. Tanioka, Y. Matsumoto, A. Fukuhara, Y. Sasaki, Y. Zoka, N. Yorino, “A Novel Energy Management Technique for Shared Solar and Storage Resources in Remote Communities,” in 2020 IEEE PES/IAS PowerAfrica, 2020, pp. 1–5.
- [11] Y. Sasaki, M. Ueoka, Y. Uesugi, N. Yorino, Y. Zoka, A. Bedawy, M.S. Kihembo, “A Robust Economic Load Dispatch in Community Microgrid Considering Incentive-based Demand Response,” IFAC-PapersOnLine, vol. 55, no. 9, pp. 389–394, 2022.
- [12] S. K. Mumbere, Y. Matsumoto, A. Fukuhara, A. Bedawy, Y. Sasaki, Y. Zoka, N. Yorino, Y. Tanioka, “An Energy Management System for Disaster Resilience in Islanded Microgrid Networks,” in 2021 IEEE PES/IAS PowerAfrica, 2021, pp. 1–5.
- [13] A. Bedawy, N. Yorino, Y. Sasaki, Y. Zoka, K. S. Mumbere, and R. Kubo, “Distributed Agent-Based Voltage Control Approach for Active Distribution Systems,” in Emerging Electronic Devices, Circuits and Systems: Select Proceedings of EEDCS Workshop Held in Conjunction with ISDCS 2022, 2023, pp. 349–362.

Contents of the Thesis and Published Papers Relationship

| Chapters | Title of chapters | Published papers |
|-----------|---|------------------------------|
| Chapter 1 | Introduction | A, B |
| Chapter 2 | Literature Review and Basic Concepts | A, B |
| Chapter 3 | A Resilient Prosumer Model for Microgrids | A-(1, 2), B-(3-8, 10-11, 13) |
| Chapter 4 | An Enhanced Solar Power Prediction Model | B-(1, 2, 12) |
| Chapter 5 | Prediction-based Optimization for Microgrid Operation | B-(9) |
| Chapter 6 | Conclusions and Future Work | |

RESEARCH AWARDS

1. IEEE PES Japan Joint Chapter Student Best Paper Award

表彰状

IEEE PES Japan Joint Chapter
学生優秀論文賞



広島大学大学院先進理工系科学研究科

Samuel Kihembo Mumbere 殿

論文名：

An energy management system for disaster resilience in
islanded microgrid networks

あなたは IEEE PES が関連する国際学会において
優秀な論文を発表されましたので学生優秀論文
賞を授与いたします。

2022 年 1 月 21 日



IEEE Power & Energy Society Japan Joint Chapter

Chairperson 野田 琢

2. IEEE ISCIT 2021 Best Student Paper Award



3. IEEE PES ISGT Europe 2021 Best Paper Award

IEEE PES
Power & Energy Society®

IEEE PES Innovative Smart Grid Technologies (ISGT) Europe 2021
Conference, Espoo, Finland

A!
Aalto University

Best Paper Award

2021

granted to the paper titled

Prosumer Control Strategy for A Robust Microgrid Energy Management System

authored by

Samuel Mumbere Kihembo, Yutaka Sasaki, Naoto Yorino, Yoshifumi Zoka, Atsushi Fukuhara, Ahmed Bedavy and Yoshiki Tanioka

The **IEEE PES ISGT Europe 2021** (ISGT Europe 2021) was organized by IEEE Power & Energy Society (PES) and Aalto University, in Espoo, Finland, on **18-21 October 2021**. This conference theme was "Smart Grids: Toward a Carbon-free Future".

Mahdi Pourakbari Kasmaei
General Chair, ISGT-Europe 2021
On behalf of ISGT-Europe 2021 Organizing Committee

IEEE

4. IEEJ Academic Encouragement Award

電力技術委員会

奨励賞

Mumbere Kihembo Samuel 殿

貴殿は電気学会電力技術委員会が主催する研究会（令和三年）に於いて優秀な研究発表を行いました
ここに貴殿の努力と成果を称え副賞を添えて表彰いたします

令和四年三月一日

電気学会 電力技術委員会

委員長 根本 孝七

